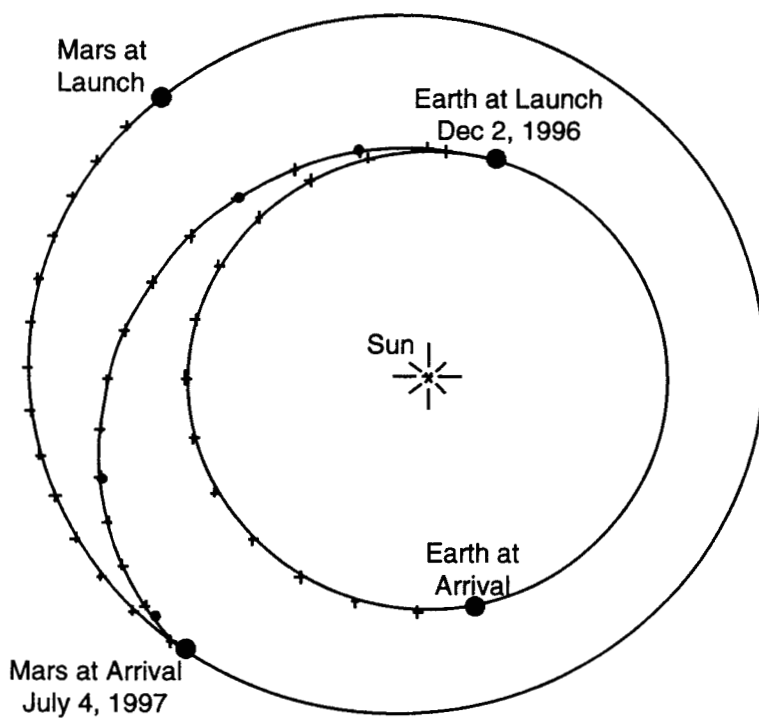Mars Pathfinder Project

PLANETARY CONSTANTS AND MODELS

December 1995

JPL

Jet Propulsion Laboratory
California Institute of Technology
Pasadena, California

Mars Pathfinder Project

PLANETARY CONSTANTS AND MODELS

Prepared by:

_____

Robin Vaughan

December 1995

JPL

Jet Propulsion Laboratory
California Institute of Technology
Pasadena, California

Revision History

Date	Changes	Status
10/95	Issued preliminary version for review by project personnel	Draft
12/95	First official release; incorporated comments from preliminary review.	Final

Contents

List of Figures

List of Tables

List of Acronyms and Abbreviations

AIM	Attitude and Information Management subsystem
ARA	Areocentric Right Ascension (used to compute local solar time)
AU	Astronomical Unit
C frame	Pathfinder spacecraft's cruise stage coordinate frame
DE403	Developmental Ephemeris - 403 (the planetary ephemeris)
DSN	Deep Space Network
DSS	Deep Space Station
ΔT	Ephemeris time minus Universal Coordinated Time
EDL	Entry, Descent, and Landing
E frame	Pathfinder spacecraft's entry vehicle coordinate frame
EME2000	Earth Mean Equator and Equinox of Epoch J2000 coordinate system
EMO2000	Earth Mean Orbit and Equinox of Epoch J2000 coordinate system
EOT	Equation Of Time
ET	Ephemeris time (equivalent to Terrestrial Dynamical Time)
FMS	Fictitious Mean Sun
GDS	Ground Data System
GM	constant of Gravitation times Mass of body
HEF	High EFficiency antenna
HST	Hybrid Solar Time
IAU	International Astronomical Union
IERS	International Earth Rotation Service
J frame	AIM's term for the EME2000 coordinate system
JED	Julian Ephemeris Date
JGM-3	TOPEX/POSEIDON Joint Gravity Model #3 for Earth
JPL	Jet Propulsion Laboratory
J2000	Julian ephemeris date 2451545.0, January 1, 2000 12:00:00 ET
L frame	Pathfinder spacecraft's lander coordinate frame
LMST	Local Mean Solar Time
LTST	Local True Solar Time

M frame	AIM's term for the Martian local level coordinate frame
MAR033.1	Martian satellite ephemeris
Mars50c	Gravity field model for Mars
Mars-GRAM	Mars Global Reference Atmospheric Model, Version 3.0
MBF frame	Mars Body-Fixed coordinate frame; AIM's term for the Mars Mean Equator and Prime Meridian of Date frame
MFX frame	Aim's term for the Martian Surface Fixed coordinate frame
MGS	Mars Global Surveyor
MIPS	Multi-Mission Image Processing System
MME	Mars Mean Equator and Equinox coordinate system
MO	Mars Observer
MPF	Mars Pathfinder
NAIF	Navigation Ancilliary Information Facility
P frame	PAM-D motor coordinate frame (used during Pathfinder launch)
PDT	Pacific Daylight Time
PST	Pacific Standard Time
RTN	Radian, Crosstrack, and Downtrack coordinate system
SCET	Spacecraft Event Time
SCLK	Spacecraft clock time
SI	International System of Units
SMAA	Semi-MAjor Axis
SMIA	Semi-MInor Axis
SSA	Star Scanner Assembly
TAI	Atomic time
TDT	Terrestrial Dynamic Time
TDB	(Solar System) Barycentric Dynamic Time
TS	True Sun
USGS	United States Geological Survey
UTC	Universal Coordinated Time
UT1	Universal Time

Chapter 1

INTRODUCTION

1.1 Purpose

This document provides a common set of astrodynamic constants and planetary models for use by the Mars Pathfinder Project. It attempts to collect in a single reference all the quantities and models in use across the project during development and for mission operations. These models are central to the navigation and mission design functions, but they are also used in other aspects of the project such as science observation planning and data reduction.

1.2 Scope

This document defines models and gives values for astrophysical quantities required to design and execute various aspects of the Mars Pathfinder mission. Current International Astronomical Union (IAU) standards and definitions are adopted wherever possible. These definitions correspond to the J2000 coordinate system adopted by the Mars Pathfinder Project. Deviations from IAU conventions are noted where they occur. Models are described to an appropriate level of detail and references are used where the model is too complex to describe completely within this document.

    The document is divided into five main sections covering the following categories of information: (i) coordinate systems, (ii) time systems, (iii) models and constants for the Earth, (iv) models and constants for Mars, and (v) fundamental (or general) constants. The section on coordinate systems is intended to be a comprehensive list of all the systems in use throughout the Mars Pathfinder project. It includes coordinate systems used to describe the spacecraft interplanetary trajectory, coordinate systems used once the spacecraft has landed on Mars, and systems fixed to the spacecraft itself. Time systems and related parameters for both Earth and Mars are included along with a definition of the spacecraft clock time. The sections on Earth and Mars include data on their mass and gravity fields, topographic information such as size and shape models and orientation and rotation parameters. Models for the Mars atmosphere and local surface conditions are included to

account for the entry, descent, and landing (EDL) and surface operations phases of the mission. The final section gives a table of general astrodynamic constants and discusses the standard planetary ephemeris adopted by the project.

This document is patterned on the Mars Observer Planetary Constants and Models document [1]. Portions of this document are taken verbatim from the MO document where applicable. Other sections have been modified slightly to reflect knowledge updates since the publication of the MO document. New sections have been inserted to reflect the special needs of the Mars Pathfinder mission.

Chapter 2

COORDINATE SYSTEMS

The definitions and values for any set of astrodynamic constants are intimately tied to the definition of appropriate coordinate systems. This section begins with a discussion of the terminology that is customarily used in the description of these systems. It then utilizes this common terminology to present the set of coordinates systems in use by the Mars Pathfinder project. These systems are (somewhat arbitrarily) divided into three classes: celestial, spacecraft, and surface systems. Celestial coordinate systems are typically used to describe the spacecraft's motion relative to various solar system bodies such as the Earth and Mars. Spacecraft coordinate systems are fixed to the spacecraft itself and are used for attitude control and instrument pointing. The surface coordinate systems comprise those systems to be used after the lander has been deployed on the Martian surface. They are usually attached to some part of the lander, which is also presumably attached to a fixed point on the Martian surface.

2.1   Definitions

A coordinate system, as utilized herein, is simply a means of relating points in three dimensional space and their motions. The state of a moving object, such as the spacecraft, is defined by two sets of ordered triples, the first giving the object's position and the second giving its velocity in that system. A coordinate system is fully specified by three fundamental characteristics - frame, center, and type. The frame and center typically define, or tie the coordinate system to, an inertial reference frame, while the coordinate type gives expressions for computing the values for the position and velocity triples. A typical example of coordinate type is Cartesian coordinates where position is given by (X, Y, Z) and velocity is given as $(\dot{X}, \dot{Y}, \dot{Z})$. The following sections elaborate on the concepts of frame, center, and coordinate type.

2.1.1   Frame

A coordinate frame represents a set of Cartesian axes: X, Y, and Z, whose directions are specified by four items: (i) body, (ii) reference plane, (iii) reference direction, and (iv)

reference time, or epoch. All coordinate frames used by MPF are orthogonal and right-handed. More specifically if the axes are specified as unit vectors, the frame is orthonormal. Mathematically, an orthonormal frame is defined as one where

$$X \cdot X = 1 \quad X \cdot Y = 0$$
$$Y \cdot Y = 1 \quad X \cdot Z = 0$$
$$Z \cdot Z = 1 \quad Y \cdot Z = 0$$

A right-handed frame is one whose axes satisfy

$$X \times Y = Z \quad Y \times Z = X \quad Z \times X = Y$$

In such a system a right threaded screw rotated through 90° from X toward Y will advance in the positive Z direction. In other words, if the right thumb is directed along $+Z$, the fingers curl in the direction of positive rotation. Similar statements apply to rotations about the X and Y axes. Figure 2-1 illustrates the directions of positive rotations in a right-handed frame.

θ is the rotation angle about each coordinate axis

Figure 2-1: Positive rotation angles for a right-handed coordinate frame

The body and reference plane are used to define the X-Y plane of the frame. The body can be any solar system body or the spacecraft, but it is most usually a major planet or the Sun. The reference plane is usually associated with some feature of the body itself or its motion in the solar system. The two most common planes are the equator and the orbit plane. For example, using Earth as the body and its equator as the reference plane specifies the family of Earth Equatorial coordinate systems. Similarly, using Earth as the body with

its orbit plane, the ecliptic, as the reference plane designates the Earth Orbital coordinate systems. Note that the specification of a body name in the coordinate frame definition says nothing about where the frame is actually centered. It is common usage to center an Earth Orbit frame at the Sun or to center an Earth Equator frame at some other solar system body, such as Mars. The Z-axis of the frame is defined to be the unit normal for the reference plane. For an equator plane, the Z-axis will be a north pole vector whereas for an orbit plane, it will be the direction of the orbital angular momentum vector.

The reference direction is simply an arbitrary, although usually physically meaningful, direction in the X-Y plane that is chosen as the frame's X-axis. Typically such a direction is obtained from the line of nodes that results from the intersection of the reference plane with some other known plane. For example, the X-axis of the Earth equator plane may be the vernal equinox, which is the node with Earth's orbit plane where the orbit ascends through the equator plane. This choice for the X-axis designates the Earth Equator and Equinox frame. A common choice for the X-axis in the Mars equator plane is the node at which the Mars equator plane ascends through the Earth equator plane. This is called the Mars Equator and IAU-vector frame since it is the standard defined by the International Astronomical Union in [7]. An X-axis that is attached to and rotates with the body can also be chosen. These systems typically use the intersection of the body's prime meridian with its equator plane to define the direction of the X-axis. One example of this type of frame is the Mars Equator and Prime Meridian frame.

The Y-axis direction is chosen to complete a right-handed, orthogonal coordinate system. It will lie in the reference plane 90° away from the X-axis specified by the reference direction.

The reference time specifies when the frame being described has, had, or will have an actual physical existence. It is necessary to designate a reference time because the reference planes that describe the coordinate frames are likely to be in some state of motion due to the fact that the bodies they are associated with are continually being subjected to the perturbing forces of the physical universe. These forces produce two motions of particular interest: precession and nutation. Precession is a "coning" motion of a planet's spin axis, and hence its equator, caused by torques applied to the planet's equatorial bulge by the Sun and its satellites, if any. This is usually a long period change, which means that it requires a substantial interval (on the order of 10^3–10^4 years) to complete a single cycle. During this length of time, the rate of precession can vary periodically on time scales that are comparatively short (on the order of 10–10^2 years). This short period change is caused by additional torques exerted by any satellites and is called nutation. Precession and nutation combined represent the true motion of a rererence plane, as well as its Z-axis. This true motion can be viewed as a cyclic motion about a mean motion that would occur due to precession alone. In other words, an Earth True Equator plane reflects the effects of both precession and nutation whereas an Earth Mean Equator plane reflects the effects of precession only.

The reference time can be specified as a fixed moment in time, called the epoch, or it can be set equal to the varying times at which a state is to be obtained in the frame. These two alternatives essentially distinguish inertial from non-inertial coordinate frames

as explained below.

An <u>inertial</u> frame is one in which the Cartesian axes are in a state of rest or uniform, i.e. unaccelerated, motion. This implies that the axes are not rotating. Since the reference planes are constantly rotating, an epoch must be specified to "freeze" their motion at some point and define an inertial frame. It is typical to begin with a mean equator or mean orbit plane - one which considers only precession - and select an epoch that represents a snapshot of that plane's position at that time. The standard epoch for inertial frames is January 1, 2000 12:00:00 ET, commonly called J2000. This is the beginning of the Julian year 2000 and corresponds to a Julian date of 2451545.0. The fundamental inertial frame for Mars Pathfinder uses the Earth as the body, its mean equator as the reference frame, the vernal equinox of its mean orbit as the reference direction, and J2000 as the reference epoch. Hence, this frame is called the Earth Mean Equator and Equinox of 2000 or simply EME2000. This inertial frame is used in navigation to integrate the equations of motion for the planets and the spacecraft.

A <u>non-inertial</u> frame is one which is undergoing some sort of non- uniform, i.e. accelerated, motion. The most common type of motion for axes in a non-inertial frame is rotation, although precession and nutation are also examples. There is no specific epoch at which to freeze the reference plane's motion in a non-inertial system. Instead, the reference time defining the orientation of the axes is taken to be the same time at which a state is to be related to the frame. The reference time is said to be "of date" for such a frame. One example of a non-inertial frame is the Mars Mean Equator and IAU-vector of date which reflects only the precession of Mars. This system is not too different from an inertial system since precession is a long period motion. Another non-inertial frame is Earth Mean Equator and Equinox of Date which incorporates both precession and nutation of Earth's pole. This deviates from an inertial frame more rapidly since the short period effects of nutation are included. Finally, there are <u>body-fixed</u> frames which incorporate the body's rotation along with precession and nutation. One such frame is the Earth True Equator and Prime Meridian of date whose X-axis, the Greenwich Prime Meridian, completes 1 rotation each day.

2.1.2   Center

The <u>center</u> of a coordinate frame is simply the origin of the system. It may be at the center of any of the nine planets, their natural satellites, minor planets, comets, or the Sun, at the solar system or a planet system barycenter, at a topographic location on the surface of any of these bodies, or at the spacecraft. The body name used in the frame definition is not related to the center, although frequently the center of the body is chosen as the frame center. It is also common to describe interplanetary trajectories in a coordinate system centered at the Sun's center using the inertial frame of Earth Mean Equator and Equinox of 2000.

2.1.3   Type

Given a center and a frame, there are several types of coordinates that can be used to represent state vectors. They are all equivalent to each other and each requires the specification of six parameters to quantify the position and velocity of a point in the frame. The most common types of coordinates are summarized in the following paragraphs. More detailed definitions of the position and velocity components for these types are given as needed in subsequent sections defining those coordinate systems used by MPF.

Cartesian coordinates

Cartesian coordinates consist of X, Y, and Z position components and time derivatives of these $\dot{X}$, $\dot{Y}$, and $\dot{Z}$ to specifiy velocity. These are most useful during the process of numerical integration of a trajectory.

Latitudinal coordinates

Latitudinal coordinates utilize a radius or altitude, a declination or latitude, and a right ascension or longitude to specify position. A speed, azimuth and flight path angle are used to specify velocity. Generally, right ascension and declination are used with an equator plane when the system's X-axis is not rotating diurnally. Star locations are typically given as right ascension and declination angles in an inertial reference frame. Latitude and longitude are commonly used for an equator plane where the X-axis does rotate diurnally. Thus locations on Earth or Mars can be given as latitude measured from the equator and longitude measured from the prime meridian. These coordinates are useful when seeking to relate the motion of a spacecraft to a nearby spherical body.

Conic element, or Keplerian, coordinates

Conic elements are a specialized set which are used to describe the orbital motion of one body about another. These elements are related to the position and velocity at a point on the orbit by certain trigonometric equations. See Chapter 3 of reference [2] for a discussion of the conic orbital elements.

B-Plane coordinates

B-Plane coordinates are another specialized set which are used to describe navigation targeting and accuracy for planetary flybys. They are derived assuming that the spacecraft approaches the target body along a hyperbolic orbit, moving with constant speed along a fixed asymptote direction when far from the body.

2.2   Celestial Systems

Celestial coordinate systems are those used to express the spacecraft trajectory in interplanetary space or to give the location of a body such as Mars or the spacecraft with respect

to the Earth or the Sun. The fundamental inertial reference frame is considered to be a celestial system since integration of the spacecraft equations of motion is performed using this system. Many other celestial coordinate systems, both inertial and non-inertial, are used for MPF. These are presented in the following sections, where they have been grouped into sets according to their center.

2.2.1   The Inertial Reference Frames

The J2000 Inertial Reference Frame is a right-handed Cartesian set of 3 orthogonal axes chosen as follows:

$+Z_{J2000}$ is normal to the Earth's mean equator of epoch J2000

$+X_{J2000}$ is parallel to the vernal equinox of Earth's mean orbit of epoch J2000

$+Y_{J2000}$ completes the right-handed system

The epoch J2000 is the Julian Ephemeris Date (JED) 2451545.0. These axes are depicted in Figure 2-2. These vectors are used as the basis for expressing the positions and velocities of objects in space, such as stars, planets, satellites, asteroids, comets, and spacecraft. Various ephemeris files provided by navigation contain polynomial coefficients representing the states of solar system bodies or the spacecraft in this reference frame. One example of such a file is the planetary ephemeris file. The current planetary ephemeris file in use by MPF is described in section 6.

$Z_{EME2000}$
(Earth's Mean North Pole,
Normal to Earth's Mean
Equator, at Epoch J2000)

$Y_{EME2000}$

$X_{EME2000}$
(Earth's Mean Vernal
Equinox at Epoch J2000)

Figure 2-2: The EME2000 Inertial Reference Frame

The center of this frame can be anywhere, not just at the planet Earth. The planetary ephemeris file uses the solar system barycenter as its center. Spacecraft ephemeris files typically change center during the different mission phases, perhaps starting out centered at Earth near launch, transitioning to be centered at the Sun's center during cruise, and then centered at Mars for approach and landing.

The reference plane of this frame is an instantaneous snapshot of the Earth's mean equator at epoch J2000. Precession of the equator is accounted for, while nutation is ignored. Referring to the discussion in section 2.1.1, it is appropriate to refer to this frame as Earth Mean Equator and Equinox of Epoch J2000 or simply EME2000.

Another fundamental inertial frame, closely related to EME2000 is the Earth Mean Orbit and Equinox of Epoch J2000 or EMO2000. This could also be called the Ecliptic of J2000. The reference plane is the plane of the Earth's mean orbit at J2000 and thus the Z-axis is the Earth's mean orbital angular momentum vector of that epoch. The X axis is again specified as the vernal equinox of the Earth's mean orbit at J2000, so that this coordinate system is related to EME2000 by a single rotation about this axis. The angle of rotation is referred to as the mean obliquity of the ecliptic at J2000 and its value is 23.439281° [9]. The relationship between the EME2000 and EMO2000 frames is discussed further in section 2.2.3.

2.2.2   Sun-Centered Systems

During the interplanetary phase of a deep space mission it is customary to relate spacecraft states to the Sun, since it dominates gravitationally during this period. However it is not very effectual to use reference frames tied to the solar equator plane. The Earth-related reference planes are typically carried over into this phase. The following inertial systems are most commonly used:

- Sun-centered Earth Mean Equator and Equinox of Epoch J2000

- Sun-centered Earth Mean Orbit and Equinox of Epoch J2000

There are no non-inertial systems centered at the Sun in use by MPF.

2.2.3   Earth-Centered Systems

Since the Mars Pathfinder mission is controlled from Earth, there are obviously many uses for coordinate systems centered at Earth itself. These range from specifying the position of the spacecraft relative to a fixed point on Earth such as a DSN tracking station to representing the positions of the Earth and Sun relative to the spacecraft in attitude control flight software. The relevant set of Earth-centered coordinate systems is described in the following sections.

Inertial

Two inertial coordinate systems are defined by simply attaching the center of the inertial frames defined in section 2.2.1 to the center of the Earth:

- Earth-centered Earth Mean Equator and Equinox of Epoch J2000

- Earth-centered Earth Mean Orbit and Equinox of Epoch J2000

These are depicted in Figure 2-3. Note that the first of these coordinate systems corresponds to the "J Frame" used by AIM (Ref. [4], section 2.2.1).

Figure 2-3: Earth-centered inertial coordinate systems

Non-Inertial

As noted earlier, it is possible to have coordinate systems centered on the Earth which, while not fixed to the solid body of the planet, are nevertheless non-inertial. This arises from the fact that an "of date" coordinate system incorporates a reference plane which is in a state of rotational motion. Two such systems can be defined:

- Earth-centered Earth Mean Equator and Equinox of Date

- Earth-centered Earth True Equator and Equinox of Date

The first system includes precession of the Earth's equator while the second includes the combined effects of precession and nutation.

These coordinate systems will find their most common usage in the launch and Earth departure phase of a deep space mission, during which it is important to relate the state of the spacecraft to the reference plane which characterizes the current orientation of the Earth. Because the X- and Y-axes are not tied to the solid body of the Earth, latitude and longitude are not used to describe the angular components of the spherical position vector. Rather, it is generally accepted to specify these angles as declination and right ascension.

Body-Fixed

Very often it is important to know the state of a spacecraft with respect to the solid rotating body of the Earth. For example, this is useful in ascertaining likely periods when the spacecraft can be tracked by a particular DSN station. For the body-fixed systems, the reference direction is taken to be the intersection of the Greenwich Meridian with the Earth's equator. Similar to the non-inertial Earth-centered systems, there are two possibilities:

- Earth-centered Earth Mean Equator and Prime Meridian of Date

- Earth-centered Earth True Equator and Prime Meridian of Date

In addition to the rotation of the Earth, the Mean Equator system includes the mean polar motion due to precession alone while the True Equator system includes polar motions due to precession and nutation. The angular components of the spherical position vector for these systems are the standard latitude and longitude as shown in Figure 2-4.

2.2.4   Mars-Centered Systems

Once the spacecraft nears the vicinity of Mars, it makes the most sense to utilize Mars-centered coordinate systems. These are systems that are centered at the center of the planet itself, not at the Mars system barycenter nor at a point on its surface. (Surface coordinate systems are discussed in section 2.4.) For Pathfinder, these systems will be used in the last few months of cruise up to the time that the spacecraft enters the Martian atmosphere.

Inertial

One inertial coordinate system is defined by simply attaching the origin of the EME2000 frame defined in section 2.2.1 to the center of Mars. This system is called

- Mars-centered Earth Mean Equator and Equinox of Epoch J2000

The only other inertial coordinate system centered at Mars is

- Mars-centered Mars Mean Equator and IAU-vector of Epoch J2000

Figure 2-4: Earth-centered Body-Fixed Coordinate Systems

The reference plane for this system is the Mars mean equator at epoch J2000. Instead of a Mars equinox, the new IAU standard for the reference direction in an arbitrary planet equatorial reference plane is used. This IAU-vector is defined to be that point in the planet equator where the equator ascends through the Earth's equator plane. This definition was chosen to obviate the need for defining a planet's mean orbit plane which would have been required for an equinox X-axis. It was felt that only the Earth's mean orbit plane was known with any precision, so that the equinox reference direction is only applicable when using Earth's equator as the reference plane. The IAU-vector is used as the X-axis for other planets. In the case of Mars, the X-axis points toward the point in the Mars Mean Equator of Epoch J2000 plane where that plane ascends through the Earth Mean Equator of Epoch J2000 plane. This is illustrated in Figure 2-5.

Figure 2-5: Mars-centered Mars Mean Equator and IAU-Vector of Epoch J2000

Non-Inertial

One non-inertial, albeit not body-fixed, Mars-centered coordinate system is of interest for MPF:

• Mars-centered Mars Mean Equator and IAU-Vector of Date

This is closely related to the inertial system of Mars Mean Equator and IAU-vector of Epoch J2000 except that the directions of the Mars polar axis and IAU-vector are not frozen at J2000, but are evaluated at the varying "of date" epoch. The motion of these axes due to the precession of the Mars pole is very slight and can probably be ignored in most realistic applications. However, to be strictly accurate this system must be classified as non-inertial.

Body-Fixed

The primary body-fixed *frame* centered at Mars is analogous to that of the Earth-centered, Earth Mean Equator and Prime Meridian of Date system. The reference plane is the Mars Mean Equator of Date and the reference direction is the intersection of the Mars Prime Meridian with this mean equator plane. The Mars prime meridian has been chosen to pass through a crater called Airy-0 located in Mars' southern hemisphere. This frame is called the MBF frame in [4]. There are actually two coordinate *systems* that use this frame; they are distinguished by coordinate *type*. The latitude and longitude components of the latitudinal position vector are defined differently in these two systems as described below. The first body-fixed system is called

- Areocentric Mars Mean Equator and Prime Meridian of Date

In this system, the latitudinal coordinates for position are a radius measured from the center of Mars to the point and longitude and latitude angles giving the direction to the point. Latitude, ϕ, is defined as the angle between the vector to the point and the equatorial plane. It is measured positive above and negative below the Mars mean equator so that $-90° \leq \phi \leq +90°$. Longitude, λ, is defined as the angle between the vector to the point and the plane of the prime meridian. Longitude is measured positive eastward and $0° \leq \lambda < 360°$. This is equivalent to traditional latitude, longitude, and radius coordinates used on Earth and depicted in Figure 2-4. The relationship between the Cartesian coordinates (x, y, z) of a point in the body-fixed frame and its latitudinal coordinates (r, ϕ, λ) is

$$
\begin{aligned}
x &= r \cos \phi \cos \lambda \\
y &= r \cos \phi \sin \lambda \\
z &= r \sin \phi
\end{aligned}
$$

The second body-fixed system is called

- Areographic Mars Mean Equator and Prime Meridian of Date

and was originally used to define the latitude and longitude of surface features on Mars for cartographic purposes. The key elements of this system are depicted in Figure 2-6. The definitions of latitude and longitude differ from the standard latitudinal definitions because this system deals with an oblate planet rather than a spherical one.

An oblate spheroid is a special type of triaxial ellipsoid that is often used as a shape model for Mars. A triaxial ellipsoid is a surface whose points satisfy the equation

$$
\frac{x^2}{a^2} + \frac{y^2}{b^2} + \frac{z^2}{c^2} = 1
$$

where a, b, and c are the semi-major axis lengths, or radii, along the X, Y, and Z coordinate axes. For planetary bodies, it is customary for the X- and Y-axes to lie in the equatorial plane with the Z-axis aligned with the spin axis (or north pole). An oblate spheroid is an ellipsoid where two of the three radii are equal and the third radius is smaller than the two equal radii. It is usually the case for a planet that the equatorial radii, a and b, are equal and the polar radius, c, is less than the equatorial radii:

$$\frac{x^2 + y^2}{a^2} + \frac{z^2}{c^2} = 1 \text{ where } c < a$$

The radial distance from the center to a point on the surface of an oblate spheroid at a given areocentric latitude (and longitude) is

$$r_s = \frac{ac}{\sqrt{a^2 \sin^2 \phi + c^2 \cos^2 \phi}}$$

Note that the radial distance is not a function of the areocentric longitude due to the rotational symmetry of the spheroid about the polar axis.

The areographic coordinates for the position of a point P are latitude and longitude angles and a height, or altitude, above a particular point on the spheroid's surface, P'. Areographic longitude, Λ, is measured similarly to areocentric longitude except that is is considered positive westward of the planet's prime meridian. Areographic latitude, Φ, and height, h, are referenced to P' where P' is that point on the oblate spheroid where the outward pointing surface normal passes through P. The areographic latitude, Φ, of P' is the angle between the equatorial plane and the normal to the spheroid at P'. The height, h, of P above (or below) P' is the distance along the normal vector from P' to P. h is positive for points above the spheroid's surface and negative for those below it. The relationship between areocentric and areographic latitude and longitude of a point P' *on the surface of the oblate spheroid* is:

$$\Lambda = 360° - \lambda \tag{2.1}$$

$$\Phi = \tan^{-1}\left[\frac{a^2}{c^2} \tan \phi\right] \tag{2.2}$$

(See [3] for a more detailed treatment of areocentric versus areographic latitude.)

Relating Inertial, Non-Inertial, and Body-Fixed Systems

It is often necessary to express the directions of the axes of a non-inertial frame at some moment in time as vectors in the fundamental inertial frame EME2000. For frames using a body's equator as the reference, this is accomplished using equations that give the direction of the body's spin axis, or north pole axis, as a function of time. This direction is typically expressed as right ascension and declination angles, α and δ, which are equivalent to the standard longitude and latitude angles. The right ascension and declination of the (north) pole are sufficient to define the axes directions for the IAU standard mean equator frame

Figure 2-6: Areographic Coordinate System

for planets such as Mars. The direction of the body's prime meridian in the equatorial plane is also required to specify the X-axis direction for body-fixed frames. This direction is typically given as an angle W measured positive eastward in the equatorial plane, from the X-axis of corresponding mean equator frame.

   Figure 2-7 depicts the relationship between the EME2000, Mars Mean Equator and IAU-Vector of Date, and Mars Mean Equator and Prime Meridian of Date coordinate frames. The subscript IAU is used to denote the coordinate axes for the Mean Equator and IAU-Vector system, while the subscript PM is used to denote the Mean Equator and Prime Meridian system. The angles α, δ, and W needed to rotate between these two systems and EME2000 are indicated. Equations giving the values of α, δ, and W as functions of time can be found in section 5.3.

2.2.5   Spacecraft-Centered Systems

It is sometimes convenient to work in an inertial coordinate system whose origin is at the spacecraft. This is another example of attaching the fundamental inertial frame to a particular center:

   • Spacecraft-centered Earth Mean Equator and Equinox of Epoch J2000

For example, the vector pointing from the spacecraft to a target body can be given in this inertial frame and then rotated into some spacecraft body-fixed system to determine

X$_{IAU}$ = Mars IAU Vector of Date

α = *Right Ascension*
δ = *Declination*
   of Mars North Pole

X$_{IAU}$ = Mars IAU Vector of Date

17
Figure 2-7: Relationship of Mars Mean Equator and IAU-Vector of Date and Mars Body-Fixed Coordinate Systems

instrument pointing.

The spacecraft-centered inertial system is presented here with the other celestial systems because it is derived from the fundamental inertial reference frame. There are also numerous body-fixed spacecraft-centered coordinate systems. Because the spacecraft is not a natural solar system body like the planets and because of their wide use throughout the project, these systems are presented separately in section 2.3.

2.2.6   Miscellaneous Systems

There are two other coordinate systems typically used by the navigation team that can be considered celestial systems. The first is the RTN system and the second is the B-plane system. These are documented here for completeness.

The RTN System

The RTN system is convenient when working with a body in a closed orbit about another body such as a planet orbiting the Sun or a spacecraft orbiting a planet. The reference plane for this system is the body's orbital plane; the Z, or N axis, also called the normal or crosstrack axis, is aligned with the body's orbital angular momentum vector. The X-axis is aligned with the radius vector from the focus of the orbit (usually the Sun or a planet) to the body. Hence, the X-axis is also called the radial or R-axis. The Y-axis is chosen to complete a right-handed system and thus it lies in the orbital plane pointing roughly along the direction that the body is moving along its orbit. The Y, or T, axis is called the tangential or downtrack direction, although it is not, in general, coincident with the body's orbital velocity vector. Figure 2-8 illustrates these definitions of the RTN axes. This is a non-inertial system since the radial and downtrack axes of this system rotate once per orbital revolution of the body about the focus. Further, this can be considered an "of date" system since it is based on the instantaneous orbital position and velocity of the body. The center of this system is usually taken to be the center of the focus body, but it can also be set at the orbiting body itself. The accuracy of a planet's orbital ephemeris is often given as standard deviations in the radial, downtrack, and crosstrack directions at a set of relevant times.

The Navigation B-Plane Coordinate System

The B-plane coordinate system is used extensively for spacecraft navigation. Historically it was proposed as a convenient system for designing and evaluating a spacecraft's encounter with a planetary body and has been used for most of JPL's past missions. The spacecraft's incoming trajectory on approach to a target body is represented as a hyperbolic orbit. When far from the target body, the spacecraft is essentially moving along an asymptote of this hyperbola with a fixed speed denoted V_∞. In other words, the V_∞ vector, $\boldsymbol{V}_\infty$, is directed along the asymptote with magnitude V_∞ and is approximately the velocity relative to the target body at the time of entry into its gravitational sphere of influence. The B-plane is a plane passing through the center of the target body and perpendicular to the

Orbiting
body

R
(Radial)

Orbit
Focus

Body's Orbital
Velocity

T
(Downtrack)

Body's Orbit

N (Crosstrack) axis:
Normal to orbit plane -
points into page

Figure 2-8: In-Orbit RTN or Radial-Crosstrack-Downtrack Coordinate System

asymptote (assuming 2-body conic motion). The "B-vector", denoted $\boldsymbol{B}$, is a vector in that plane, from the target body center to the piercing-point of the trajectory asymptote. The B-vector specifies where the point of closest approach would be if the target body had no mass and did not deflect the flight path. The coordinate frame is defined by three orthogonal unit vectors, $\hat{S}$, $\hat{T}$, and $\hat{R}$. The $\hat{S}$ vector is parallel to $\boldsymbol{V}_\infty$. $\hat{T}$ is arbitrary, but typically specified to lie in the ecliptic plane (the mean plane of the Earth's orbit), or in a body equatorial plane. Finally, $\hat{R}$ completes a right-handed orthogonal triad with $\hat{S}$ and $\hat{T}$. The center, or origin for the B-plane system is at the center of the target body. The B-plane system is illustrated in Figure 2-9. Note that $\hat{T}$ usually points to the right and $\hat{R}$ points down as seen looking along the incoming asymptote. For Pathfinder navigation, the B-plane coordinate system is centered at Mars with the $\hat{T}$ axis chosen to lie in the Mars Mean Equator of Date plane.

Figure 2-9: The B-Plane Coordinate System

The six components characterizing position and velocity in the B- plane coordinate system are $\boldsymbol{B} \cdot \hat{R}$, $\boldsymbol{B} \cdot \hat{T}$, T_L, $\hat{S} \cdot \hat{R}$, $\hat{S} \cdot \hat{T}$, and $C_3 = (V_\infty)^2$. $\boldsymbol{B} \cdot \hat{R}$ and $\boldsymbol{B} \cdot \hat{T}$ are the components of the B-vector along the $\hat{R}$ and $\hat{T}$ axes. T_L is called the linearized time-of-flight and specifies what the time to encounter would be from some given epoch if the magnitude of the B-vector were zero. In other words, T_L represents the time to encounter if the spacecraft were traveling on a rectilinear orbit relative to the central body. $\hat{S} \cdot \hat{R}$ and $\hat{S} \cdot \hat{T}$ are the components of $\hat{S}$ along the $\hat{R}$ and $\hat{T}$ axes. Obviously, these are nominally zero since these axes form an orthogonal triad. C_3 is proportional to the total energy of the two-body conic orbit.

Trajectory errors in the B-plane are often characterized by a 1σ dispersion ellipse as shown in Figure 2-9. SMAA and SMIA denote the semi-major and semi-minor axes of the

ellipse; θ is the angle measured clockwise from the $\hat{T}$ axis to SMAA. Dispersions normal to the B-plane are typically given as a 1σ time-of-flight error. Alternatively, these dispersions are sometimes given as a 1σ distance error along the $\hat{S}$ direction, numerically equal to the time-of-flight error multiplied by the magnitude of $\boldsymbol{V}_\infty$.

Formally, the 1σ spacecraft trajectory uncertainty is computed as a 6x6 covariance matrix with entries for each of the six B-plane coordinate components. The entries for $\boldsymbol{B} \cdot \hat{R}$ and $\boldsymbol{B} \cdot \hat{T}$ are typically transformed to SMAA, SMIA, and θ and the T_L entry can be transformed to a downtrack distance error as discussed above. The entries for $\boldsymbol{B} \cdot \hat{R}$ and $\boldsymbol{B} \cdot \hat{T}$ represent dispersions in the asymptote direction while the entries for C_3 represents variations in the magnitude of the approach velocity. These are not often quoted when presenting orbit determination accuracy, but the full covariance matrix is used for maneuver design and in Monte Carlo simulations analyzing landing accuracy for MPF.

2.3 Spacecraft Systems

A number of Pathfinder spacecraft coordinate frames are defined in reference [4]. Only four of these are described here, namely those referenced to the cruise stage, entry vehicle system, and lander and one that describes the configuration of the spacecraft in the launch vehicle payload fairing. Other coordinate systems related to lander surface operations are presented in section 2.4.

2.3.1 Cruise Stage

The Mars Pathfinder spacecraft consists of a cruise stage and an entry vehicle containing the lander. For launch and during interplanetary cruise, the entry vehicle and lander remain attached to the cruise stage. The cruise stage is jettisoned shortly before entry into the Mars atmosphere. A cruise stage coordinate system, called the C Frame in [4] and denoted by axes X_c, Y_c, Z_c, will be used until separation occurs near Mars arrival. The reference plane of the cruise stage frame is the plane of the entry vehicle interface pads located at the top of the backshell interface plate (also called the entry vehicle separation plane). The Z_c-axis is normal to this plane, coincident with the nominal spacecraft spin vector, and directed positively outward towards the entry vehicle and away from the solar array (through the spacecraft center of mass). In contrast to the celestial systems, the Y-axis serves as the reference direction for cruise stage coordinates. The Y_c-axis lies in the entry vehicle separation plane and is directed positively outward over the boresight of the Star Scanner Assembly (SSA). The X_c-axis also lies in the separation plane and completes a right-handed system. The center of the cruise stage coordinate system is the geometric center of the three mounting bolt holes for the bolts that connect the cruise stage to the entry vehicle. MPF cruise stage coordinates are depicted in Figure 2-10.

2.3.2 Entry Vehicle

The entry vehicle coordinate system, denoted X_e, Y_e, Z_e, and called the E frame in [4], is identical to the cruise stage coordinate system. The center and reference planes are the

same and the star scanner location on the cruise stage is again used to define the reference direction for the Y_e-axis. Figure 2-11 shows these axes in relation to the entry vehicle.

2.3.3   Lander

The Mars Pathfinder lander is a tetrahedral structure. One of its faces is called the base petal and houses most of the lander equipment. The other three faces, or petals, open after surface impact to expose these sytems. The rover is mounted to one of these petals. The lander coordinate system, called the L Frame in [4], has the lander base petal as its reference plane and its center coincident with the geometric center of the base petal. The reference direction specifies the Y_L-axis direction and passes through the geometric center of the rover petal. While the entry vehicle and lander remain attached to the cruise stage, lander coordinate axes X_L, Y_L, Z_L, are aligned with those of the cruise stage and entry vehicle systems. The center of the lander system is translated 1.127 m in the $Z_c = Z_e$ direction from the origin of cruise stage coordinates. The Z_L-axis is normal to the reference plane and coincident with the nominal spacecraft spin vector. When the lander is upright on the surface, the Z_L-axis is directed positively downward to the ground. MPF lander coordinates are depicted in Figure 2-12.

Figure 2-13 shows the relative orientation of the cruise stage, entry vehicle, and lander coordinate systems using an exploded view of the Pathfinder spacecraft.

2.3.4   Launch Configuration

The configuration of the MPF spacecraft inside the payload fairing of the Delta launch vehicle is shown in Figure 2-14. A coordinate system referenced to the PAM-D motor, called the P Frame in [4] and denoted by axes X_P, Y_P, Z_P, is used to describe the position of the spacecraft in the fairing. The orientations of the PAM-D coordinate axes with respect to cruise stage axes are:

$$X_P = Z_c$$
$$Y_P = Y_c$$
$$-Z_P = X_c$$

A launch separation plane is defined as the plane normal to Z_c located 0.031 m below the origin of cruise stage coordinates. The origin of PAM-D coordinates is located 10.387 m above this separation plane, or 10.356 m along the $+Z_c$-axis from the origin of cruise stage coordinates. There are no translations in the X or Y directions from the origin of cruise stage coordinates to the origin of PAM-D coordinates.

Figure 2-10: Mars Pathfinder Cruise Stage Coordinate System

Figure 2-13: Relative Orientation of Pathfinder Spacecraft Coordinate Systems

Figure 2-11: Mars Pathfinder Entry Vehicle Coordinate System

Figure 2-12: Mars Pathfinder Lander Coordinate System

Figure 2-14: Mars Pathfinder Launch Configuration

2.4   Surface Systems

2.4.1   Martian Local Level Coordinate System

The Martian local level coordinate system is defined relative to the Mars body-fixed frame defined in section 2.2.4. This system is called the M frame in [4] and its axes are denoted X_M, Y_M, Z_M. Its center coincides with that of lander coordinates. The position of this center can be expressed as areocentric radius, latitude and longitude. The Z_M-axis is aligned with the radius vector but points in the opposite direction downward from the lander to the ground. The reference direction is the X_M-axis which is points along the longitude meridian containing the center towards the Martian north pole (the Z-axis of the Mars body-fixed frame). The Y_M-axis completes a right-handed system and points along the latitude circle containing the center eastward in the direction of Mars' rotation. This frame is thus a North, East, Nadir frame. The X_M, Y_M, Z_M axes are illustrated in Figure 2-15.

Figure 2-15: Mars Pathfinder Local Level Coordinate System

2.4.2   Martian Surface Fixed Coordinate System

The Martian surface fixed coordinate system is another North, East, Nadir frame defined relative to the Mars body-fixed frame of section 2.2.4. In contrast to the local level system, the surface fixed system references areographic radius, latitude, and longitude. This system

is called the MFX frame in [4] and its axes are denoted X_{MFX}, Y_{MFX}, Z_{MFX}. Its center initially coincides with that of lander and local level coordinates. The Z_{MFX}-axis is aligned with the surface normal of the Mars IAU reference ellipsoid at the landing site and points downward from the lander into the ellipsoid. (See section 5.2.1 for a definition of the IAU reference ellipsoid.) The X_{MFX}- and Y_{MFX}-axes are defined similarly to X_M and Y_M and lie in the plane that is tangent to the reference ellipsoid at the landing site. X_{MFX} points along the areographic longitude meridian containing the lander towards the Martian north pole (the Z-axis of the Mars body-fixed frame). The Y_{MFX}-axis completes a right-handed system and points along the areographic latitude circle containing the lander eastward in the direciton of Mars' rotation.

2.4.3 Relating Lander, Local Level, and Surface Fixed Coordinates

Lander and Mars local level coordinates share the same origin. The location of this origin relative to Mars body-fixed coordinates is given as areocentric radius, or distance from Mars' center, and areocentric latitude and longitude. This location is initially set to the nominal landing site. Its value is uplinked to the lander flight software — the lander currently has no way to measure this location *in situ*. It may be updated after landing if more accurate solutions for the actual landing site can be determined (through navigation solutions using tracking data acquired after landing and/or reconstruction of the atmospheric entry trajectory). After the lander petals have been deployed, an initial estimate of lander orientation will be made using accelerometer measurements and IMP Sun search frames. These measurements will define the orientation of lander coordinates with respect to Mars local level coordinates. The accelerometers measure the local gravity vector which is assumed to be aligned with the radial vector from the lander towards Mars center. (Note that this assumption is only true for a sphere of uniform density, but the difference is fairly small in the vicinity of Pathfinder's chosen landing site.) This measurement establishes the direction of the Z_L-axis. The Sun search frames establish the direction of the X_L-axis. The lander flight software keeps track of the orientation of lander coordinates with respect to Mars local level coordinates and this is returned in engineering telemetry. This information may be updated by subsequent accelerometer and Sun search measurements after the initial sequence. Any additional measurement sequences will be commanded from the ground as necessary.

It is initially assumed that the Mars surface fixed frame shares the same origin as local level and lander coordinates. It is possible that the lander may change position after the initial accelerometer and Sun search imaging sequences. The origin of Mars surface fixed coordinates remains at the same location, fixed in the Mars body-fixed frame. The origin of local and lander coordinates moves with any subsequent translations of the lander.

Because the Z axes of local level and surface fixed coordinates differ, there will always be a rotation required to convert between them. Prior to landing, this transformation can be determined from the angle between the radius vector at the nominal landing site and the surface normal vector for the Mars reference ellipsoid at that point. The surface normal vector, also called the nadir vector, at the actual landing site may differ from this nominal

value.

As for the local level frame, an initial series of IMP sun search images and other images taken after lander deployment are used to determine the true relationship of surface fixed coordinates to Mars body-fixed coordinates and local level coordinates. Rotations and translations between local level and surface fixed coordinates that may result from lander motions after these initial measurements are determined from analysis of stereo images taken daily with the lander camera. This analysis will be performed by the Multi-Mission Image Processing System (MIPS).

The transformations required to convert between lander, Mars local level, and Mars surface-fixed coordinates will be available in appropriate NAIF SPICE kernel files. The MOS (Mission Operation System) flight team will be responsible for providing the rotation between lander and local level coordinates. A TBD party (MIPS or part of the IMP team?) will be responsible for providing the translation and rotations between surface fixed and local level coordinates. These transformations will be defined as time-varying functions. It is expected that these values will change most frequently in the first few days of surface operations. They should remain relatively stable after this, with infrequent updates possible for the duration of the mission.

It should be noted that the definition of surface fixed coordinates is currently being reviewed. Although the basic definition of the system's axes is not expected to change, there may be some changes in the methods used to determine its relationship with other frames such as the local level and Mars body-fixed frames. This section will be revised, if necessary, as soon as an agreement is reached by the appropriate team members.

Chapter 3

TIME SYSTEMS

There are several time systems that will be used for Pathfinder mission operations. Earth-based time systems are the most familiar. Historically these have all been tied to the diurnal rotation of the Earth and its yearly orbit around the sun. These are described in section 3.1. Similar time systems tied to rotation of a body can be defined for other planets. Pathfinder will make use of such Mars-based time systems for surface operations. Martian time systems are discussed in section 3.2. Finally, the spacecraft itself carries a clock to control the times at which it must perform certain actions. The relationship of spacecraft clock time to other time systems is explained in section 3.3.

3.1 Earth

The three major Earth-based time systems for Mars Pathfinder are

- Universal Coordinated Time

- Pacific standard or daylight time — the local time in Pasadena, California, where the mission operation center is located

- Dynamical (or ephemeris) time.

A short description of these systems is presented below. Much of the material has been taken from [6] and Chapter 2 of [7]. Refer to these documents for more complete explanations of these time systems.

3.1.1 Universal Coordinated Time

The fundamental unit of time in the SI system is the second which is now defined by the oscillation of the undisturbed cesium atom. <u>International Atomic Time</u> (TAI or atomic time) is a simply a count of atomic seconds that have occurred since the instant of midnight January 1, 1958 at the Royal Observatory in Greenwich, England. Atomic time is kept by the International Earth Rotation Service (IERS) in Paris, France.

Formerly, the second was based upon the rotation or the orbital motion of the Earth, which was determined by astronomical observation. Before 1960, it had been defined as a specified fraction of the mean solar day. Between 1960 and 1971, it was defined as a specified fraction of the year. As measurement accuracies increased, certain irregularities in the Earth's motion became apparent. At the same time, advances in physics led to the construction of precise atomic time standards. The new definition of the second was introduced to produce a more uniform measure of the passage of time.

Unfortunately, the calendar systems developed by humans to organize daily activities are all tied to astronomical phenomena such as Earth's rotation and its motion in orbit around the Sun. This means that there must be occasional adjustments between atomic time and the calendar systems to keep the calendar systems aligned with the current state of Earth's rotation (which we all personally observe).

<u>UT1</u> is tied to the true rotation of the Earth and is related to the prime meridian angle W. It is derived from the mean sidereal time at the Greenwich Observatory and determined by astronomical observations of stars and radio sources. Although it is angular in nature, it can be expressed using a calendar system having the familiar six components of year, month, day, hours, minutes, and seconds that specify an instant of time. Midnight is defined as 0 hours, minutes, and seconds, or 00:00:00. Due to irregularities in the Earth's rate of rotation, UT1 proceeds at a different rate than atomic time. This is done to keep a UT1 "day" close to the mean duration of the solar day. Hence, the conversion between UT1 and TAI is a constantly varying function.

<u>UTC</u>, or Universal Coordinated Time, is another angular system related to the rotation of the Earth where the rate is chosen to be the same as that of atomic time. One UTC second is the same as one SI second or one second of atomic time. UTC also uses the six components of year, month, day, hour, minute, and second to specify an instant in time. UTC is the basis for all civil time-keeping and has been defined to match as closely as possible with UT1. Ideally, UTC times where the hours, minutes, and seconds components are all 0 should correspond to Greenwich midnight of the same calendar day. However, it is not possible to match these exactly since the the Earth's rotation is irregular compared to the uniform rate of atomic time. UTC is occasionally adjusted to keep the difference between midnight in the two systems smaller than 0.9 seconds. The mechanism for this adjustment is the addition of leap seconds to UTC as discussed in the following paragraphs.

The hours and minutes components of UT1 or UTC are integers. The hours component may have any value between 0 and 23, while the minutes component may have any value from 0 to 59. The seconds component is a floating point number. For UT1, this component always ranges between 0 and 59.999.... For UTC, the seconds component normally ranges between 0 and 59.999.... Thus the usual progression of UTC times around midnight on January 1 of any given year is:

...	December	31	23:59:58
...	December	31	23:59:59
...	January	1	00:00:00

When Greenwich UT1 midnight lags behind UTC midnight by more than 0.7 seconds, the IERS will announce that a leap second will added, traditionally after the last "normal" UTC

second of December 31 or June 30. When a UTC leap second is added, the progression above includes a new entry as shown below:

...	December	31	23:59:58
...	December	31	23:59:59
...	December	31	23:59:60	← leap second inserted
...	January	1	00:00:00

Similarly, a negative leap second will be declared by IERS when Greenwich UT1 midnight runs of ahead of UTC midnight by more than 0.7 seconds. In this case, the last "normal" UTC second will be removed from the progression as:

...	December	31	23:59:57
...	December	31	23:59:58
			← leap second removed
...	January	1	00:00:00

Since 1972 when leap seconds and the UTC system were introduced, a negative leap second has not occurred.

UTC midnight actually falls in the nighttime portion of the day at Greenwich, England. However, it does not correspond to "the middle of the night" at other locations on Earth. The standard time zones have been introduced as local time systems around the globe. Offsets are chosen between UTC and the local system so that midnight in the local system occurs during the actual night in that region. JPL, in Pasadena, California, falls in the Pacific time zone. The difference between UTC and Pacific standard and daylight times is:

$$UTC = PST + 8 \text{ hours } (08:00:00)$$
$$UTC = PDT + 7 \text{ hours } (07:00:00)$$

Currently the change from PST to PDT occurs at 02:00 PST (03:00 PST) on the first Sunday in April and the change from PDT to PST occurs at 02:00 PDT (01:00 PST) on the last Sunday in October each year. Note that the offset between UTC and PST/PDT is a fixed, integral number of hours, so that any leap second changes are included in the official PST/PDT times. In other words, for a year where a leap second is added in December:

	UTC			PST				
...	December	31	23:59:58	December	31	15:59:58	
...	December	31	23:59:59	December	31	15:59:59	
...	December	31	23:59:60	December	31	15:59:60	← leap second inserted
...	January	1	00:00:00	December	31	16:00:00	

3.1.2 Dynamical Time

Dynamical time represents the independent variable in the equations of motion of bodies in the solar system. There are two forms of dynamical time: Barycentric Dynamical Time (TDB) and Terrestrial Dynamical Time (TDT). As their names imply, these two forms differ

in the center of the coordinate system to which they are referenced. TDT is associated with a geocentric coordinate system, while TDB is associated with the solar system barycenter. The existence of two forms of dynamical time and their relationship is a consequence of certain aspects of the theory of relativity. As far as measurements have been able to detect, TDT and TAI change at the same rate. The origin, or epoch, for TDT has been chosen so that TDT = TAI + 32.184 sec. Since UTC is directly tied to TAI, TDT can easily be converted to UTC once the corresponding TAI value is known.

TDB is the "atomic time" that would be measured if the atomic clocks were moved from Earth to the solar system barycenter. This is the time scale used in all navigation, trajectory, and ephemeris tasks at JPL. The planet ephemeris file and the spacecraft trajectory files produced by the navigation team will give positions and velocities as functions of TDB. For historic reasons, this is also referred to as ephemeris time or ET.[1] Due to relativistic effects, the atomic clocks at the two locations measuring TDB and TDT would appear to run at different rates at different times of the year. Thus, the difference between ET (TDB) and TDT is a periodic function whose value is always less than 0.002 seconds. For most purposes, this small difference can be safely ignored and ET (TDB) can be converted to TAI using the fixed offset of 32.184 seconds.

Precise conversions between UT1, TAI, and ET are required to reduce the radiometric navigation data. The small differences mentioned above cannot be neglected in orbit determination analyses. The time as measured by equipment at the DSN complex where the data is received must also be considered. A detailed formulation of the equations used for these conversions in the navigation software can be found in [11, 12].

Ephemeris time can be given as a count of ephemeris seconds (equivalent to atomic seconds) past the reference epoch of J2000. However, it is also desirable to use a calendar labeling for ephemeris time to make these times more readily recognizable to (most) humans. Calendar date and time strings assigned to instants of ephemeris time *are not* identical to those assigned to UTC instants. Leap seconds are not applied to ephemeris time, so that the seconds component always falls between 0 and 59.999.... Also, the offset from atomic time (32.184 sec) must be applied. The difference between UTC and ET at some instant is the sum of the constant offset of 32.184 seconds and the total number of leap seconds that have occurred up to that time. As of this writing (September, 1995), 29 (positive) leap seconds have been declared, the last one announced for the end of June, 1994. Thus, ET appears to be running ahead of UTC by 61.184 seconds, or $\Delta T = ET - UTC = 61.184$ sec. Figure 3-1 is a plot of changes in the value of ΔT from 1972 to the present. Predictions of additional leap seconds to 1998, the end of Pathfinder's extended mission, are also shown.

Another dating scheme frequently used by navigation is the Julian ephemeris date or JED. Julian dates are expressed as an integral number of Julian days and a fraction that corresponds to the time of day and indicates the portion of the day that has elapsed to that point. Integral values of Julian date have been defined to refer to instants of Greenwich mean noon The origin, or JED 0.0, is the day starting at Greenwich mean noon on 1 January 4713 B.C, Julian proleptic calendar. Thus, the reference epoch J2000 is the integer Julian

---

[1] This should not be confused with "ephemeris time" as defined in section 2.55 of [7]. In this document ephemeris time is synonymous with TDB.

Figure 3-1: Historical and Predicted Values for ΔT = ET - UTC

day 2451545, JED 2451545.0, or January 1, 2000 12:00:00 ET. There are 86400 seconds in a Julian day, 365.25 Julian days in a Julian year, and 100 Julian years or 36525 days in a Julian century. When converting Julian ephemeris dates to ET calendar date and time, the usual leap year conventions apply.

The following example illustrates the conversion between ET expressed as calendar date and time, seconds past the reference epoch, and JED. Let the target date be October 1, 1995 00:00:00.0 ET. The Julian year of 1995 is not a leap year, so it has 365 days. There are 92 of these days left at the beginning of October 1. The Julian year of 1996 is a leap year, so it has 366 days. The three remaining years to 2000 – 1997,1998, and 1999 – are not leap years and have 365 days each. Thus, there are 92 + 366 + 3(365) = 1553 Julian days to January 1, 2000 00:00:00.0 ET. Another 1/2 day must be added to reach J2000, so the target date becomes 2451545.0 - 1553.5 = 2449991.5 JED. The target date is 1553.5·86400 = 134222400 seconds prior to J2000, so October 1, 1995 00:00:00.0 ET corresponds to -134222400.0 seconds past J2000 ET. Finally, to convert from ET to UTC, which is always expressed as a calendar date and time, apply the appropriate value of ΔT. From July 1994 to the present, $\Delta T = 61.184$ sec. Hence, October 1, 1995 00:00:00 ET is September 30, 1995 23:58:58.816 UTC. The following times are all equivalent:

October 1, 1995 00:00:00.00 ET   2449991.5 JED
September 30, 1995 23:58:58.816 UTC   -134222400.0 seconds past J2000 ET

3.2   Mars

3.2.1   Seasons

The seasons of Mars are measured by the longitude of the Sun, L_s, with respect to the vernal equinox of Mars. The vernal equinox is defined as the intersection of the instantaneous orbital and equatorial planes of Mars. L_s is measured eastward from the vernal equinox *in the orbital plane of Mars* as shown in Figure 3-2. The beginning dates of the Martian seasons over the duration of Pathfinder's mission are listed in Table 3-1. Pathfinder is scheduled to land at a site in the northern hemisphere of Mars on July 4, 1997. $L_s = 143°$ on the landing day, placing Pathfinder's arrival late in the northern summer.

3.2.2   Local True Solar Time

Local true solar time, or LTST, is one of two types of Martian solar time used to express the time of day at a point on the surface of Mars. LTST is measured relative to the true position of the Sun as seen from a point on the planet's surface.

The coordinate system used to define LTST is a Mars Mean Equator and Equinox (MME) system similar to the EME frame. The frame's center is the center of the planet. The reference plane is the Mars mean equator of date, so that the Z-axis is the Mars north pole vector (or spin axis). The X-axis is chosen to point in the direction of the vernal equinox of Mars' orbit. The vernal or autumnal equinox vectors are found by searching the planetary ephemeris for those times where the vector from Mars' center to the Sun

Figure 3-2: Longitude of the Sun for Determining the Seasons of Mars

Date	Event	Season	L_s
August 26, 1996	Vernal Equniox	Northern Spring	0
March 13, 1997	Summer Solstice	Northern Summer	90
September 12, 1997	Autumnal Equinox	Southern Spring	180
February 6, 1998	Winter Solstice	Southern Summer	270
July 14, 1998	Vernal Equinox	Northern Spring	0
January 29, 1999	Summer Solstice	Northern Summer	90

(Event dates determined from DE403 planetary ephemeris.)

Table 3-1: Martian Seasons over Mars Pathfinder Mission

is perpendicular to Mars' north pole vector. The vernal equinox is the time where the Sun appears to rise above Mars' equator. The vernal equinox closest to Mars Pathfinder's landing date, as determined using the DE403 planetary ephemeris, occurs on August 26, 1996 19:50 ET. The Y-axis is chosen to complete a right-handed system.

Positions of points in the MME frame can be expressed as a radius and areocentric "right ascension" and "declination" angles. The areocentric right ascension angle, or ARA, is measured positve eastward in the Mars mean equator plane from the vernal equinox vector to the intersection of the meridian containing the point with the equator. Similarly, the areocentric declination is the angle between the Mars mean equator plane and the vector to the point. LTST is a function of the difference between the ARAs of the vectors to the Sun and to the point on the planet's surface. Specifically,

$$\text{LTST} = (\alpha_P - \alpha_{TS}) \frac{24}{360} + 12$$

where

LTST	=	the local true solar time in true solar hours
α_P	=	ARA of the point on Mars' surface in degrees
α_{TS}	=	ARA of the true sun in degrees

The conversion factor of 24/360 is applied to transform the angular measure in decimal degrees into hours-minutes-seconds of arc. This standard representation divides 360° into 24 hours, each hour into 60 minutes, and each minute into 60 seconds of arc. The hours, minutes, and seconds of arc are called "true solar" hours, minutes, and seconds when used to measure LTST. The constant offset of 12 hours is added to the difference in ARAs to place local noon (12:00:00 in hours, minutes, seconds) at the point where the Sun is directly overhead; at this time, the ARA of the true sun is the same as that of the surface point so that $\alpha_P - \alpha_{TS} = 0$. Figure 3-3 illustrates the use of ARA in defining LTST.

The calculation of the LTST at a given point on Mars at some UTC or ET time requires the determination of Mars' orientation in inertial space and its position along its orbit around the Sun at that time. Since the surface point rotates with the planet, the vector from Mars' center to the surface point is not constant in the MME frame. α_P is thus dependent on the rotation rate of Mars. α_{TS} depends on the apparent vector from Mars to the Sun as seen from the point on the surface, which must be obtained from the planetary ephemeris file.

The use of "true solar" time units can be extended to define a true solar day as 24 true solar hours. Due to the eccentricity of Mars' orbit and the inclination of its orbit plane to the equatorial plane (the obliquity for Mars), the Sun does not move at a uniform rate over the course of a Martian year. Consequently, the number of SI seconds in a true solar day, hour, minute or second is not constant. The length of a true solar day, defined as the difference in seconds between ET times corresponding to noon LTST on two consecutive days, varies in length by about 50 seconds over the course of a Martian year. Figure 3-4 shows the variation in the duration of the true solar day for the period of Pathfinder's nominal surface operations and for the first day in each month of the extended mission.

Figure 3-3: Local true solar time (LTST) from areocentric right ascensions in the MME frame

Figure 3-4: Length of Mars' true solar day over Pathfinder's mission

3.2.3 Local Mean Solar Time

The desire to work with solar days, hours, minutes, and seconds of uniform length led to the concept of the fictitious mean Sun or FMS. The FMS is a defined as a point that moves on the celestial equator of Mars at a constant rate that represents the average mean motion of the Sun over a Martian year. Local mean solar time, or LMST, is defined, by analogy with LTST, as the difference between the areocentric right ascensions of a point on the surface and of the FMS. The difference between LTST and LMST varies over time and is expressed as the difference in ARA between the FMS and the true sun. The term "equation of time" or EOT is used to refer to this difference. In other words, the value of EOT is the offset that must be added to LMST obtain the equivalent LTST (LTST = LMST + EOT).

Mathematical expressions for locating the FMS and calculating the EOT for Mars have recently been developed for use by the Mars Global Surveyor mission [8] and will be used for Mars Pathfinder as well. The ARA of the FMS, α_{FMS}, relative to the Mars vernal equinox of August 26, 1996 is given by

$$\alpha_{FMS} = 0.5240429 \, \Delta T$$

where α_{FMS} is measured in degrees, ΔT is the time from September 15, 1996 13:07 ET in days, and 0.5240429°/day is the average mean motion of the Sun around Mars. (Note that in this equation 1 day is 86400 SI seconds.) LMST is computed as

$$\text{LMST} = (\alpha_P - \alpha_{FMS}) \frac{24}{360} + 12$$

where

LMST	=	the local mean solar time in mean solar hours
α_P	=	ARA of the point on Mars' surface in degrees
α_{TS}	=	ARA of the FMS in degrees

The equation of time is simply

$$\text{EOT} = \alpha_{FMS} - \alpha_{TS}$$

where α_{FMS} is computed from the equation given above and α_{TS} is determined by querying the planetary ephemeris file for the apparent vector from Mars to the Sun at the desired time. Figure 3-5 illustrates the relationship between α_{TS}, α_{FMS}, and EOT when computing LMST. Figure 3-6 plots the value of EOT from Pathfinder's landing date to the end of the extended mission. True solar time varies from 40 solar minutes ahead to 51 solar minutes behind mean solar time over this period.

The length of a mean solar day is constant and can be computed from the mean motion of the FMS and the rotation rate for Mars given in section 5.3. The mean solar day is also called a "sol". Its duration in SI seconds is

$$
\begin{aligned}
1 \text{ sol} &= \frac{360°}{350.8919830°/\text{day} - 0.5240429°/\text{day}} \\
&= 1.02749127 \text{ days} \cdot 86400 \text{seconds/day} \\
&= 88775.245 \text{ seconds}
\end{aligned}
$$

Mean solar hours, minutes, and seconds can also be defined in the same way as the true solar units. Using the duration of the mean solar day given above, the mean solar time units are:

1 mean solar hour	=	3698.968 seconds
1 mean solar minute	=	61.649 seconds
1 mean solar second	=	1.02749127 seconds

Figure 3-5: Local Mean Solar Time from areocentric right ascensions in the MME frame

Figure 3-6: Equation of Time for Mars from July 4, 1997 to September 1, 1998 UTC

3.2.4   Pathfinder's Hybrid Solar Time

LTST is most relevant for Pathfinder since the spacecraft will land on the surface of Mars. Local environmental conditions such as thermal cycles experienced by the lander are functions of the true solar time at the landing site. Also, it may be desirable to schedule certain types of science observations when the true sun is at a certain position as seen from the lander. However, it is somewhat awkward to work with LTST for planning purposes since the planetary ephemeris file must be queried to determine LTST values that correspond to UTC or ET times. The variability of the true solar time units is another inconvenience when using LTST. To avoid these problems, a hybrid solar time — HST — is in use by some parts of the Pathfinder project. An epoch is chosen at a certain true solar time at the landing site on a given day. The corresponding UTC and ET are found from Mars' rotation model and the planetary ephemeris file. HST equals LTST at this epoch. Mean solar time units are then used to propagate HST values away from the epoch. At any given instant of time expressed as UTC or ET, the difference between this time and the HST epoch is computed in ET seconds. This is then converted to an interval in mean solar seconds by dividing by 1.02749127 seconds/mean solar second. The offset in mean solar seconds is then added to the LTST of the epoch to obtain the HST value corresponding to the given UTC or ET.

Obviously, HST is only an approximation of LTST. The accuracy of the approximation depends on the length of the interval from the hybrid time epoch to the time of interest and on the rate of change in the EOT for Mars during the interval. From Figure 3-6, the rate of change in EOT is fairly slow over the first 30 days representing Pathfinder's nominal mission. If the HST epoch is chosen at LTST noon on July 4, 1997 (01:30:35.174 UTC), the difference between HST and LTST is only 4.6 solar minutes near the end of the nominal mission on August 3, 1997 00:00 UTC. The rate of change in EOT is significantly larger over the months of the extended mission. Keeping the HST epoch at LTST noon on the landing day results in differences of up to 82 solar minutes between HST and LTST as shown in Figure 3-7. Clearly, the HST epoch must be updated to keep the difference between HST and LST at a reasonable level.

As an example of a limiting the deviation of HST from LTST, a schedule of HST epoch updates has been developed to maintain $|HST - LTST| \leq 5$ solar minutes. The frequency of the epoch changes and the duration of the intervals over which HST was propagated from each epoch were chosen based on the rate of change in the EOT for Mars. The schedule of HST epoch updates over the 424-day period from July 4, 1997 00:00 UTC to September 1, 1998 00:00 UTC, covering Pathfinder's nominal and extended missions, is summarized below:

Mission Period	HST Epoch Update Frequency
0 — 115 days	30 days
115 — 155 days	10 days
155 — 260 days	7 days
260 — 290 days	10 days
290 — 310 days	20 days
310 — 340 days	30 days
340 — 360 days	20 days
360 — 424 days	10 days

A list of the selected epochs, all chosen at LTST noon on the corresponding UTC day, is given in appendix B. Figure 3-8 plots HST − LTST when the HST epoch is updated according to this schedule. The magnitude of this difference is always less than 5 solar minutes, as desired.

In summary, care must be exercised when using HST as an approximation to LTST. The HST epoch and the propagation interval must be properly selected if the deviation between HST and LTST is to be kept within some desired bounds. An epoch of LTST noon on Pathfinder's landing day can be used to keep HST within 5 solar minutes of LTST over the 30-sol nominal mission. The HST epoch update strategy discussed above can be used as a guideline to maintain HST within 5 solar minutes of LTST during the extended mission. More frequent epoch updates will be required to obtain agreement of less than 5 solar minutes.

3.3   Spacecraft Clock

The Mars Pathfinder spacecraft carries an onboard clock used to control various spacecraft activities. The Pathfinder clock functions similarly to the Mars Observer and Cassini clocks. Time tags indicating the spacecraft clock time associated with various events are included in the downlink telemetry stream. A spacecraft clock time, or SCLK, for Mars Pathfinder takes the form:

$$SSSSSSSSSS.FFF$$

where

SSSSSSSSSS	is (approximately) the number of integer seconds
FFF	indicates the fractional seconds as an integer number of 1/256 second increments

The spacecraft clock hardware stores the integer seconds using 32 bits. Thus the maximum number of integer seconds that can be represented, or the maximum value for SSSSSSSSSS, is 4,294,967,295. The fractional seconds are stored using 16 bits, but only the most significant 8 bits are used to construct the time tags returned in the downlink. This means that FFF represents a modular count of 1/256-second units and its maximum value is 255. The maximum SCLK value for MPF — 4294967295.255 — is approximately 136 years.

Figure 3-7: Deviation of HST from LTST for a single epoch on July 4, 1997

Figure 3-8: Deviation of HST from LTST for a schedule of multiple epoch updates

Since the spacecraft clock hardware is not as accurate as the atomic clocks and other high-precision timing devices available on Earth, the rate at which it runs varies over time. As a consequence, the relationship between SCLK and ET or UTC is usually a nonlinear function. In practice, this function is approximated as a piecewise linear function. In other words, the conversion between SCLK and ET or UTC is represented as

$$T = T_i + \rho_i \, (\text{SCLK} - \text{SCLK}_i)$$

over the interval $\text{SCLK}_i \leq \text{SCLK} < \text{SCLK}_{i+1}$ where

SCLK	$=$	the spacecraft clock time to be converted
T	$=$	the ET or UTC time corresponding to SCLK
ρ_i	$=$	the clock rate over the interval
T_i	$=$	the ET or UTC time mapped to SCLK_i

Similarly,

$$\text{SCLK} = \text{SCLK}_i + \frac{T - T_i}{\rho_i}$$

over the interval $T_i \leq T < T_{i+1}$. The clock rate ρ_i is given in units of

$$\frac{\text{SI seconds}}{\text{SCLK primary units}} = \frac{\text{seconds of UTC, ET, TAI}}{1 \text{ tick of the SSSSSSSSS portion of SCLK}}$$

Ideally, $\rho_i \equiv 1.0$ for all i. The values of SCLK_i, T_i, and ρ_i for $i = 1, \ldots, n$ are maintained in a file for use by ground software.[2] The same equation is applied for $\text{SCLK} \geq \text{SCLK}_n$ or $T \geq T_n$ with $i = n$. When T is UTC, it is typically referred to as <u>spacecraft event time</u> or SCET.

The following convention for converting between SCLK and UTC times have been adopted for development and simulation purposes. The "zero point" or epoch for spacecraft clock time has been chosen to be near January 1, 1958 00:00:00 ET, which is close to the epoch of TAI. As of this writing, the last leap second was added on June 30, 1994. 1,151,712,000 seconds of ET have elapsed between January 1, 1958 00:00:00 ET and July 1, 1994 00:00:00 ET. But, ET is currently running ahead of UTC by 61.184 seconds, so that July 1, 1994 00:00:00 UTC is about 1,151,712,061 seconds from January 1, 1958 00:00:00 ET. Therefore, SCLK is "set" to the value 1151712061:000 at July 1, 1994 00:00:00 UTC. It is further assumed that the spacecraft clock rate is the same as that of atomic time. The entries in the SCLK coefficients file are:

SCLK_1	$=$	1151212061:000
T_1	$=$	July 1, 1994 00:00:00 UTC
ρ_1	$=$	1.00

---

[2]In the NAIF system, this file is called the SCLK kernel file. The MPF GDS software has a similar file called the SCLK_SCET file. There are also utility routines supplied by both these groups that automate the conversion between SCLK and UTC/ET. It is strongly recommended that these existing routines be accessed by any application software that requires this conversion.

Using the equation given above, the time July 4, 1997 12:00:00 UTC, on Pathfinder's landing day, becomes:

$$\text{SCLK} = 1151212061.000 + \frac{\text{July 4, 1997 12:00:00 UTC - July 1, 1994 00:00:00 UTC}}{1.00}$$

$$= 1151212061.000 + 94996800.000$$

$$= 1246708861.00$$

The approximate range of SCLK from launch to the end of the nominal mission is:

Event	UTC	SCLK
Start of Nominal Launch Window	December 2, 1996 00:00:00	1228176061.000
End of Primary Surface Operations	September 1, 1997 00:00:00	1251763261.000

Note that this ignores any leap seconds that may be announced in the future.

The initial operational setting of the spacecraft clock will be done to correspond as closely as possible to the mapping described above. Calibrations will be performed to precisely determine the mapping between the initial SCLK and UTC and the initial clock rate. Periodic calibrations will be performed in flight to update this mapping and to measure any drift in the rate at which the spacecraft clock is proceeding relative to atomic time. The set of triples $\text{SCLK}_i, \text{T}_i, \rho_i$ will be updated as needed. This includes updates due to leap seconds that may occur over the mission duration. The responsibility for maintaining the SCLK file for Pathfinder is TBD, but it is expected that this service will be performed by the Multi-Mission Data Management group of section 391.

Chapter 4

EARTH DATA

4.1 Mass & Gravity Field

4.1.1 Earth GM

The value for the gravitational parameter (GM) for Earth, or the product of the universal gravitational constant (G) and the mass of Earth $(M_\oplus)$, is taken from the JPL planetary ephemeris DE403 [9] and is given below:

$$GM_{\oplus\,DE403} = 398600.436 \text{ km}^3/\text{sec}^2$$

Using the value $G = 6.67259 \times 10^{-20} \text{ km}^3/\text{sec}^2 \text{ kg}$, the corresponding mass of Earth is

$$M_{\oplus\,DE403} = 5.9737 \times 10^{24} \text{ kg}$$

Using Newton's laws, the gravitational acceleration at the surface of the Earth can be computed from the planet's GM and its equatorial radius (given in section 4.2.1):

$$
\begin{aligned}
g_\oplus &= \frac{GM_{\oplus\,DE403}}{R^2_{\oplus\,EQRTL\,IAU}} \\
&= \frac{398600.436\,\text{km}^3/\text{sec}^2}{(6378.14\,\text{km})^2} \\
&= 9.798 \times 10^{-3}\,\text{km}/\text{sec}^2 \\
&= 9.798\,\text{m}/\text{sec}^2
\end{aligned}
$$

This is commonly called $1g$.[1] The equivalent value for Mars is 3.719 m/sec^2 (from section 5.1.1). Thus, Mars' gravitational acceleration is $0.379g$, about 62% less than that of Earth.

---

[1]The standard value for $1g$ is usually given as 9.80665 m/sec^2. This is actually the value of g at sea level and latitude 45°.

4.1.2   Gravity Field Model: JGM-3

Many complex models have been developed for Earth's gravity field, primarily for use in orbit determination for Earth-orbiting spacecraft. Most of these express the gravitational potential field as a series expansion of associated Legendre polynomials. Each polynomial has a set of associated harmonic coefficients. The model provides the values and associated uncertainties for these coefficients for a fixed limit of degree and order of the associated Legendre polynomials. Currently, the best available Earth gravity field model is the JGM-3 model which is includes terms up to degree and order 70. This model is being used for TOPEX/POSEIDON orbit determination solutions [15]. The Earth GM value associated with the JGM-3 gravity field is

$$GM_{\oplus JGM-3} = 398600.4415 \, \text{km}^3/\text{sec}^2$$

This is in close agreement with the value given for DE403 shown in the preceding section. Since Mars Pathfinder will not orbit the Earth before being injected onto its interplanetary trajectory, it will not be necessary to employ the full 70×70 gravity field for Pathfinder navigation solutions. A truncation to degree and order 20 will be more than sufficient for Pathfinder navigation purposes. Values for the harmonic coefficients of this truncated version of JGM-3 can be found in Appendix A.1, Table A-1 and Table A-2.

4.2   Topographic Data

4.2.1   IAU Reference Spheroid

The IAU reference surface for Earth is an oblate spheroid with the mean equatorial and polar radii values shown below [5]:

$$
\begin{aligned}
R_{\oplus EQTRL\,IAU} &= 6378.14 \quad \text{km} \\
R_{\oplus POLAR\,IAU} &= 6356.75 \quad \text{km}
\end{aligned}
$$

These radii correspond to a flattening coefficient of

$$f_{\oplus} = \frac{R_{\oplus EQRTL} - R_{\oplus POLAR}}{R_{\oplus EQTRL}} = 0.00335364 \, \text{or} \, \sim 1/298.18$$

4.2.2   Launch Site

Mars Pathfinder will be launched from Launch Complex 17 A at Cape Canaveral Air Station, Florida in December of 1996. The launch vehicle is the McDonnell Douglas Delta II 7925. The location of the launch site in the geocentric, body-fixed frame in latitudinal coordinates is:

Radius	6373.329364	km
Latitude	28.285577	°
Longitude	80.565299	°W

50

Station	Antenna Size	X (m)	Y (m)	Z (m)
		Goldstone		
DSS14	70m	-2353621.29	-4641341.53	+3677052.36
DSS15	34m	-2353538.83	-4641649.49	+3676670.03
		Canberra		
DSS43	70m	-4460894.66	+2682361.55	-3674748.50
DSS45	34m	-4460935.32	+2682765.71	-3674381.32
		Madrid		
DSS63	70m	+4849092.62	-360180.52	+4115109.15
DSS65	34m	+4849336.70	-360488.81	+4114748.82

Station	Antenna Size	Radius (km)	Latitude (°)	Longitude (°)
		Goldstone		
DSS14	70m	6371.993	+35.244	243.110
DSS15	34m	6371.966	+35.240	243.113
		Canberra		
DSS43	70m	6371.689	-35.221	148.981
DSS45	34m	6371.676	-35.217	148.978
		Madrid		
DSS63	70m	6370.051	+40.241	355.752
DSS65	34m	6370.022	+40.237	355.749

Table 4-1: Geocentric Coordinates of DSN Stations at epoch 1995.0

4.2.3 Deep Space Network Station Sites

Mars Pathfinder will use X-band frequencies for radiometric tracking and telecommunications. The spacecraft will be tracked using antennas at the three Deep Space Network (DSN) sites in Goldstone, California; Madrid, Spain; and Canberra, Australia. The radiometric tracking data will be acquired primarily through the 34-meter high-efficiency (HEF) stations at these sites. The 70-m stations will also be used for some portions of the mission. The locations of these stations expressed as Cartesian and latitudinal coordinates in a geocentric, body-fixed frame are listed in Table 4-1. These coordinates represent the current best estimate of station locations to match the DE403 planetary ephemeris [14]. These locations are subject to update and will be revised as further reports are issued.

4.3   Orientation & Rotation

A wealth of observational data has been obtained on the orientation of Earth's north pole and its rotation. Very sophisticated models have been developed that account for both large and small variations seen in the observations. One of these models that includes precession, nutation, and Earth's crustal motions is used in navigation computations. This model is based on extensive and precise observations of Earth's polar motion and rotation; the parameters describing crustal motion are updated frequently. This model is intimately tied to the timing systems models. More accurate models are needed for these quantities for Earth since the observation platforms for navigation tracking data — the DSN stations — are situated on Earth's surface. Descriptions of the navigation models for timing and polar motion can be found in [10, 11, 12].

The IAU has defined a simpler, approximate model for Earth's orientation and rotation [5]. This model is presented below and should be sufficient for most purposes other than spacecraft navigation tasks.

4.3.1   Earth Rotation Pole

The IAU has defined the right ascension and declination of the Earth mean north pole, or spin axis, as the following linear function of time in the EME2000 coordinate system [5]:

$$\alpha_\oplus = 0.00 - 0.641\,T$$
$$\delta_\oplus = 90.00 - 0.557\,T$$

where

$\alpha_\oplus$ = right ascension of the Earth spin axis in degrees (°)
$\delta_\oplus$ = declination of the Earth spin axis in degrees (°)
T = interval in Julian centuries from the epoch J2000(1 Julian century = 36525 days)

4.3.2   Earth Prime Meridian & Rotation Rate

The IAU has defined the location of the prime meridian of Earth by specifying an angle $W_\oplus$ that is measured along the Earth mean equator of date eastward from the ascending node of the Earth's mean equator *of date* on its mean equator *of J2000* to the point where the prime meridian crosses the Earth's mean equator of date. The following linear function of time gives the value for the angle $W_\oplus$ [5]:

$$W_\oplus = 190.16 + 360.9856235\,d$$

where $W_\oplus$ is measured in degrees (°) and

d = interval in days from the epoch J2000

The factor multiplying d in this equation is the mean rotation rate of Earth:

$$\dot{W}_\oplus = 360.9856235°/\text{day}$$

Thus the length of Earth's day - the mean rotation period - is 0.9973 days. The prime meridian (0° longitude) is defined physically to pass through Greenwich, England.

Chapter 5

MARS DATA

This section contains those constants and models describing the planet Mars in use by the Pathfinder project. Overall physical properties such as mass, size, and shape along with a general model for atmospheric properties such as density are presented. Localized properties such as expected temperatures, winds, etc. at the Pathfinder landing site are also included.

5.1 Mass & Gravity Field

5.1.1 Mars GM

The value for the gravitational parameter (GM) for Mars, or the product of the universal gravitational constant (G) and the mass of Mars (M_σ), is taken from the JPL planetary ephemeris DE403 [9] and is given below:

$$GM_{\sigma\,DE403} = 42828.314\,\mathrm{km}^3/\mathrm{sec}^2$$

Using the value $G = 6.67259 \times 10^{-20}\mathrm{km}^3/\mathrm{sec}^2\,\mathrm{kg}$, the corresponding mass of Mars is

$$M_{\sigma\,DE403} = 6.4185 \times 10^{23}\,\mathrm{kg}$$

Using Newton's laws, the gravitational acceleration at the surface of Mars can be computed from the planet's GM and its equatorial radius (given in section 5.2.1):

$$
\begin{aligned}
g_\sigma &= \frac{GM_{\sigma\,DE403}}{R_{\sigma\,EQRTL\,IAU}^2} \\
&= \frac{42828.314\,\mathrm{km}^3/\mathrm{sec}^2}{(3393.4\,\mathrm{km})^2} \\
&= 3.719 \times 10^{-3}\,\mathrm{km/sec}^2 \\
&= 3.719\,\mathrm{m/sec}^2
\end{aligned}
$$

The equivalent value for Earth, commonly called $1g$, is 9.798 m/sec^2 (from section 4.1.1). Thus, Mars' gravitational acceleration is $0.379g$, about 62% less than that of Earth.

5.1.2 Gravity Field Model: Mars50c

The gravity field model adopted by the Mars Pathfinder project is the Mars50c model recently developed by B. Sjogren and A. Konopliv at JPL. A complete description of this model and its derivation can be found in [17]. The gravitational potential field is expressed as a series expansion of associated Legendre polynomials. Each polynomial has a set of associated harmonic coefficients. The model provides the values and associated uncertainties for these coefficients for a fixed limit of degree and order of the associated Legendre polynomials. The Mars50c solution is a complete gravity field to degree and order 50, including solutions for the gravitational mass of Mars and its satellites. The data set for this solution includes Doppler tracking data from Mariner 9 and Vikings 1 and 2. The Mars GM value obtained with the Mars50c solution is

$$GM_{\mars\, Mars50c} = 42828.370371\,\text{km}^3/\text{sec}^2$$

This is in close agreement with the value given for DE403 shown in the preceding section. Values for the harmonic coefficients can be found in Appendix A.2, Table A-3 and Table A-4. Note that it will not be necessary to use the full 50×50 gravity field for MPF navigation purposes. Since Pathfinder will enter the Mars atmosphere and land directly from its interplanetary trajectory, only a truncated gravity field model will be applied in MPF orbit determination solutions. The 50×50 model is needed for navigation of orbiting spacecraft such as MGS. The full gravity field model is presented here for completeness.

5.2 Topographic Data

5.2.1 Reference Surfaces

A triaxial ellipsoid or an oblate spheroid is frequently employed as the shape model for Mars. However, the surface of Mars is more irregular than that of Earth, so there are several slightly different ellipsoids used for different purposes. Chapter 1 of [22] gives radii for a general triaxial ellipsoid model; the USGS has defined an oblate spheroid for mapping purposes as presented in chapter 5 of [1]. The IAU report [5] also gives an oblate spheroid as the reference surface for Mars. The polar and equatorial radii for this surface, given in the next section will be the reference surface for Mars Pathfinder. Note that these values are taken from the text of section 3 and are slightly different from the radii for the "best-fit" spheroid for Mars given in Table IV of [5]. There is also a reference surface defined for the Mars-GRAM atmosphere model as discussed in section 5.4.

IAU Reference Spheroid

The IAU reference surface for Mars is an oblate spheroid with the mean equatorial and polar radii values shown below [5]:

$$R_{\mars\, EQRTL\, IAU} = 3393.4\ \text{km}$$
$$R_{\mars\, POLAR\, IAU} = 3375.8\ \text{km}$$

These radii correspond to a flattening coefficient of

$$f_\sigma = \frac{R_{\sigma\,EQRTL} - R_{\sigma\,POLAR}}{R_{\sigma\,EQTRL}} = 0.005186 \text{ or } \sim 1/192.81$$

5.2.2   Landing Site

The nominal landing site chosen for Mars Pathfinder is located at the outflow of a catastrophic flood system in the Ares Valles region of Chryse Planitia. The position of the landing site in Mars body-fixed coordinates is given in Table 5-1 along with the locations of the two Viking landers [13].

Viking 1 - Chryse Planitia		
Areocentric Radius	3389.32 km	±0.06 km
Areocentric Latitude	22.269°	±0.003°
Areographic Latitude	22.480°	±0.003°
Longitude (positive West)	47.968°	0.1°
Viking 2 - Utopia Planitia		
Areocentric Radius	3381.86 km	±0.06 km
Areocentric Latitude	47.669°	±0.003°
Areographic Latitude	47.967°	±0.003°
Longitude (positive West)	225.737°	±0.1°
Mars Pathfinder - Ares Valles, Chryse Planitia		
Areocentric Radius	3377.7 km	
(to surface of IAU reference spheroid)		
Areocentric Latitude	19.5°	
Areographic Latitude	19.688°	
Longitude (positive West)	32.8°	

Table 5-1: Mars Pathfinder & Viking Landing Site Locations

5.3   Orientation & Rotation

5.3.1   Mars Rotation Pole

The IAU has defined the right ascension and declination of the Mars north pole, or spin axis, as the following linear function of time in the EME2000 coordinate system [5]:

$$\alpha_\sigma = 317.681 - 0.108\,T$$
$$\delta_\sigma = 52.886 - 0.061\,T$$

where

α_σ = right ascension of the Mars spin axis in degrees (°)

δ_σ = declination of the Mars spin axis in degrees (°)

T = interval in Julian centuries from the epoch J2000
(1 Julian century = 36525 days)

5.3.2   Mars Prime Meridian & Rotation Rate

The IAU has defined the location of the prime meridian of Mars by specifying an angle W_σ that is measured along the Martian equator eastward from IAU-vector of epoch J2000 to the point where the prime meridian crosses the Martian equator. Recall that the IAU-vector is defined as the vector pointing to the ascending node of the Martian equator on the Earth Mean Equator of J2000. The following linear function of time gives the value for the angle W_σ [5]:

$$W_\sigma = 176.901 + 350.8919830\, d$$

where W_σ is measured in degrees(°) and

$$d = \text{interval in days from the epoch J2000}$$

The factor multiplying d in this equation is the rotation rate of Mars:

$$\dot{W}_\sigma = 350.8919830\,°/\text{day}$$

Thus the length of the Martian day - the rotation period - is 1.026 days. The prime meridian (0° longitude) is defined physically to bisect the crater Airy-0 which is located at about 5° South latitude. Refer to Figure 2-7 for an illustration of the angles α_σ, δ_σ, and W_σ. Figure 5-1 below depicts the same relationship from a slightly different viewpoint.

5.4   Atmosphere

Two principal Mars atmosphere models are in use by the Pathfinder project: the Mars Global Reference Atmospheric Model (Mars-GRAM) [19] and a hydrostatic equilibrium model [21]. Version 3.0 of Mars-GRAM has been used for analyses prior to October of 1995. Mars-GRAM has recently been updated and the current version is now 3.33. Mars-GRAM includes mean density, temperature, pressure, and wind profiles along with statistical perturbation magnitudes for density variations. Diurnal, seasonal, and positional (i.e. dependent on latitude and longitude) variations can be simulated. Additional effects due to local and global dust storms, solar flux, and terrain-influenced atmospheric waves are also available. Mars-GRAM is based on data collected from the Mariner and Viking missions.

Mars-GRAM has its own reference ellipsoid which is used to compute "absolute" altitude above the planet's surface. This is a true ellipsoid, not an oblate spheroid – the two equatorial radii are not equal. The ellipsoid radii for the Mars-GRAM reference ellipsoid are

$$R_{\sigma\,X-EQRTL\,Mars-GRAM} = 3393.67\ \text{km}$$
$$R_{\sigma\,Y-EQRTL\,Mars-GRAM} = 3393.21\ \text{km}$$
$$R_{\sigma\,POLAR\,Mars-GRAM} = 3376.78\ \text{km}$$

Figure 5-1: Mars Spin Axis Right Ascension and Declination and Mars Prime Meridian

A terrain model is also included and is used to compute "terrain" altitude.

The full formulation of Mars-GRAM is too complex to be duplicated here. Mean values of density, pressure, and temperature as a function of altitude above the reference ellipsoid are plotted in Figures 5-2 to 5-5.[1] Figure 5-3 shows 1σ high and low density variations from the mean as a function of altitude. The altitude limit for these plots is 125 km, which defines the atmospheric entry interface for Mars Pathfinder. See [19] for further details or contact Dave Spencer for the Mars-GRAM software.

Recent observations of Mars have indicated that its atmosphere is significantly cooler and has a lower dust content than was measured at the time of the Viking landings. Another atmosphere model based upon a hydrostatic equilibrium atmosphere formulation has been developed which is correlated to the more recent data [20, 21]. Given a value for surface pressure and a profile of temperature variation as a function of altitude above the surface, pressure and density profiles are constructed using the hydrostatic equation and the ideal gas law. The temperature profiles used for this model are taken from the Clancy atmosphere model mentioned in [20] and reflect the more recent measurements. The reference ellipsoid shape used to define the surface when computing altitudes is the same as that used for Mars-GRAM. This hydrostatic model will be used in the upcoming simulations of Pathfinder's EDL trajectory.

The temperature profile generated by the hydrostatic equilibrium atmosphere model consists of six linear segments joined at particular "breakpoint" altitudes. The breakpoint altitudes are chosen to reflect discontinuities in the Clancy and Mars-GRAM temperature profiles. Temperature is assumed to change at a constant lapse rate in each layer bounded by two consecutive breakpoint altitudes. The assumed temperature at the surface of the reference ellipsoid is taken from the Clancy model. Near the surface, the temperature increases with altitude at a rate of $2.5°K/km$. Surface temperature at the Pathfinder landing site is computed using this rate and its assumed altitude above the ellipsoid. Temperatures at the breakpoint altitudes for the next two layers above the landing site are also computed using this rate and their altitude difference from the previous layer, along with the addition of a fixed temperature offset. Bounding temperatures for the remaining layers are computed using only a fixed offset from the temperature of the preceding layer. The temperature lapse rate within a layer is computed as the slope of a line segment defined by its bounding breakpoint altitudes and temperatures. See Table 1 of [21] for a list of the breakpoint altitudes and the corresponding temperature values.

Pressures are computed using the hydrostatic equation for an ideal gas at a constant temperature:

$$p_2 = p_1 \exp\left(\frac{m\, g(z_1 - z_2)}{R\, T}\right)$$

where

---

[1]The spikes seen in the pressure curve of Figure 5-4 at larger altitudes are an artifact of the Mars-GRAM software and do not represent actual pressure variations.

Figure 5-3: Mars-GRAM 1σ density variations from mean

Figure 5-4: Mars-GRAM mean pressure as a function of altitude

Figure 5-6: Mean temperature as a function of altitude for Mars-GRAM, Clancy, and hydrostatic equilibrium models

Figure 5-7: Mean pressure variation from Mars-GRAM value as a function of altitude for the hydrostatic equilibrium atmosphere model

Figure 5-8: Mean density variation from Mars-GRAM value as a function of altitude for the hydrostatic equilibrium atmosphere model

5.5   Local Surface Environment

The Pathfinder lander and rover will conduct various engineering and scientific investigations on the surface of Mars for a period of about 30 Martian days following the landing on July 4, 1997. An extended mission of continuing surface operations out to August 1998 is also possible. Appropriate design of lander systems and successful coordination of activities on the surface requires knowledge of the local surface environment likely to be experienced at the Pathfinder landing site.

Pathfinder arrives at Mars in the late northern summer when $L_s \sim 143°$ (see section 3.2.1 for a definition of L_s and its relationship to Martian seasons). The spacecraft is expected to land in the Ares Tiu outflow area at 19.5°N latitude and 32.8°W longitude. At this time of year, the seasonal surface pressure cycle is at a minimum, temperatures at the landing site are at a maximum, and the atmosphere is expected to be relatively free of dust. Probabilities for global dust storms increase to a maximum several months later in the early southern summer, although these storms do not occur every year. There was, however, a global dust storm in 1994, whose effects extended over $L_s = 200 - 300°$.

This section gives predictions of the Mars surface environmental conditions expected after Pathfinder's landing and describes environmental models currently used by project engineering teams. It concentrates on the period immediately after landing, but some information is presented on variations expected throughout the Martian year. The topics discussed include surface pressure, temperature, winds, dust content, insolation, local slopes, and rock distribution. Most of the material presented here is taken directly from references [23] and [24]. The information on local slopes and rock distribution has been updated to reflect more recent analyses.

The Viking landers provided the best records of surface conditions at two very different latitudes and elevations on Mars. Viking 1 at 22.5°N, 48.0°W is the most relevant to Pathfinder, as it is at a very similar latitude and altitude. Much of the data and many of the models described in the following sections are derived from Viking 1 measurements.

5.5.1   Surface Pressure

Viking 1 provided excellent records of surface pressure. Variations in daily mean pressures and standard deviations in pressure about the daily mean for the first Viking 1 year are shown in Figure 5-9 as a function of day number and L_s [25]. An enhanced version of this plot that also includes Viking 2 data is shown in Figure 5-10 [26, 27][2] The annual pressure cycle is near a minimum at $L_s = 143°$ with daily mean pressures of 6.85 mbar and daily fluctuations in pressure of ± 0.1 mbar (1σ). During dust storms these fluctuations can increase by a factor of 3-4. Actual daily pressure variations near $L_s = 143°$ during the first Viking 1 year are shown in Figure 5-11(a) [28]. Viking 1 obtained pressure data for 4 Mars years. These data indicate that year-to-year changes at $L_s = 143°$ are small compared with the daily cycle.

---

[2]This plot was obtained from James Tillman's web page on Martian Meteorology, which can be accessed at the URL http://www.atmos.washington.edu/local-httpdocs/mars-meteorology.html.

Daily mean surface pressures at the Pathfinder lander site can be accurately related to Viking 1 surface pressures by the approximate expression:

$$P_P(t) = P_{V_1}(t)e^{-\Delta z/H}$$

where

$P_P(t)$ is the mean surface pressure at the Pathfinder lander site at time t in the Mars year

$P_{V_1}(t)$ is the Viking 1 mean surface pressure at the same time

Δz is (Pathfinder-Viking 1) altitude relative to the Mars reference surface

H is the atmospheric pressure scale height appropriate to the lower few km of the Martian atmosphere.

H is computed as

$$H = RT/mg$$

where

R is the gas constant

T is temperature

g is the local acceleration due to gravity on Mars (given in section 5.1.1.)

m is the mean atmospheric molecular weight

As $\Delta z \approx -0.2$ km and $H \approx 10$km, Pathfinder pressures are expected to be approximately 2% higher than those recorded by Viking 1. This is not a very significant increase over the surface pressure models recommended in [23] which were taken directly from Viking 1.

5.5.2 Surface Temperature

Surface and near surface atmospheric temperatures relevant to the Pathfinder lander are determined by the balance between surface heating and cooling and are only weakly influenced by the overlying atmosphere. Under clear conditions, the daily temperature cycle varies with season and the albedo, emissivity, and thermal inertia of the surface. Although local surface properties are unknown for Pathfinder, large-scale albedo, emissivity, and thermal inertia are similar at the Viking 1 and Pathfinder landing sites, so that the Viking temperature record provides the best nominal model for Pathfinder. During global dust storms, high dust opacities reduce the amplitude of the daily temperature cycle dramatically. Daytime maxima fall significantly, nighttime minima rise somewhat, and daily mean temperatures fall.

The Viking 1 lander monitored temperatures 1.6 m above the surface, and surface brightness temperature variations were measured by the Viking orbiter Infrared Thermal Mapper (IRTM) instrument. Figure 5-11(b) shows daily atmospheric temperature cycles

at 1.6 m near $L_s = 143°$ [28]. Clearly these cycles are quite repetitive. In Figure 5-12, a nominal daily temperature cycle at 1.6 m is compared with measured maxima and minima for the whole Martian year and for high dust optical depths of 3.0 and 5.0 [23]. Figure 5-13, taken from [30], shows a 15-day average of the daily variation of the difference between atmospheric temperature at 1.6 m and surface temperature near $L_s = 120°$ at the Viking 1 lander site. For clear conditions, this difference is not expected to vary significantly with season and can be applied to $L_s = 143°$.

From the model in [29], daily surface temperatures variations at the Pathfinder lander site near $L_s = 143°$ are expected to range from 176 to 276°K, whereas annual extremes lie between 173 and 281°K. These values are derived from the thermal model of [29]. Margins of ±5 K in the minimum and ±10 K in the maximum for daily surface and near surface atmospheric temperature extremes are recommended, due primarily to likely differences in surface albedo and thermal inertia between the Pathfinder and Viking 1 lander sites.

5.5.3 Surface Winds

Near surface winds vary in speed and direction with weather, time of day, and season. Figure 5-14 shows the daily variation of wind speed and direction recorded by Viking 1, near $L_s = 143°$, 1.6 m above the surface [28]. These variations are fairly repetitive and are determined primarily by large-scale surface slopes, with maximum winds blowing downslope near noon. Surface slopes at the Pathfinder lander site are not well known but are likely to be comparable with or less than those at the Viking 1 lander site. Based on these data, Pathfinder can be expected to encounter sustained daytime winds of 2–8 m/sec with a mean of 4 m/sec and sustained nighttime winds of 0–3 m/sec with a mean of 1 m/sec in the days following the landing.

From [28], peak sustained winds during the daytime reach 12 m/sec approximately 15 days after the landing, but fall below 8 m/sec for the following 35 days. The maximum sustained winds observed at Viking lander 1 later in the year were 25 m/sec [23].

5.5.4 Dust Optical Depth

The variation of dust optical depth at 0.6 μm at the Viking lander sites is shown in Figure 5-15 [31]. Near $L_s = 143°$ and away from global dust storm periods, background dust optical depths lie in the range 0.3 - 0.5. However recent observations of Mars suggest that conditions are now clearer with background optical depths in the range 0.1 - 0.2 [32]. A most probable optical depth of 0.2 with a likely range of 0.1 to 0.5 is therefore recommended.

Estimates of probable optical depth are complicated by the occurrence of global and local dust storms. Two global dust storms occurred during year 1 of the Viking lander 1 dust opacity record of Figure 5-15. During these storms, optical depths reached peak values of 5 or more, and remained above unity for half the Martian year. However, dust opacities returned to background levels by $L_s = 143°$ in the following year. Global dust storms generally occur later in the Martian year than $L_s = 143°$. Furthermore, they do not occur every year and there is some evidence that their incidence was higher in the Viking years than it has been recently [33]. Local dust storms can raise dust optical depth to 5 for

periods of a few days, and occur more frequently than their global relatives. Figure 5-16 shows that local dust storms are most common at low latitudes in the southern spring and summer [31]. The Pathfinder lander season of $L_s = 143°$ lies just at the end of a period of minimum local dust storm incidence.

Given the poor quality of observational statistics for both global and local dust storms, it is difficult to quantify the probability of encountering dust opacities that are significantly higher than recommended above. An attempt was made to model this using a Rayleigh probability distribution based on the Viking data set in [23]. This validity of this model is questionable due to its inherent assumptions and the fact that more recent observations were not taken into account. Dust opacities based on the whole Viking data set are likely to be too high for the following reasons:

1. Global and local dust storms incidence is near a minimum at $L_s = 143°$.

2. Mars has recently been clearer than in the Viking years.

5.5.5   Insolation

A knowledge of insolation at the surface of Mars is required to evaluate lander solar panel performance. Insolation is determined by the solar constant, the Mars orbit, the solar zenith angle, and absorption and scattering by the Martian atmosphere. Absorption and scattering by the gaseous atmosphere and by ice particles are small compared with absorption and scattering by dust.

Dust optical depth, dust optical constants, and a scattering radiative transfer model are required to calculate direct and diffuse insolation as a function of zenith angle. The Pathfinder project currently uses the optical constants of [34] and the radiative transfer model of [35]. It has recently been pointed out that the optical constants of [34] are inaccurate, particularly at wavelengths beyond $1.0\mu m$ [36], and solar cell performance calculations have been repeated independently using a more sophisticated radiative transfer model [37]. However, reference [38] shows that the original and new models give similar results for GaAs/Ge solar cell performance. For dust optical depths below unity, the new model predicts power levels 2-5% higher than the original. When optical depth is 5, the power levels calculated using the new model are 15-25% lower than the original model. Agreement is best at low solar zenith angles and deteriorates at larger zenith angles. For Pathfinder most of the integrated daily insolation originates at low zenith angles, so that both models produce similar results. Continued use of the original model is recommended for dust optical depths below unity, where it is expected to be slightly conservative.

The main uncertainty in insolation calculations is dust optical depth. Under dust storm conditions, the models indicate that insolation can fall by a factor of 3. However, for dust optical depths in the most probable 0.1-0.5 range, insolation variations are relatively small (10%) because most of the radiation scattered from the direct beam is preserved in the diffuse beam.

5.5.6   Local Slopes

The root mean square slope observed at the Viking 1 landing site is 5.5°. Recent radar observations have measured a slightly lower root mean square slope of 4–5° at Ares Valles, the Pathfinder landing site. An exponential probability distribution has been developed to express the statistical variation in slope from the root mean square value [39]. The probability P that the slope is less than s degrees is given by

$$P = 1 - e^{-s/S_m}$$

where S_m is the root mean square slope. Using this equation, the mean value for local slope, defined to be the value of s where $P = .5$ or 50%, is between 3.5 and 2.8°. The fraction of all slopes less than 5° is between 63 and 71%. The distribution also indicates that there is an 86–92% chance that local slopes will be less than 10°.

The local slopes in craters can be very large, approaching an angle or repose of about 30°. Fortunately, the likelihood of landing in a crater is relatively small. Examination of the landing footprint at Ares Tiu [43] has determined that there are approximately 30 craters larger than 1 km in diameter. There are roughly 100 craters between about 100 m and 1 km in diameter in the landing ellipse. The size frequency distribution of craters in the ellipse can be approximated by a −2 power-law distribution. The probability of landing on a crater larger than 10 m in diameter can be calculated by summing the total area covered by craters and dividing by the total area of the landing ellipse. The results indicate that there is about a 1% chance of landing in such a crater. A similar exercise has been carried out for large hills distributed in the landing ellipse. The results indicate that there is less than a 1% chance of landing on a hill whose diameter is on the order of 100 m or larger. Slopes on the margins of these hills average around 10°.

5.5.7   Rock Distribution

Thermal inertia and other data indicate that the Ares Tiu site has a rock abundance of approximately 20%. This is comparable to the percentage of rocks observed at the Viking 2 landing site. The model developed to represent frequency distribution as a function of rock size for the Viking 2 site [39] can therefore be applied to the Pathfinder site. The cumulative frequency distribution for rocks bigger than 14 cm in diameter is expressed as

$$N = 0.013\, D^{-2.66}$$

where N is the number of rocks per square meter that are larger than D m in diameter. The largest rock present in this distribution should be limited to a diameter of about 1 m or the cumulative area covered by the rocks in this distribution will exceed those actually present [40, 41, 42].

Other rock size-frequency distributions for rocks greater than 10 cm in diameter have also been developed and used in Pathfinder planning. The exponential functions given below provide a more rapid drop off in large rock sizes so they do not have to be limited at

large diameters:

$$N = 4.61\,e^{-6.85D}$$
$$F = 0.175\,e^{-2.752D}$$

where

F is the cumulative fractional area covered by rocks of a given diameter or larger

N is the number of rocks per square meter that are larger than D m in diameter (for $D \geq 10cm$).

D is the rock diameter in meters

The constant before the exponential function in this relation is the total rock coverage at the site [42].

Center Block: Daily mean pressures at the two Viking Landers for 700 sols.
Upper and lower blocks: Standard Deviations of pressure within each sol.

All pressures and standard deviations are in mb. The abscissa is time measured in VL-1
(Viking Lander -1) sols. The scale labeled Ls is the aerocentric longitude of the Sun.
The dates of initiation of two global dust storms are marked. Gaps are due to irretrievably
lost data.

Figure 5-9: Statistics for daily pressure variations at the Viking 1 landing site.

Figure 5-10: Viking mission's atmospheric pressure for 3.3 Mars years superimposed on a one year timeline. (courtesy of James E. Tillman).

Figure 5-11: Actual daily pressure and temperature variations over the first year at the
Viking 1 landing site.

Daily Atmospheric Temperature Profile
July 4, 1997

Figure 5-12: Nominal daily temperature cycle at 1.6 m above the surface.

Average differences between ground temperature and gas temperature at 1.6 m above the surface for VL-1 (Viking Lander 1) sols 31-45 (from[30]). The time unit on the abscissa is 3600 sec.

Figure 5-13: Daily variation in the difference between surface and near-surface atmospheric temperature at the Viking 1 landing site.

Figure 5-14: Daily variation in wind speed and direction at the Viking 1 landing site.

Visible optical depths derived from the Sun-diode measurements made at the two Viking landers (Colburn, et. al., 1989). Line indicates the opacity of a global haze inferred from Viking Lander 1 surface-pressure data (Zurek 1981). Initial appearance of detection of all observed regional dust clouds, hazes of obscurations (vertical lines) and of planet-encircling dust storms (arrows) are indicated at the top of the upper panel. (Figure taken from [31]), as adopted from [33]).

Figure 5-15: Variation in dust optical depth at the Viking landing sites.

Latitude and time-of-year occurrence of local dust storms detected by the Viking Orbiters, from either infrared or visible imaging observations, and those observed from Earth, as compiled by Wells (1979). Solid line represents the sub-solar latitude. (Figures taken from [31], as copied from Peterfreund, 1985).

Figure 5-16: Local Dust Storms as Detected by the Viking Orbiters.

5.6   Martian Satellites

The two satellites of Mars, Phobos and Deimos, were discovered by Asaph Hall during the 1877 opposition. These bodies are of secondary interest for Mars Pathfinder which is designed to explore the Martian surface. Few, if any, observations of the satellites will be undertaken by the Pathfinder lander. Nevertheless, some information on Phobos and Deimos is given here for the sake of completeness.

Both satellites are in near equatorial orbits that are very nearly circular. As is the case for the planets' trajectories around the sun, the orbital trajectories of these satellites around Mars is contained in a satellite ephemeris file. The satellite ephemeris file currently in use by Mars Pathfinder is MAR033.2 [44]. This file covers the period from October 26, 1996 to January 9, 2000. The 1-σ uncertainties for the ephemerides in this file are 15 km for Phobos and 30 km for Deimos.

5.6.1   Satellite Masses

The values for the gravitational parameters (GM) for the Martian satellites are taken from the satellite ephemeris MAR033 and are given below:

$$GM_{\text{Phobos MAR033.1}} = 0.69 \times 10^{-3} \, \text{km}^3/\text{sec}^2$$
$$GM_{\text{Deimos MAR033.1}} = 0.12 \times 10^{-3} \, \text{km}^3/\text{sec}^2$$

Using the value $G = 6.67259 \times 10^{-20} \text{km}^3/\text{sec}^2 \, \text{kg}$, the corresponding masses of Phobos and Deimos are

$$M_{\text{Phobos MAR033.1}} = 1.034 \times 10^{16} \, \text{kg}$$
$$M_{\text{Deimos MAR033.1}} = 1.798 \times 10^{15} \, \text{kg}$$

5.6.2   Satellite Shapes

The Martian satellites are rocky bodies with irregular shapes. A triaxial ellipsoid is used to approximate these shapes. The IAU values for the radii of these ellipsoids are shown below [5]:

$$\begin{array}{lc} \text{Phobos} & 13.4 \times 11.2 \times 9.2 \text{ km} \\ \text{Deimos} & 7.5 \times 6.1 \times 5.2 \text{ km} \end{array}$$

5.6.3   Satellites' Orientation & Rotation

The expressions for the poles and prime meridian angles for the satellites are slightly more complicated than the simple linear functions of time used for Mars itself. There are additional terms which are expressed as trigonometric functions of quantities which are linear functions of time. The equation for the prime meridian angle also contains a term that is quadratic in time. These terms are added to account for the precession and nutation of the satellites.

Satellites' Rotation Poles

The IAU has defined the right ascension and declination of the Mars satellite north poles, or spin axes, as the following functions of time in the EME2000 coordinate system [5]:

$$
\begin{aligned}
\alpha_{\text{Phobos}} &= 317.68 - 0.108\,T + 1.79\,\sin M1 \\
\delta_{\text{Phobos}} &= 52.90 - 0.061\,T - 1.08\,\cos M1 \\
M1 &= 169.51 - 0.4357640\,d
\end{aligned}
$$

and

$$
\begin{aligned}
\alpha_{\text{Deimos}} &= 316.65 - 0.108\,T + 2.98\,\sin M3 \\
\delta_{\text{Deimos}} &= 53.52 - 0.061\,T - 1.78\,\cos M3 \\
M3 &= 53.47 - 0.0181510\,d
\end{aligned}
$$

where

$$
\begin{aligned}
\alpha_{\text{Phobos}} &= \text{right ascension of Phobos' spin axis in degrees } (^\circ) \\
\delta_{\text{Phobos}} &= \text{declination of Phobos' spin axis in degrees } (^\circ) \\
\alpha_{\text{Deimos}} &= \text{right ascension of Deimos' spin axis in degrees } (^\circ) \\
\delta_{\text{Deimos}} &= \text{declination of Deimos' spin axis in degrees } (^\circ) \\
T &= \text{interval in Julian centuries from the epoch J2000} \\
&\quad\ (1 \text{ Julian century} = 36525 \text{ days}) \\
d &= \text{interval in days from the epoch J2000} \\
&\quad\ (1 \text{ day} = 86400 \text{ SI seconds})
\end{aligned}
$$

and $M1$ and $M3$ are measured in degrees ($^\circ$).

Satellites' Prime Meridians & Rotation Rates

The IAU has defined the location of the prime meridians of the Martian satellites as the following functions of time [5]:

$$
\begin{aligned}
W_{\text{Phobos}} &= 35.06 + 1128.8445850\,d + 8.864\,T^2 - 1.42\,\sin M1 - 0.78\,\sin M2 \\
M2 &= 192.93 + 1128.4096700\,d \\
W_{\text{Deimos}} &= 79.41 + 285.1618970\,d - 0.520\,T^2 - 2.58\,\sin M3 - 0.19\,\cos M3
\end{aligned}
$$

where W_{Phobos}, $M2$, and W_{Deimos} are measured in degrees($^\circ$), $M1$ and $M3$ are the same quantities defined in the previous section, and

$$
d = \text{interval in days from the epoch J2000}
$$

83

Recall that the W angle is defined as the angle from the body's IAU-vector to its prime meridian measured eastward in the body's equatorial plane and that the IAU-vector is defined as the ascending node of the satellite's equator with the Earth's mean equator plane of epoch J2000.

The factor multiplying d in these equations for W is approximately the rotation rate of each satellite. Thus the rotation periods for the satellites are:

Phobos	0.3189 days	7.654 hours
Deimos	1.262 days	30.299 hours

The rotation of both satellites is synchronous with the long axis of the triaxial ellipsoid pointed toward Mars and the short axis normal to the orbit plane.

Chapter 6

SUMMARY OF FUNDAMENTAL CONSTANTS

6.1   General Parameters

Table 6-1 presents a summary of the fundamental constants in use by Mars Pathfinder. Most of these data have been described and referenced in earlier sections of this document. The values for the speed of light, length of the astronomical unit, and the GMs for the planets and the moon are taken from the DE403 planetary ephemeris. The Earth and Mars shape and orientation data are taken from [5] and are discussed in detail in sections 5.2.1, 5.3, 4.2.1, and 4.3. All coordinate system dependent data are referenced to the EME2000 inertial reference frame.

6.2   Planetary Ephemeris

The fundamental planetary ephemeris adopted by the Mars Pathfinder project is the JPL Developmental Ephemeris 403, or simply DE403. A description of the planetary orbit solutions contained in this file, including tabulations of the observations from which they were estimated, can be found in [9]. The planetary ephemeris is the source for values of the following constants:

- Length of the astronomical unit, AU

- Speed of light, c

- GM's of the nine planets, the Sun, and moon

Values for these quantities given elsewhere in this document are taken from DE403 unless otherwise noted.

Symbol	Value	Units	Comments
c	299792.458	km/sec	Speed of light
AU	149597870.691	km	Length of 1 AU
$GM_{\male}$	22032.08048641792	km^3/sec^2	Mercury
$GM_{\female}$	324858.5988264597	km^3/sec^2	Venus
$GM_{\oplus}$	398600.4356081032	km^3/sec^2	Earth
$GM_{\mars}$	42828.31425806710	km^3/sec^2	Mars
$GM_{\jupiter}$	126712767.8577960	km^3/sec^2	Jupiter
$GM_{\saturn}$	37940626.06113727	km^3/sec^2	Saturn
$GM_{\uranus}$	5794549.007071872	km^3/sec^2	Uranus
GM_{Ψ}	6836534.063879259	km^3/sec^2	Neptune
GM_{P}	981.6008877070042	km^3/sec^2	Pluto
$GM_{\odot}$	132712440017.9870	km^3/sec^2	Sun
$GM_{\leftmoon}$	4902.799107879768	km^3/sec^2	Moon

GM is for the planetary system, including natural satellites where applicable.

Symbol	Value	Units	Comments
$R_{\oplus\,EQRTL}$	6378.14	km	Earth equatorial radius
$R_{\oplus\,POLAR}$	6356.75	km	Earth polar radius
$f_{\oplus}$	0.00335364		Earth flattening
$R_{\mars\,EQRTL}$	3393.4	km	Mars equatorial radius
$R_{\mars\,POLAR}$	3375.8	km	Mars polar radius
$f_{\mars}$	0.005186		Mars flattening

Symbol	Value	Units	Comments
$\alpha_{\oplus}$	$0.00 - 0.641\,T$	° (deg)	Earth pole right ascension
$\delta_{\oplus}$	$90.00 - 0.557\,T$	°	Earth pole declination
$W_{\oplus}$	$190.16 + 360.9856235\,d$	°	Earth prime meridian
$\alpha_{\mars}$	$317.681 - 0.108\,T$	°	Mars pole right ascension
$\delta_{\mars}$	$52.886 - 0.061\,T$	°	Mars pole declination
$W_{\mars}$	$176.901 + 350.8919830\,d$	°	Mars prime meridian

where $T = (JED - 2451545.0)/36525$ centuries and $d = (JED - 2451545.0)$ days

Symbol	Value	Units	Comments
ΔT = ET - UTC	61.184(known)	sec	7/1/94 – 12/31/95
	62.184(predicted)	sec	1/1/96 – 12/31/96
	63.184(predicted)	sec	1/1/97 – 12/31/97
	64.184(predicted)	sec	1/1/98 – 12/31/98

Table 6-1: Astrodynamic Constants for Mars Pathfinder

REFERENCES

[1] **Mars Observer Planetary Constants and Models**, Project Document 642-321, JPL Document D-3444, November 1990.

[2] Battin, R. H., **An Introduction to the Mathematics and Methods of Astrodynamics**, AIAA Education Series, New York, 1987.

[3] Bate, R., Mueller, D., and White, J., **Fundamentals of Astrodynamics**, Dover Publications, Inc., New York, 1971.

[4] **Mars Pathfinder AIM Phasing and Coordinate Frame Document**, Project Document PF-300-4.0-03, JPL Document D-12103, K. Lau and J. Mellstrom, June 26, 1995.

[5] Davies, M. E., et. al., "Report of IAU/IAG/COSPAR Working Group on Cartographic Coordinates and Rotational Elements of the Planets and Satellites: 1991," *Celestial Mechanics and Dynamical Astronomy*, Vol. 53, No. 4, 1992, pp 377-397. (1994 report to be published soon. Values given in this document are from the 1994 report.)

[6] **NAIF Fundamental Concepts**, W. L. Taber, NAIF document No. 205.0, JPL, October 3, 1990.

[7] **Explanatory Supplement to the Astronomical Almanac**, P. K. Seidelmann (ed)., University Science Books, Mill Valley, CA, 1992.

[8] Lee, Wayne, "Mars Fictitious Mean Sun and Equation of Time", JPL IOM 312/95.5-4353, April 17, 1995.

[9] Standish, E. M., Newhall, X. X., Williams, J. G., and Folkner, W. M, "JPL Planetary and Lunar Ephemerides, DE403/LE403," JPL IOM 314.10-127, May 22, 1995.

[10] **DPTRAJ-ODP User's Reference Manual**, Volume 1, Model Descriptions - Time and Polar Motion, JPL Section 312 Navigation and Flight Mechanics.

[11] Moyer, T. D., *Mathematical Formulation of the Double-Precision Orbit Determination Program (DPODP)*, JPL TR 32-1527, May 15, 1971.

[12] Moyer, T. D., "Transformation from Proper Time on Earth to Coordinate Time in Solar System Barycentric Space - Time Frame of Reference, Parts 1 and 2," *Celestial Mechanics*, 23, 1981, pp 33–56 and 57–68.

[13] Michael, W. H., Jr., "Viking Lander Contributions to Mars Mapping," *The Moon and Planets*, Vol. 20, 1979, pp 149-152.

[14] Folkner, W. M., "Current DSN Station Locations," JPL IOM 335.1-95-027, October 16,1995.

[15] Nerem, R. S., et. al., "Gravity Model Development for TOPEX/Poseidon: Joint Gravity Models 1 and 2," *J. Geophys. Res.*, 99(C12), 1994. (Publication pending for Joint Gravity Model 3 (JGM-3) update.)

[16] **Mars Pathfinder Project Mission Plan**, Revision A, Project document PF-100MP-02, JPL document D-11355, April 1995.

[17] **The JPL Mars Gravity Field, Mars50c, Based Upon Viking and Mariner 9 Doppler Tracking Data**, A. Konopliv and W. Sjogren, JPL Publication 95-5, February 1995.

[18] Heiskanen, W. A. and Moritz, H., **Physical Geodesy**, W. H. Freeman and Co., San Francisco, CA, 1967.

[19] **The Mars Global Reference Atmosphere Model (Mars-GRAM)**, C. G. Justus and G. Chimonas, Georgia Tech Project G-35-685, Prepared for NASA Marshall Space Flight Center under Grant No. NAG8-078, July, 1989.

[20] Spencer, D. A., and Braun, R. D., "Mars Pathfinder Atmospheric Entry Trajectory Design," paper AAS 95-379, AAS/AIAA Astrodynamics Specialist Conference, Halifax, Nova Scotia, Canada, August 14-17, 1995.

[21] Spencer, D. A., "Hydrostatic Equilibrium Mars Atmosphere Model Development," JPL IOM 312/95.2-2079, October 30, 1995.

[22] **Mars**, Kieffer, H., Jakosky, B., Snyder, C., and Matthews, M., (eds.), The University of Arizona Press, 1992.

[23] Spencer, D. and Cook, R., "Revised EDL and Surface Environmental Assumptions," JPL IOM 210/RAC-94.017 Rev. A, August 1, 1994.

[24] Schofield, T. and Cook, R., "Mars Surface Environment for Pathfinder," JPL IOM S&I DFM 95-016, June 27, 1995.

[25] Hess, S., Ryan, J., Tillman, J., Henry, R., and Leovy, C. "The annual pressure cycle of Mars measured by Viking landers 1 & 2," *Geophysical Research Letters*, 7, 1980, pp 197-200.

[26] Tillman, J. E., "Mars Global Atmospheric Oscillations: Annually Synchronized, Transient Normal-Mode Oscillations and the Triggering of Global Dust Storms," *Journal of Geophysical Research*, Vol. 93, No. D8, August 20, 1988, pp. 9433-9451.

[27] Tillman, J. E., Johnson, N. C., Guttorp, P., and Percival, D. B., "The Martian Annual Atmospheric Pressure Cycle: Years Without Great Dust Storms," *Journal of Geophysical Research* (special edition), Vol. 84, No. 10, June, 1993, pp 10963-10971.

[28] Murphy, J. Leovy, C., and Tillman, J., Material presented at the second Mars Pathfinder Project Science Group meeting, 9-10th June 1994.

[29] Keiffer, H., Martin, T., Peterfreund, A., Jakosky, B., Miner, E., and Palluconi, F., "Thermal and Albedo Mapping of Mars during the Viking Primary Mission," *Journal of Geophysical Research*, 82, 1977, pp 4249-4291.

[30] Sutton, J., Leovy, C.B., and Tillman, J.E., "Diurnal variations of the Martian surface layer meteorological parameters during the first 45 sols at two Viking lander sites", *Journal of the Atmospheric Sciences*, 35, 1978, pp 2346-2355.

[31] Kahn, R., Martin, T., Zurek, R., and Lee.S., "The Martian Dust Cycle," in **Mars** Keiffer, H., Jakosky, B., Snyder, C., and Matthews, M. (eds.), 1992., pp 1017-1053.

[32] Schofield, J., Herkenhoff, K., and Zurek, R., "Cold Mars Atmosphere - Impact on the Pathfinder Mission," JPL IOM S&I DFM 95-014, May 22, 1995.

[33] Zurek, R. and Martin, L., "Interannual variability of planet-encircling dust storms on Mars," *Journal of Geophysical Research*, 98, 1992, pp 3247-3259.

[34] Pollack, J., Colburn, D., Flaser, F., Kahn, R., Carlston, C., and Pidek, C., "Properties and effects of dust particles suspended in the Martian atmosphere," *Journal of Geophysical Research*, 84, 1979, pp 2929-2945.

[35] Applebaum, J., Landis, G.A., and Sherman, I., "Solar Radiation on Mars update 1991", *Solar Energy*, 50, 1993, pp 35-51.

[36] Clancy, R., Lee, S., Gladstone, G., Mcmillan, W., and Rousch, T., "A new model of Mars atmospheric dust based upon analysis of ultraviolet through infrared observations from Mariner-9, Viking, and Phobos," *Journal of Geophysical Research*, 100, 1995, pp 5251-5263.

[37] Crisp, D., Paige, D., Pathare, A., and Sullivan, M., "The performance of solar cells at the Martian surface," June 7th 1994.

[38] Ewell, Richard, "Comparison of solar cell performance on the surface of Mars predictions", JPL IOM 342-APS-RCE-94-017, September 15, 1994.

[39] Moore, H. "Surface Models of Mars (1975)", NASA SP-8020, September 1975.

[40] Golombek, M., "Mars Yard Rock Distributions," JPL IOM Pathfinder Science and Instruments Design File Memo 95-024, September 20, 1995.

[41] Golombek, M., "Air Bag Drop Test Rock Size-Frequency Distributions", JPL IOM Pathfinder Science and Instruments Design File Memo 95-033, October 25, 1995.

[42] Golombek, M., and Rapp, D., "Size-frequency distributions of rocks on Mars," (expanded abstract), Mars Pathfinder Landing Site Workshop II: Characteristics of the Ares Vallis Region and Field Trips in the Channeled Scabland, Washington, M. P. Golombek, K. S. Edgett, and J. W. Rice Jr. (eds.), September 28-29, 1995, Spokane, Washington, Lunar and Planetary Institute Technical Report 95-01, Part 1, p. 13-15.

[43] Golombek, M. and Parker, T., "Mars Pathfinder Landing Site Data," JPL IOM Pathfinder Science and Instruments Design File Memo 95-028, October 26, 1995.

[44] Jacobson, R. A., "Ephemerides of the Martian Satellites," JPL IOM 312.1-95-142, October 27, 1995.

Appendix A

GRAVITY FIELD MODELS

The standard representation of a gravitational potential field is:

$$V = \frac{\mu}{r}\left[1 - \sum_{n=2}^{\infty}\left(\frac{R}{r}\right)^n J_n\, P_n^0(\sin\phi) + \sum_{n=2}^{\infty}\left(\frac{R}{r}\right)^n \sum_{m=1}^{n} P_n^m(\sin\phi)\left\{C_{nm}\cos(m\lambda) + S_{nm}\sin(m\lambda)\right\}\right]$$

(A.1)

where

μ	=	GM of the body
r	=	radial distance of the point (or spacecraft) from the planet's center
ϕ	=	planetocentric latitude of the point
λ	=	planetocentric longitude of the point
R	=	the mean radius of the planet
P_n^m	=	associated Legendre polynomial of degree n, order m
J_n	=	$-C_{n0}$, nth order zonal harmonic coefficients
C_{nm}	=	tesseral harmonic coefficients
S_{nm}	=	sectorial harmonic coefficients

The Mars50c and JGM-3 models were developed using a fully normalized version of the standard equation. The Legendre polynomial terms and the harmonic coefficients are multiplied by normalization factors whose products are 1 so that the terms in the potential equation remain the same. The relationship between the normalized and unnormalized Legendre polynomial functions and the harmonic coefficients from [18] is:

$$\text{Normalized} = \text{Normalization factor} \times \text{Unnormalized}$$
$$\bar{P}_n^0 = \sqrt{2n+1}\,P_n^0$$
$$\bar{P}_n^m = \sqrt{2(2n+1)\frac{(n-m)!}{(n+m)!}}\,P_n^m \quad m>0$$
$$\bar{C}_{n0} = \frac{1}{\sqrt{2n+1}}\,C_{n0}$$
$$\bar{C}_{nm} = \sqrt{\frac{(n+m)!}{2(2n+1)(n-m)!}}\,C_{nm} \quad m>0$$

$$\bar{S}_{nm} \;=\; \sqrt{\frac{(n+m)!}{2(2n+1)(n-m)!}}\, S_{nm} \quad m > 0$$

where $\bar{C}_{n0} = -\bar{J}_n$.

A.1   The JGM-3 Gravity Field Model for Earth

The values of μ and R in equation A.1 for the Earth's JGM-3 gravity field model are:

$$\mu \;=\; GM_{\oplus\,JGM-3} = 398600.4415 \text{ km}^3/\text{sec}^2$$
$$R \;=\; R_{\oplus\,JGM-3} = 6378.1363 \text{ km}$$

The values for the normalized zonal harmonic coefficients, $\bar{J}_n$, for the JGM-3 model are given in Table A-1. Table A-2 gives the values for the normalized tesseral and sectorial coefficients, $\bar{C}_{nm}$ and $\bar{S}_{nm}$. Note that these tables only list terms up to degree and order 20, a truncation of the full 70×70 model.

n	$\bar{J}_n$
2	0.48416537545647D−03
3	−0.957170590888D−06
4	−0.539777068357D−06
5	−0.686589879865D−07
6	0.149671561786D−06
7	−0.907229416432D−07
8	−0.491180031747D−07
9	−0.273850609501D−07
10	−0.541304457388D−07
11	0.501613145957D−07
12	−0.363823406237D−07
13	−0.399464287317D−07
14	0.218038615472D−07
15	−0.316595109262D−08
16	0.543023208844D−08
17	−0.181083750598D−07
18	−0.726918460072D−08
19	0.351855030981D−08
20	−0.187899865498D−07

Table A-1: Zonal Harmonic Coefficients for JGM-3

n	m	$\bar{C}_{nm}$	$\bar{S}_{nm}$
1	1	0.000000000000D+00	0.000000000000D+00
2	1	−0.186987640000D−09	0.119528010000D−08
2	2	0.243926074866D−05	−0.140026639759D−05
3	1	0.203013720555D−05	0.248130798256D−06
3	2	0.904706341273D−06	−0.618922846478D−06
3	3	0.721144939823D−06	0.141420398474D−05
4	1	−0.536243554299D−06	−0.473772370616D−06
4	2	0.350670156459D−06	0.662571345943D−06
4	3	0.990868905774D−06	−0.200987354847D−06
4	4	−0.188481367425D−06	0.308848036904D−06
5	1	−0.627273696977D−07	−0.941946321344D−07
5	2	0.652459102764D−06	−0.323334352444D−06
5	3	−0.451837048088D−06	−0.214954193464D−06
5	4	−0.295123393022D−06	0.497414272309D−07
5	5	0.174831577700D−06	−0.669392937249D−06
6	1	−0.761035804073D−07	0.268998189326D−07
6	2	0.483274721249D−07	−0.373815919444D−06
6	3	0.570209657580D−07	0.888947380083D−08
6	4	−0.862280326198D−07	−0.471405112321D−06
6	5	−0.267112271720D−06	−0.536410164664D−06
6	6	0.950165183386D−08	−0.237261478895D−06
7	1	0.280286522037D−06	0.947773178133D−07
7	2	0.329760227424D−06	0.931936968310D−07
7	3	0.250501526750D−06	−0.217320108453D−06
7	4	−0.275540963074D−06	−0.124441512485D−06
7	5	0.164400381464D−08	0.180753352335D−07
7	6	−0.358842633079D−06	0.151778084434D−06
7	7	0.137951705641D−08	0.241285940808D−07
8	1	0.233337516872D−07	0.584992749394D−07
8	2	0.800706639316D−07	0.655185590975D−07
8	3	−0.192517643314D−07	−0.862858365342D−07
8	4	−0.244358064393D−06	0.698570748504D−07
8	5	−0.254984100103D−07	0.890902974946D−07
8	6	−0.658593538644D−07	0.308920641580D−06
8	7	0.672627018487D−07	0.748131967687D−07
8	8	−0.123970613955D−06	0.120441006688D−06

Table A-2: Tesseral and Sectorial Harmonic Coefficients for JGM-3

n	m	$\bar{C}_{nm}$	$\bar{S}_{nm}$
9	1	0.142230258927D−06	0.219096183494D−07
9	2	0.226206423558D−07	−0.321749849622D−07
9	3	−0.161064278972D−06	−0.745454640614D−07
9	4	−0.820173668779D−08	0.200680932868D−07
9	5	−0.163250615159D−07	−0.542714732480D−07
9	6	0.628331869224D−07	0.222677310949D−06
9	7	−0.118158852176D−06	−0.968993858400D−07
9	8	0.187984269547D−06	−0.301544406579D−08
9	9	−0.477248219232D−07	0.965855776308D−07
10	1	0.837588323327D−07	−0.131554065398D−06
10	2	−0.935579256828D−07	−0.514158905849D−07
10	3	−0.719673670736D−08	−0.154179881185D−06
10	4	−0.843353523953D−07	−0.784853461718D−07
10	5	−0.495197408181D−07	−0.502926935779D−07
10	6	−0.374188337367D−07	−0.794642182750D−07
10	7	0.820840625208D−08	−0.314913584011D−08
10	8	0.404678418711D−07	−0.919166827344D−07
10	9	0.125402502523D−06	−0.377364777537D−07
10	10	0.100382331314D−06	−0.238094044472D−07
11	1	0.161070777387D−07	−0.278921528407D−07
11	2	0.184297954611D−07	−0.984521172044D−07
11	3	−0.305606980075D−07	−0.148803090512D−06
11	4	−0.400241077823D−07	−0.635965302134D−07
11	5	0.374358745677D−07	0.498286316800D−07
11	6	−0.146078140555D−08	0.341731612304D−07
11	7	0.470618247402D−08	−0.897772350571D−07
11	8	−0.614060310693D−08	0.245722545052D−07
11	9	−0.314555162277D−07	0.420407136882D−07
11	10	−0.521293085885D−07	−0.183022780022D−07
11	11	0.462269459741D−07	−0.695925137860D−07
12	1	−0.541917013363D−07	−0.420117757677D−07
12	2	0.139857384606D−07	0.310477696443D−07
12	3	0.389785207778D−07	0.245765809599D−07
12	4	−0.684196981871D−07	0.295432560593D−08
12	5	0.311070755273D−07	0.763878831243D−08

Table A-2: (cont.) Tesseral and Sectorial Harmonic Coefficients for JGM-3

n	m	$\bar{C}_{nm}$	$\bar{S}_{nm}$
12	6	0.332441946804D$-$08	0.393688334845D$-$07
12	7	$-$0.186031065417D$-$07	0.355708292492D$-$07
12	8	$-$0.257024774027D$-$07	0.166667944646D$-$07
12	9	0.417930777117D$-$07	0.253245799090D$-$07
12	10	$-$0.616938471209D$-$08	0.309862629190D$-$07
12	11	0.113208272884D$-$07	$-$0.634422554485D$-$08
12	12	$-$0.234927522693D$-$08	$-$0.109594265534D$-$07
13	1	$-$0.529668682614D$-$07	0.398768164474D$-$07
13	2	0.560391252754D$-$07	$-$0.626993413009D$-$07
13	3	$-$0.218171319486D$-$07	0.982089990775D$-$07
13	4	$-$0.147093724418D$-$08	$-$0.126138487865D$-$07
13	5	0.582531254154D$-$07	0.658456489681D$-$07
13	6	$-$0.353119887404D$-$07	$-$0.605833152976D$-$08
13	7	0.270636492003D$-$08	$-$0.771105789145D$-$08
13	8	$-$0.988717875865D$-$08	$-$0.972893716175D$-$08
13	9	0.247536300548D$-$07	0.453592577207D$-$07
13	10	0.408921474586D$-$07	$-$0.370989434214D$-$07
13	11	$-$0.447390745655D$-$07	$-$0.483289206073D$-$08
13	12	$-$0.314100213465D$-$07	0.881063493744D$-$07
13	13	$-$0.612113410742D$-$07	0.684087856909D$-$07
14	1	$-$0.190237519415D$-$07	0.274718260627D$-$07
14	2	$-$0.369789660624D$-$07	$-$0.298910748984D$-$08
14	3	0.368094358394D$-$07	0.203134043800D$-$07
14	4	0.171206603690D$-$08	$-$0.206880440006D$-$07
14	5	0.298994624501D$-$07	$-$0.168579108384D$-$07
14	6	$-$0.194009817301D$-$07	0.241295941300D$-$08
14	7	0.368511326315D$-$07	$-$0.422236458897D$-$08
14	8	$-$0.348668529184D$-$07	$-$0.148884147887D$-$07
14	9	0.323766387782D$-$07	0.286982125507D$-$07
14	10	0.388384894621D$-$07	$-$0.146465029369D$-$08
14	11	0.153565394629D$-$07	$-$0.390385031097D$-$07
14	12	0.850466461661D$-$08	$-$0.309217277403D$-$07
14	13	0.321667471351D$-$07	0.452000811994D$-$07
14	14	$-$0.517834363669D$-$07	$-$0.501357060897D$-$08

Table A-2: (cont.) Tesseral and Sectorial Harmonic Coefficients for JGM-3

n	m	$\bar{C}_{nm}$	$\bar{S}_{nm}$
15	1	0.120190484678D$-$07	0.817326710799D$-$08
15	2	$-$0.217462728532D$-$07	$-$0.317330396220D$-$07
15	3	0.524030646688D$-$07	0.151598623104D$-$07
15	4	$-$0.421626914461D$-$07	0.782709969099D$-$08
15	5	0.134508958467D$-$07	0.898233496299D$-$08
15	6	0.334633862208D$-$07	$-$0.377525321326D$-$07
15	7	0.599127013549D$-$07	0.605619232715D$-$08
15	8	$-$0.319895524164D$-$07	0.222709138831D$-$07
15	9	0.130267220243D$-$07	0.378764137042D$-$07
15	10	0.103113307523D$-$07	0.149563291952D$-$07
15	11	$-$0.951744918496D$-$09	0.187163366675D$-$07
15	12	$-$0.327289916045D$-$07	0.157197765289D$-$07
15	13	$-$0.282889609266D$-$07	$-$0.429439585260D$-$08
15	14	0.530448112798D$-$08	$-$0.244424846227D$-$07
15	15	$-$0.192275325578D$-$07	$-$0.470437177403D$-$08
16	1	0.275334993498D$-$07	0.337081990437D$-$07
16	2	$-$0.223952940063D$-$07	0.262066133546D$-$07
16	3	$-$0.351007890045D$-$07	$-$0.232415199680D$-$07
16	4	0.412189767399D$-$07	0.460566969766D$-$07
16	5	$-$0.134952635757D$-$07	$-$0.167885070609D$-$08
16	6	0.143210546505D$-$07	$-$0.344453592516D$-$07
16	7	$-$0.781296622069D$-$08	$-$0.851014325206D$-$08
16	8	$-$0.215378422697D$-$07	0.524757504003D$-$08
16	9	$-$0.227767152892D$-$07	$-$0.389238874533D$-$07
16	10	$-$0.121287100211D$-$07	0.120646359931D$-$07
16	11	0.192658351833D$-$07	$-$0.297475752027D$-$08
16	12	0.196977425594D$-$07	0.691450927978D$-$08
16	13	0.138373301892D$-$07	0.993931047643D$-$09
16	14	$-$0.191259290846D$-$07	$-$0.388601607315D$-$07
16	15	$-$0.144605112506D$-$07	$-$0.326991029842D$-$07
16	16	$-$0.375294246599D$-$07	0.359110383412D$-$08
17	1	$-$0.263888623964D$-$07	$-$0.298528557535D$-$07
17	2	$-$0.173785969947D$-$07	0.919674929740D$-$08
17	3	0.742256153378D$-$08	0.819465237243D$-$08
17	4	0.752025612808D$-$08	0.233819948710D$-$07
17	5	$-$0.170580525942D$-$07	0.535320656218D$-$08

Table A-2: (cont.) Tesseral and Sectorial Harmonic Coefficients for JGM-3

n	m	$\bar{C}_{nm}$	$\bar{S}_{nm}$
17	6	$-0.134666100110D-07$	$-0.282748374362D-07$
17	7	$0.240111196379D-07$	$-0.588355438684D-08$
17	8	$0.376245618668D-07$	$0.376095603594D-08$
17	9	$0.329048997604D-08$	$-0.285857664019D-07$
17	10	$-0.430407782970D-08$	$0.180384439877D-07$
17	11	$-0.157255191146D-07$	$0.110208682279D-07$
17	12	$0.286891287894D-07$	$0.207440697008D-07$
17	13	$0.166030667389D-07$	$0.203048086784D-07$
17	14	$-0.140607941032D-07$	$0.113757053430D-07$
17	15	$0.533185582731D-08$	$0.538710072517D-08$
17	16	$-0.300610168116D-07$	$0.372408860961D-08$
17	17	$-0.340641085422D-07$	$-0.197332149060D-07$
18	1	$0.421001670372D-08$	$-0.390758931456D-07$
18	2	$0.128282488663D-07$	$0.135863599790D-07$
18	3	$-0.375966759094D-08$	$-0.310905629936D-08$
18	4	$0.530922910408D-07$	$0.145969988307D-08$
18	5	$0.731442203594D-08$	$0.246503511368D-07$
18	6	$0.133778399892D-07$	$-0.156609960659D-07$
18	7	$0.652858771149D-08$	$0.628026301655D-08$
18	8	$0.310661164348D-07$	$0.247013406569D-08$
18	9	$-0.191831235593D-07$	$0.361443872003D-07$
18	10	$0.556615602556D-08$	$-0.459538683139D-08$
18	11	$-0.764247535871D-08$	$0.211715136603D-08$
18	12	$-0.296030199745D-07$	$-0.161924646618D-07$
18	13	$-0.637993303475D-08$	$-0.349797303124D-07$
18	14	$-0.800283215532D-08$	$-0.130783750357D-07$
18	15	$-0.405355669223D-07$	$-0.202494268224D-07$
18	16	$0.106709138405D-07$	$0.696543691109D-08$
18	17	$0.360031919416D-08$	$0.451037605479D-08$
18	18	$0.262060609734D-08$	$-0.108100584063D-07$
19	1	$-0.696750144486D-08$	$0.158048507374D-09$
19	2	$0.314350515722D-07$	$-0.432954797743D-08$
19	3	$-0.989999332042D-08$	$-0.988212084385D-09$
19	4	$0.158267868073D-07$	$-0.566193768936D-08$
19	5	$0.120582237929D-07$	$0.272044440646D-07$

Table A-2: (cont.) Tesseral and Sectorial Harmonic Coefficients for JGM-3

n	m	C_{nm}	S_{nm}
19	6	$-0.238500620077D-08$	$0.179516595915D-07$
19	7	$0.736778591222D-08$	$-0.866484817195D-08$
19	8	$0.310521890736D-07$	$-0.104626088472D-07$
19	9	$0.303046616376D-08$	$0.645155665369D-08$
19	10	$-0.333774895894D-07$	$-0.709017930783D-08$
19	11	$0.160807201977D-07$	$0.110003173288D-07$
19	12	$-0.298865572632D-08$	$0.930967987884D-08$
19	13	$-0.744655150908D-08$	$-0.283983038541D-07$
19	14	$-0.452943207373D-08$	$-0.131134526890D-07$
19	15	$-0.178384586154D-07$	$-0.141059161725D-07$
19	16	$-0.214212124130D-07$	$-0.695745086793D-08$
19	17	$0.291057530676D-07$	$-0.151525371480D-07$
19	18	$0.347143402904D-07$	$-0.943857745550D-08$
19	19	$-0.237085820000D-08$	$0.477960914790D-08$
20	1	$0.834776750113D-08$	$0.624452941693D-08$
20	2	$0.200304480295D-07$	$0.148844700886D-07$
20	3	$-0.593499490668D-08$	$0.355711511711D-07$
20	4	$0.545717472347D-08$	$-0.224101011983D-07$
20	5	$-0.114523183889D-07$	$-0.693507758649D-08$
20	6	$0.115654010973D-07$	$-0.423417320021D-09$
20	7	$-0.203015102281D-07$	$-0.129958892264D-09$
20	8	$0.492220313056D-08$	$0.406716184366D-08$
20	9	$0.180439125534D-07$	$-0.586487138672D-08$
20	10	$-0.325490346724D-07$	$-0.576018319921D-08$
20	11	$0.145627627208D-07$	$-0.189297512983D-07$
20	12	$-0.640921540838D-08$	$0.181542209426D-07$
20	13	$0.273234905392D-07$	$0.703251296621D-08$
20	14	$0.118943770266D-07$	$-0.144722338577D-07$
20	15	$-0.258327376783D-07$	$-0.765802414907D-09$
20	16	$-0.120637046415D-07$	$0.330018839924D-09$
20	17	$0.443472483728D-08$	$-0.137034054600D-07$
20	18	$0.149166321827D-07$	$-0.983692915354D-09$
20	19	$-0.296262452972D-08$	$0.109596496475D-07$
20	20	$0.404458409553D-08$	$-0.123466183379D-07$

Table A-2: (cont.) Tesseral and Sectorial Harmonic Coefficients for JGM-3

A.2 The Mars50c Gravity Field Model

The values of μ and R in equation A.1 for the Mars50c gravity field model are:

$$\mu = GM_{\sigma\,Mars50c} = 42828.370371 \text{ km}^3/\text{sec}^2$$
$$R = R_{\sigma\,Mars50c} = 3394.2 \text{ km, the mean radius of Mars}$$

The values for the normalized zonal harmonic coefficients, $\bar{J}_n$, for the Mars50c model are given in Table A-3. Table A-4 gives the values for the normalized tesseral and sectorial coefficients, $\bar{C}_{nm}$ and $\bar{S}_{nm}$.

n	$\bar{J}_n$	n	$\bar{J}_n$
1	0.000000000000D+00	26	0.183098144323D−06
2	0.875919760273D−03	27	0.202687019376D−06
3	0.119340679166D−04	28	−0.429103749124D−07
4	−0.515052493229D−05	29	−0.731785560117D−07
5	0.182402897065D−05	30	−0.385694619253D−07
6	−0.145665966143D−05	31	0.449236654034D−08
7	−0.840128810448D−06	32	0.994070250913D−08
8	−0.498316049196D−06	33	0.333016477465D−07
9	0.738627001499D−06	34	0.597738890173D−07
10	−0.137778585004D−05	35	0.426732151228D−08
11	0.899843993543D−06	36	−0.132004765406D−06
12	−0.965604124650D−06	37	−0.155989004466D−07
13	0.879642981649D−06	38	0.101627936744D−06
14	−0.698734778005D−06	39	0.411241523485D−07
15	−0.544256504521D−06	40	−0.838452765079D−07
16	−0.792720657847D−06	41	−0.332760239974D−07
17	−0.303213778972D−06	42	0.564327325392D−07
18	0.303014626246D−06	43	0.383110894648D−07
19	−0.308367385325D−06	44	−0.297436536507D−07
20	−0.366257053953D−06	45	−0.353213024282D−07
21	−0.136162789788D−06	46	0.119490799001D−07
22	−0.158771990938D−06	47	0.169071830029D−07
23	−0.126368695427D−07	48	0.148809772801D−08
24	−0.575286829294D−07	49	0.654895835191D−08
25	−0.237001079235D−07	50	−0.144664459485D−07

Table A-3: Zonal Harmonic Coefficients for Mars50c

99

n	m	$\bar{C}_{nm}$	$\bar{S}_{nm}$
1	1	0.000000000000D+00	0.000000000000D+00
2	1	0.132033468405D−07	0.675285290457D−09
2	2	−0.843122022711D−04	0.496785329690D−04
3	1	0.386567700057D−05	0.252774247650D−04
3	2	−0.159257903505D−04	0.846687289437D−05
3	3	0.354141266874D−04	0.251996626619D−04
4	1	0.423920765688D−05	0.374755584188D−05
4	2	−0.111646822443D−05	−0.896339096830D−05
4	3	0.651418723273D−05	−0.272352421181D−06
4	4	0.113002982991D−06	−0.128953895406D−04
5	1	0.483319737757D−06	0.209711155235D−05
5	2	−0.424950879878D−05	−0.122480912838D−05
5	3	0.330314698123D−05	0.254191256762D−06
5	4	−0.468758582735D−05	−0.332592263843D−05
5	5	−0.442180487607D−05	0.383605422433D−05
6	1	0.189292146731D−05	−0.162575855711D−05
6	2	0.952881708647D−06	0.161247203944D−05
6	3	0.951313518098D−06	0.244050571795D−06
6	4	0.103496966548D−05	0.265185330216D−05
6	5	0.178175240614D−05	0.162897120977D−05
6	6	0.278529844665D−05	0.785346403849D−06
7	1	0.114392658047D−05	−0.121424715130D−06
7	2	0.279913674214D−05	−0.731916050571D−06
7	3	0.840389648008D−06	−0.423723215581D−06
7	4	0.239819519371D−05	−0.525983697776D−06
7	5	−0.308772049354D−06	−0.133474272819D−05
7	6	−0.572301952896D−06	−0.193627126643D−05
7	7	0.419198548050D−06	−0.177122313587D−05
8	1	0.202856025184D−06	0.626151101085D−06
8	2	0.166759972810D−05	0.659128506006D−06
8	3	−0.108712385793D−05	−0.132729727828D−05
8	4	0.162651101420D−05	0.415430115159D−07
8	5	−0.279554256497D−05	−0.162629432881D−05
8	6	−0.100692473264D−05	−0.176741453509D−05
8	7	−0.493709063200D−06	0.165618103486D−05
8	8	−0.306068555105D−06	−0.263871691654D−06

Table A-4: Tesseral and Sectorial Harmonic Coefficients for Mars50c

n	m	$\bar{C}_{nm}$	$\bar{S}_{nm}$
9	1	0.140363590542D−07	−0.207516804135D−06
9	2	0.119844490144D−05	0.154699271725D−06
9	3	−0.116773247490D−05	−0.894217268137D−06
9	4	0.403772948857D−06	0.169654071153D−05
9	5	−0.237146990403D−05	−0.150668977275D−05
9	6	0.890911573225D−06	0.567620690171D−06
9	7	−0.544184128735D−06	0.927288769489D−06
9	8	0.119623090937D−05	−0.176326258378D−06
9	9	−0.122398213822D−05	−0.621796126516D−06
10	1	0.158786445100D−05	−0.255763576813D−06
10	2	−0.491836523970D−07	−0.979693910877D−06
10	3	−0.279738766054D−07	0.321517077932D−06
10	4	−0.121444932529D−05	−0.339009651008D−07
10	5	0.488010771436D−06	−0.816604192291D−06
10	6	0.524197094579D−06	0.113698897944D−05
10	7	0.241893048541D−06	−0.711182999553D−06
10	8	0.542076876382D−06	0.810443071435D−06
10	9	−0.157547419097D−05	−0.145853461120D−05
10	10	−0.214668677035D−06	0.804047386684D−06
11	1	−0.170391788843D−05	0.235974580489D−06
11	2	−0.317420358984D−06	−0.111161454012D−05
11	3	−0.178089770929D−05	0.874697152544D−06
11	4	−0.168428003460D−05	−0.526974890309D−06
11	5	0.984946718174D−06	0.499118792403D−06
11	6	−0.395888790094D−07	0.135573601986D−07
11	7	0.865932712067D−06	−0.883521924590D−06
11	8	−0.110468186687D−05	0.828470431610D−06
11	9	−0.353118514737D−06	−0.390369703823D−06
11	10	0.402555992455D−06	0.191273007238D−05
11	11	−0.198478684681D−08	−0.351770949067D−06
12	1	−0.320515084591D−06	−0.543883615163D−06
12	2	−0.229519671147D−06	0.803027109797D−06
12	3	−0.934916884252D−06	0.159409607358D−06
12	4	−0.208603920375D−06	−0.880100786557D−07
12	5	0.130881403739D−05	0.140562434295D−05

Table A-4: (cont.) Tesseral and Sectorial Harmonic Coefficients for Mars50c

n	m	$\bar{C}_{nm}$	$\bar{S}_{nm}$
12	6	$-0.673178251723\mathrm{D}-06$	$-0.157083494651\mathrm{D}-05$
12	7	$0.294517324548\mathrm{D}-06$	$-0.158228247144\mathrm{D}-06$
12	8	$-0.170226706506\mathrm{D}-05$	$-0.396452890201\mathrm{D}-06$
12	9	$0.803475989972\mathrm{D}-06$	$0.489987802063\mathrm{D}-06$
12	10	$0.538936243709\mathrm{D}-06$	$0.143789813660\mathrm{D}-05$
12	11	$0.750453836744\mathrm{D}-06$	$-0.156253193668\mathrm{D}-05$
12	12	$-0.108426942456\mathrm{D}-07$	$-0.127625689215\mathrm{D}-06$
13	1	$-0.116157654916\mathrm{D}-05$	$0.727165007562\mathrm{D}-06$
13	2	$0.199407129798\mathrm{D}-06$	$0.630766606326\mathrm{D}-06$
13	3	$-0.170311035197\mathrm{D}-06$	$0.528329437565\mathrm{D}-06$
13	4	$0.357488299225\mathrm{D}-06$	$0.834269150794\mathrm{D}-06$
13	5	$-0.671824456273\mathrm{D}-06$	$-0.908788212065\mathrm{D}-06$
13	6	$0.329946959489\mathrm{D}-06$	$-0.936227671576\mathrm{D}-06$
13	7	$-0.545945058714\mathrm{D}-06$	$0.540894350996\mathrm{D}-06$
13	8	$-0.121383633822\mathrm{D}-07$	$0.900945617440\mathrm{D}-07$
13	9	$0.101806453979\mathrm{D}-05$	$0.925047097170\mathrm{D}-06$
13	10	$-0.832276152927\mathrm{D}-07$	$-0.740625789546\mathrm{D}-06$
13	11	$0.818834052946\mathrm{D}-06$	$-0.931654872731\mathrm{D}-06$
13	12	$-0.148613779707\mathrm{D}-05$	$-0.337593775696\mathrm{D}-06$
13	13	$0.490423074112\mathrm{D}-06$	$0.854388138909\mathrm{D}-06$
14	1	$0.113989065748\mathrm{D}-05$	$0.836423389669\mathrm{D}-07$
14	2	$0.396567859225\mathrm{D}-06$	$-0.359163227676\mathrm{D}-06$
14	3	$0.738029261652\mathrm{D}-06$	$-0.589776024107\mathrm{D}-06$
14	4	$-0.647584810251\mathrm{D}-07$	$-0.953646259357\mathrm{D}-06$
14	5	$0.377631492911\mathrm{D}-06$	$-0.460961663349\mathrm{D}-06$
14	6	$-0.391009963432\mathrm{D}-06$	$-0.616404002178\mathrm{D}-08$
14	7	$-0.880650788852\mathrm{D}-06$	$0.235999415324\mathrm{D}-06$
14	8	$0.566476205161\mathrm{D}-06$	$0.368440967706\mathrm{D}-06$
14	9	$0.215580122913\mathrm{D}-06$	$0.918463769687\mathrm{D}-06$
14	10	$-0.246156756021\mathrm{D}-06$	$-0.144208991596\mathrm{D}-05$
14	11	$-0.889384049227\mathrm{D}-06$	$0.186652043336\mathrm{D}-06$
14	12	$-0.493568496043\mathrm{D}-06$	$-0.361271637182\mathrm{D}-06$
14	13	$0.943509653845\mathrm{D}-06$	$0.198378324659\mathrm{D}-05$
14	14	$-0.251035046400\mathrm{D}-07$	$-0.769520740452\mathrm{D}-06$
15	1	$0.488368237627\mathrm{D}-07$	$0.275000436214\mathrm{D}-06$
15	2	$-0.419940952223\mathrm{D}-06$	$-0.849436935494\mathrm{D}-06$
15	3	$-0.823808468326\mathrm{D}-06$	$-0.145805804443\mathrm{D}-06$
15	4	$-0.684092787970\mathrm{D}-06$	$-0.793343028438\mathrm{D}-06$
15	5	$-0.163033075959\mathrm{D}-05$	$-0.698430505020\mathrm{D}-06$

Table A-4: (cont.) Tesseral and Sectorial Harmonic Coefficients for Mars50c

n	m	C_{nm}	S_{nm}
15	6	0.678254672503D−07	0.548702265549D−06
15	7	0.128844302331D−05	0.201934767012D−06
15	8	0.137560156395D−05	0.464014346899D−06
15	9	−0.308309543225D−06	−0.343280470537D−06
15	10	−0.500474142466D−07	−0.414256218027D−06
15	11	−0.915004242739D−06	0.657490101043D−06
15	12	0.998051437998D−06	0.718425107319D−06
15	13	−0.195265947211D−07	0.697130989896D−06
15	14	0.895354479261D−07	−0.137359167723D−05
15	15	−0.391904000704D−06	0.109654629833D−06
16	1	−0.146571435746D−06	−0.477986185031D−06
16	2	−0.433836125172D−06	−0.919322035075D−07
16	3	−0.519790674538D−06	0.242960922398D−06
16	4	−0.895459018679D−06	0.487610238224D−07
16	5	0.207154561401D−06	0.695889305395D−06
16	6	0.231431903769D−06	0.158964017471D−06
16	7	0.212340362835D−06	0.260260981808D−06
16	8	0.697327537499D−07	0.320004929138D−06
16	9	−0.216269107129D−06	−0.106535994156D−05
16	10	−0.590086083260D−06	0.471477806049D−06
16	11	0.103927336356D−07	−0.461287564577D−06
16	12	0.495660177889D−06	0.724310222300D−06
16	13	0.973226327861D−07	−0.669496615132D−06
16	14	−0.134954321144D−06	−0.852703354341D−06
16	15	−0.763923621211D−06	0.378793945791D−06
16	16	0.268136244954D−06	0.660883051773D−07
17	1	−0.123950773795D−06	−0.896138796426D−06
17	2	−0.575083834744D−07	0.175431492233D−06
17	3	0.675910579289D−07	0.137156850402D−06
17	4	0.531213159090D−06	0.444608364231D−07
17	5	0.550656672744D−06	0.343988054121D−06
17	6	0.731597068633D−06	−0.171166237196D−06
17	7	0.582069037722D−06	−0.355753253276D−06
17	8	−0.133069952097D−06	−0.247800691498D−06
17	9	−0.181076890190D−06	−0.122229108397D−06
17	10	−0.330881739744D−06	0.929014764021D−07

Table A-4: (cont.) Tesseral and Sectorial Harmonic Coefficients for Mars50c

n	m	$\bar{C}_{nm}$	$\bar{S}_{nm}$
17	11	0.315594769386D$-$06	0.665056302759D$-$07
17	12	0.138703833636D$-$06	$-$0.375237631283D$-$07
17	13	$-$0.488897282836D$-$06	$-$0.625081651348D$-$06
17	14	$-$0.357791610917D$-$06	$-$0.410466832147D$-$06
17	15	$-$0.355862049163D$-$06	0.527713352294D$-$06
17	16	0.113093899119D$-$05	0.551896091938D$-$06
17	17	0.107900030599D$-$06	0.337819418165D$-$06
18	1	$-$0.322427941902D$-$06	$-$0.144897429561D$-$06
18	2	$-$0.165489642279D$-$06	0.167583953054D$-$06
18	3	$-$0.450575862365D$-$06	$-$0.419319303612D$-$06
18	4	0.770409588360D$-$06	0.304994712822D$-$06
18	5	0.272471868479D$-$06	$-$0.705929272090D$-$06
18	6	0.112051106108D$-$06	$-$0.603057965680D$-$06
18	7	$-$0.267280986730D$-$06	0.194696920755D$-$07
18	8	$-$0.532667333492D$-$07	$-$0.242325288245D$-$06
18	9	$-$0.358834867726D$-$07	0.227445226011D$-$06
18	10	0.533629785189D$-$06	0.202164550127D$-$06
18	11	0.384435187578D$-$06	$-$0.234774677542D$-$06
18	12	0.571854379548D$-$07	$-$0.411966907665D$-$07
18	13	$-$0.348626956925D$-$06	$-$0.175292734906D$-$06
18	14	$-$0.499804087016D$-$06	0.216699040696D$-$06
18	15	0.347930744287D$-$06	0.773084195293D$-$06
18	16	0.424628349724D$-$06	0.155954545416D$-$06
18	17	$-$0.160225561358D$-$06	$-$0.108249638128D$-$05
18	18	0.502526713811D$-$06	0.306879789080D$-$06
19	1	0.431653384663D$-$06	0.360749964560D$-$06
19	2	$-$0.975699313895D$-$07	0.136217005230D$-$06
19	3	0.142905418288D$-$07	$-$0.218023846594D$-$06
19	4	$-$0.437182375465D$-$07	0.429770864452D$-$06
19	5	0.543138704591D$-$07	$-$0.356811607183D$-$06
19	6	$-$0.159468836066D$-$06	$-$0.826647381841D$-$07
19	7	$-$0.427647224967D$-$06	0.127481863822D$-$06
19	8	0.293719663721D$-$06	$-$0.144873389049D$-$06
19	9	0.142302567115D$-$06	0.372160855662D$-$06
19	10	0.637325008324D$-$06	$-$0.188021013383D$-$06

Table A-4: (cont.) Tesseral and Sectorial Harmonic Coefficients for Mars50c

n	m	$\bar{C}_{nm}$	$\bar{S}_{nm}$
19	11	$-0.283414678615\mathrm{D}-06$	$-0.398421933197\mathrm{D}-06$
19	12	$-0.239144590294\mathrm{D}-06$	$-0.145171212420\mathrm{D}-06$
19	13	$-0.245709869050\mathrm{D}-06$	$-0.846038897859\mathrm{D}-07$
19	14	$0.212786874315\mathrm{D}-06$	$0.447850969436\mathrm{D}-06$
19	15	$0.683529042031\mathrm{D}-06$	$0.438374824955\mathrm{D}-06$
19	16	$-0.146097177196\mathrm{D}-06$	$-0.188643587354\mathrm{D}-06$
19	17	$-0.154870469047\mathrm{D}-06$	$-0.749093158592\mathrm{D}-06$
19	18	$-0.615123076598\mathrm{D}-06$	$0.535791296332\mathrm{D}-06$
19	19	$-0.412239771169\mathrm{D}-06$	$-0.813439822956\mathrm{D}-06$
20	1	$0.194903089617\mathrm{D}-06$	$0.437432561589\mathrm{D}-06$
20	2	$0.610899157592\mathrm{D}-07$	$-0.289410984813\mathrm{D}-06$
20	3	$0.118392865149\mathrm{D}-06$	$0.204371724986\mathrm{D}-06$
20	4	$-0.222886492877\mathrm{D}-06$	$0.400629906600\mathrm{D}-06$
20	5	$-0.677150869887\mathrm{D}-07$	$-0.761274840950\mathrm{D}-07$
20	6	$0.287586043050\mathrm{D}-06$	$0.629725922496\mathrm{D}-06$
20	7	$0.245275527495\mathrm{D}-06$	$-0.325572489742\mathrm{D}-06$
20	8	$0.426143456711\mathrm{D}-06$	$0.166648640046\mathrm{D}-06$
20	9	$-0.462618455189\mathrm{D}-07$	$0.936724491694\mathrm{D}-07$
20	10	$-0.373595691451\mathrm{D}-06$	$-0.336942349277\mathrm{D}-07$
20	11	$-0.119047212461\mathrm{D}-07$	$-0.847505346729\mathrm{D}-07$
20	12	$-0.440640724286\mathrm{D}-06$	$-0.598213061471\mathrm{D}-08$
20	13	$0.609406476295\mathrm{D}-07$	$0.216239425806\mathrm{D}-06$
20	14	$0.375102497716\mathrm{D}-06$	$0.168547566271\mathrm{D}-06$
20	15	$0.284248949906\mathrm{D}-06$	$-0.423067344167\mathrm{D}-06$
20	16	$0.235746984773\mathrm{D}-06$	$-0.252717874987\mathrm{D}-06$
20	17	$-0.209385860816\mathrm{D}-06$	$-0.297554465778\mathrm{D}-07$
20	18	$0.518156550911\mathrm{D}-07$	$0.722624953757\mathrm{D}-06$
20	19	$0.265902459955\mathrm{D}-06$	$-0.138952738638\mathrm{D}-06$
20	20	$-0.432422123770\mathrm{D}-06$	$0.185282363539\mathrm{D}-06$
21	1	$-0.197337569401\mathrm{D}-06$	$-0.924239300593\mathrm{D}-07$
21	2	$0.172466386837\mathrm{D}-06$	$-0.302364474829\mathrm{D}-06$
21	3	$-0.120400832146\mathrm{D}-06$	$0.101793945760\mathrm{D}-06$
21	4	$-0.184001883371\mathrm{D}-06$	$0.248610318949\mathrm{D}-07$
21	5	$0.506655263473\mathrm{D}-06$	$0.140339481499\mathrm{D}-06$
21	6	$0.969970324895\mathrm{D}-07$	$0.210511435387\mathrm{D}-06$
21	7	$0.152310270141\mathrm{D}-06$	$-0.389071817981\mathrm{D}-06$
21	8	$-0.182827055200\mathrm{D}-07$	$0.220851088659\mathrm{D}-06$
21	9	$-0.126372331381\mathrm{D}-06$	$-0.195349647054\mathrm{D}-06$
21	10	$-0.365010618904\mathrm{D}-06$	$0.200332141692\mathrm{D}-06$

Table A-4: (cont.) Tesseral and Sectorial Harmonic Coefficients for Mars50c

n	m	$\bar{C}_{nm}$	$\bar{S}_{nm}$
21	11	$-0.177206992560\text{D}-06$	$-0.234120096082\text{D}-06$
21	12	$0.175859291180\text{D}-06$	$-0.537104936891\text{D}-07$
21	13	$0.116914389414\text{D}-06$	$0.168703127376\text{D}-06$
21	14	$0.111580198703\text{D}-06$	$-0.365209801482\text{D}-06$
21	15	$-0.357183944018\text{D}-06$	$-0.519977038370\text{D}-06$
21	16	$-0.400192057411\text{D}-06$	$-0.145686770495\text{D}-11$
21	17	$-0.317486460879\text{D}-06$	$-0.300548028585\text{D}-06$
21	18	$0.351650994189\text{D}-06$	$0.583821705688\text{D}-06$
21	19	$0.193831079546\text{D}-07$	$-0.502685404381\text{D}-06$
21	20	$-0.249576024707\text{D}-06$	$-0.439429613674\text{D}-06$
21	21	$0.739134669161\text{D}-06$	$0.229680574057\text{D}-06$
22	1	$-0.163836199971\text{D}-06$	$-0.208085542205\text{D}-06$
22	2	$0.158465589671\text{D}-06$	$0.174755702672\text{D}-06$
22	3	$-0.247766585012\text{D}-06$	$0.731045671043\text{D}-07$
22	4	$0.170891036849\text{D}-06$	$-0.239372069599\text{D}-06$
22	5	$0.106028055958\text{D}-06$	$0.152520825831\text{D}-06$
22	6	$-0.783216002116\text{D}-07$	$-0.270183113540\text{D}-06$
22	7	$0.401305876619\text{D}-06$	$-0.365280658889\text{D}-07$
22	8	$-0.181992749200\text{D}-06$	$-0.256933196103\text{D}-06$
22	9	$-0.400281576026\text{D}-08$	$0.177258217959\text{D}-06$
22	10	$-0.587797365200\text{D}-07$	$0.392377281124\text{D}-06$
22	11	$0.925369171343\text{D}-07$	$-0.519496179183\text{D}-07$
22	12	$0.371507550710\text{D}-06$	$0.133261544899\text{D}-06$
22	13	$-0.163806004416\text{D}-06$	$-0.155267450272\text{D}-06$
22	14	$-0.520305696793\text{D}-08$	$-0.543489117628\text{D}-06$
22	15	$-0.333401361423\text{D}-06$	$0.242705951891\text{D}-06$
22	16	$-0.131169441950\text{D}-06$	$-0.665018953393\text{D}-07$
22	17	$0.186748175912\text{D}-06$	$0.204921209966\text{D}-06$
22	18	$-0.150605587408\text{D}-06$	$0.132304862851\text{D}-06$
22	19	$0.281316677750\text{D}-06$	$-0.686840013370\text{D}-06$
22	20	$-0.376843396631\text{D}-06$	$0.188868951222\text{D}-06$
22	21	$0.235215196336\text{D}-06$	$0.651434581808\text{D}-06$
22	22	$-0.226629219837\text{D}-06$	$-0.413504561303\text{D}-06$
23	1	$0.123171901135\text{D}-06$	$0.280167732355\text{D}-06$
23	2	$0.110148406407\text{D}-06$	$0.418425922378\text{D}-06$
23	3	$-0.212544014064\text{D}-07$	$-0.780286972014\text{D}-07$
23	4	$0.321419821052\text{D}-06$	$0.180516891379\text{D}-08$
23	5	$-0.337650739952\text{D}-06$	$0.396586692672\text{D}-07$

Table A-4: (cont.) Tesseral and Sectorial Harmonic Coefficients for Mars50c

n	m	$\bar{C}_{nm}$	$\bar{S}_{nm}$
23	6	0.197754904477D−06	−0.284209773511D−06
23	7	−0.130062912148D−06	0.136559361124D−06
23	8	−0.197915513701D−06	−0.232349385415D−06
23	9	−0.987621655339D−08	0.121854161391D−06
23	10	−0.160549180767D−06	0.298925554929D−08
23	11	0.325950129001D−06	−0.663338901065D−07
23	12	−0.236167942362D−06	0.472125557766D−07
23	13	−0.101171556236D−06	0.352249396674D−08
23	14	−0.143503402140D−06	−0.181051880504D−06
23	15	−0.186432659779D−06	0.604146831133D−06
23	16	0.448830357759D−06	0.139726410148D−06
23	17	0.418981451817D−06	0.732410506430D−06
23	18	−0.227721136118D−06	−0.589488347754D−06
23	19	0.523347857815D−06	0.879326327729D−07
23	20	−0.505095722848D−06	0.790975467947D−07
23	21	0.362655308018D−06	0.667675393158D−06
23	22	−0.171728944719D−07	−0.128046908547D−06
23	23	−0.638681905004D−06	0.293597348197D−06
24	1	0.845320164875D−07	0.171836683405D−06
24	2	0.342367333660D−07	0.464783678534D−07
24	3	0.202542884064D−06	−0.255181610114D−06
24	4	−0.103624405849D−06	0.147927289361D−06
24	5	−0.157606210655D−06	−0.179227506461D−06
24	6	0.178246944609D−06	0.818393207073D−07
24	7	−0.420600153995D−06	0.184808520968D−06
24	8	0.155302955474D−06	−0.101994834211D−07
24	9	−0.107999298326D−06	0.187829357050D−06
24	10	−0.908600393447D−07	−0.391717340954D−06
24	11	−0.359936284840D−07	0.129998444180D−06
24	12	−0.325148237352D−06	−0.218485291793D−06
24	13	0.451093312898D−07	0.487981972098D−07
24	14	−0.618524579090D−07	0.354661066910D−06
24	15	0.165019639170D−06	−0.932853736512D−08
24	16	0.527099796294D−06	0.264663905387D−06
24	17	−0.670277450815D−07	−0.164027498957D−06
24	18	0.280993402294D−06	−0.646052714797D−06
24	19	−0.390970415257D−06	0.376025485391D−06
24	20	−0.396394839801D−07	−0.318202136437D−06

Table A-4: (cont.) Tesseral and Sectorial Harmonic Coefficients for Mars50c

n	m	$\bar{C}_{nm}$	$\bar{S}_{nm}$
24	21	0.118030823146D−06	0.470386289655D−06
24	22	−0.204201803466D−07	−0.585394740589D−06
24	23	−0.535439314676D−06	0.162459297708D−06
24	24	0.449342838403D−06	0.101603891792D−06
25	1	−0.509073460693D−07	−0.248566601823D−06
25	2	−0.662822694519D−07	−0.256010274982D−06
25	3	0.587337138017D−07	−0.661956305269D−07
25	4	−0.310210377388D−06	−0.567733859159D−08
25	5	0.551960919486D−07	−0.206663962314D−06
25	6	−0.198905651065D−06	0.312335889335D−06
25	7	0.668409262457D−07	0.275159135230D−07
25	8	0.309024715865D−06	0.102840382227D−06
25	9	−0.613989477185D−08	−0.201075966856D−07
25	10	0.162399226382D−06	−0.869368219006D−07
25	11	−0.280921712717D−06	0.214888379321D−06
25	12	−0.880498929972D−07	−0.180810988630D−06
25	13	0.168560882105D−06	0.351860290796D−07
25	14	0.353710045287D−07	0.904928662669D−07
25	15	0.260859144244D−06	−0.232070082848D−06
25	16	0.150623198563D−06	0.448658214245D−07
25	17	−0.283510994422D−06	−0.708306548304D−06
25	18	0.551369617473D−07	−0.101670336688D−06
25	19	−0.505364456862D−06	−0.653757113804D−07
25	20	0.321454634673D−06	0.567843666686D−07
25	21	−0.545408537593D−06	0.269723746697D−06
25	22	0.214149849095D−06	−0.448739337543D−06
25	23	−0.391006458226D−06	0.466775569968D−06
25	24	0.403047166570D−06	−0.317173373691D−08
25	25	0.114971043802D−06	−0.382135286992D−06
26	1	−0.116078881285D−06	−0.264146209299D−06
26	2	−0.140760039213D−06	−0.298565089752D−07
26	3	−0.926661158092D−07	0.184567828246D−06
26	4	−0.396057676461D−07	0.195228192966D−07
26	5	0.227736681591D−06	0.180429824449D−06
26	6	−0.173144367613D−06	0.529181709687D−07
26	7	0.287613640742D−06	−0.157904165552D−06
26	8	0.795364028549D−07	0.107376759677D−06
26	9	0.120634106923D−06	−0.383836639869D−06
26	10	0.159242959946D−06	0.120490893409D−06

Table A-4: (cont.) Tesseral and Sectorial Harmonic Coefficients for Mars50c

n	m	$\bar{C}_{nm}$	$\bar{S}_{nm}$
26	11	$-0.234764912220\mathrm{D}{-}06$	$-0.108008057405\mathrm{D}{-}06$
26	12	$0.104922041511\mathrm{D}{-}06$	$0.229295814739\mathrm{D}{-}08$
26	13	$0.853075525495\mathrm{D}{-}08$	$-0.521991300256\mathrm{D}{-}07$
26	14	$0.115174904279\mathrm{D}{-}06$	$-0.140614568763\mathrm{D}{-}06$
26	15	$-0.289333016155\mathrm{D}{-}08$	$-0.364562523654\mathrm{D}{-}07$
26	16	$-0.304552868678\mathrm{D}{-}06$	$-0.126713473140\mathrm{D}{-}06$
26	17	$-0.520804378649\mathrm{D}{-}07$	$-0.177737734821\mathrm{D}{-}06$
26	18	$-0.218173256398\mathrm{D}{-}06$	$0.430756845144\mathrm{D}{-}06$
26	19	$0.450446241717\mathrm{D}{-}07$	$-0.152653445838\mathrm{D}{-}06$
26	20	$0.256204594786\mathrm{D}{-}06$	$0.375566265045\mathrm{D}{-}06$
26	21	$-0.299216713114\mathrm{D}{-}06$	$-0.372565520752\mathrm{D}{-}06$
26	22	$0.424710688680\mathrm{D}{-}06$	$0.427328415230\mathrm{D}{-}07$
26	23	$-0.187278051288\mathrm{D}{-}06$	$0.210072563541\mathrm{D}{-}06$
26	24	$0.535649922850\mathrm{D}{-}06$	$-0.553738394350\mathrm{D}{-}07$
26	25	$0.174458058109\mathrm{D}{-}06$	$-0.359548772088\mathrm{D}{-}06$
26	26	$-0.207128263830\mathrm{D}{-}06$	$0.490986468381\mathrm{D}{-}06$
27	1	$0.276536236233\mathrm{D}{-}07$	$0.108882059315\mathrm{D}{-}07$
27	2	$-0.997684871347\mathrm{D}{-}07$	$0.165766540562\mathrm{D}{-}06$
27	3	$-0.177638776978\mathrm{D}{-}07$	$0.155217068346\mathrm{D}{-}06$
27	4	$0.269794980781\mathrm{D}{-}06$	$-0.125737636137\mathrm{D}{-}08$
27	5	$0.876305091114\mathrm{D}{-}07$	$0.229145642073\mathrm{D}{-}06$
27	6	$0.539278188439\mathrm{D}{-}07$	$-0.228042365720\mathrm{D}{-}06$
27	7	$0.112736314195\mathrm{D}{-}06$	$-0.119186573270\mathrm{D}{-}06$
27	8	$-0.103326335154\mathrm{D}{-}06$	$-0.121516848953\mathrm{D}{-}06$
27	9	$0.380402446444\mathrm{D}{-}07$	$-0.258072605461\mathrm{D}{-}06$
27	10	$-0.144672213145\mathrm{D}{-}06$	$0.103943274807\mathrm{D}{-}07$
27	11	$-0.199474502816\mathrm{D}{-}06$	$-0.168395729943\mathrm{D}{-}06$
27	12	$0.725592682310\mathrm{D}{-}07$	$0.129514769575\mathrm{D}{-}06$
27	13	$-0.151003229257\mathrm{D}{-}06$	$-0.141062512924\mathrm{D}{-}06$
27	14	$0.539725009371\mathrm{D}{-}07$	$0.768257144043\mathrm{D}{-}07$
27	15	$-0.107275035299\mathrm{D}{-}06$	$0.574027272844\mathrm{D}{-}07$
27	16	$-0.963302096937\mathrm{D}{-}07$	$-0.799746557926\mathrm{D}{-}07$
27	17	$0.142784093434\mathrm{D}{-}06$	$0.368462058009\mathrm{D}{-}06$
27	18	$-0.839590971191\mathrm{D}{-}07$	$0.156608812894\mathrm{D}{-}06$
27	19	$0.466621801299\mathrm{D}{-}06$	$0.133302855510\mathrm{D}{-}06$
27	20	$-0.828226674172\mathrm{D}{-}07$	$-0.263701603675\mathrm{D}{-}07$

Table A-4: (cont.) Tesseral and Sectorial Harmonic Coefficients for Mars50c

n	m	$\bar{C}_{nm}$	$\bar{S}_{nm}$
27	21	0.168936705595D−06	−0.277749156562D−06
27	22	0.672756445277D−07	0.320142652997D−06
27	23	0.429773488114D−07	−0.273416790581D−06
27	24	0.127832616929D−06	0.341709532900D−08
27	25	−0.126875689546D−06	−0.496638831866D−06
27	26	−0.247554663873D−06	0.270324345658D−06
27	27	0.438011809305D−06	−0.160415335107D−06
28	1	0.131154094216D−06	0.149238560348D−06
28	2	0.672152109057D−07	0.609367498891D−07
28	3	0.118072371192D−06	−0.779526132368D−07
28	4	0.175963117757D−06	−0.111884193087D−06
28	5	−0.806949976143D−07	−0.894022985544D−07
28	6	0.105117428616D−06	−0.184298715467D−06
28	7	−0.169035430495D−06	0.228462761617D−07
28	8	−0.172354625189D−06	−0.146471894138D−06
28	9	−0.477798904383D−07	0.155596523234D−06
28	10	−0.197559350122D−06	0.545478311491D−07
28	11	0.147562049341D−06	0.112065984325D−06
28	12	−0.119784754037D−07	0.107696839364D−06
28	13	0.310178263843D−07	0.506193455705D−07
28	14	0.231949860476D−07	0.161032286404D−06
28	15	−0.295542708274D−07	0.357982376764D−07
28	16	0.179489745538D−06	−0.251005077739D−08
28	17	0.135992649530D−06	0.227192978189D−06
28	18	0.126433706142D−06	−0.234156418425D−06
28	19	0.230721968937D−06	0.386534547396D−07
28	20	−0.126734209236D−06	−0.369976169875D−06
28	21	0.161614647514D−06	−0.108791758083D−07
28	22	−0.264904969312D−06	−0.259521676741D−07
28	23	0.344762481441D−06	−0.670478521782D−07
28	24	−0.235662386265D−06	0.478528304501D−07
28	25	0.155115817607D−07	−0.288350711445D−06
28	26	−0.218918636059D−06	0.522006985023D−06
28	27	0.260382479798D−06	−0.442672335602D−08
28	28	−0.323595953698D−06	−0.335488754901D−06

Table A-4: (cont.) Tesseral and Sectorial Harmonic Coefficients for Mars50c

n	m	$\bar{C}_{nm}$	$\bar{S}_{nm}$
29	1	$-0.292982077383D-07$	$0.657049259751D-07$
29	2	$0.513138379265D-07$	$-0.919492731360D-07$
29	3	$-0.156584143425D-07$	$-0.169080574690D-06$
29	4	$-0.104364219035D-06$	$-0.357803503487D-07$
29	5	$-0.170256610283D-06$	$-0.143165583041D-06$
29	6	$-0.432997183900D-07$	$0.420848249532D-07$
29	7	$-0.161552278184D-06$	$0.111299238319D-06$
29	8	$-0.123066332776D-07$	$0.119057583731D-06$
29	9	$-0.158021618374D-07$	$0.211050965555D-06$
29	10	$0.761363967184D-07$	$0.572340425985D-07$
29	11	$0.207101702791D-06$	$0.382870403366D-07$
29	12	$-0.173422532548D-07$	$-0.551496552208D-07$
29	13	$0.151799385876D-06$	$0.623334144790D-07$
29	14	$0.325375175979D-07$	$-0.631073359865D-07$
29	15	$0.259591768939D-07$	$-0.357707313611D-08$
29	16	$0.561127191633D-07$	$0.268347402310D-07$
29	17	$0.355122195435D-08$	$-0.782630791766D-07$
29	18	$0.146429412351D-07$	$-0.205883993578D-06$
29	19	$-0.243915179010D-06$	$-0.922512835278D-07$
29	20	$-0.592480575353D-07$	$-0.204828231324D-06$
29	21	$-0.110944078962D-06$	$0.172421232576D-06$
29	22	$-0.959846436755D-07$	$-0.427552571238D-07$
29	23	$0.123209238720D-06$	$0.227849063941D-06$
29	24	$-0.918821898612D-07$	$-0.121069832525D-06$
29	25	$0.218180879406D-06$	$0.229799363457D-06$
29	26	$-0.957371601915D-07$	$0.141301598007D-06$
29	27	$0.356073138915D-06$	$-0.597708769378D-07$
29	28	$0.263862154736D-07$	$-0.145967247419D-06$
29	29	$-0.184856132304D-06$	$0.275868920862D-06$
30	1	$-0.598681987738D-07$	$-0.713453316704D-07$
30	2	$-0.246218371027D-07$	$-0.121329628794D-07$
30	3	$-0.676615681755D-07$	$0.129599090581D-07$
30	4	$-0.157015557695D-06$	$0.352870509445D-07$
30	5	$-0.453742576515D-07$	$0.436547224500D-07$

Table A-4: (cont.) Tesseral and Sectorial Harmonic Coefficients for Mars50c

n	m	$\bar{C}_{nm}$	$\bar{S}_{nm}$
30	6	$-0.214752315904\mathrm{D}-07$	$0.153164696691\mathrm{D}-06$
30	7	$0.270495786482\mathrm{D}-07$	$0.521160025321\mathrm{D}-07$
30	8	$0.186993050991\mathrm{D}-06$	$0.113219377679\mathrm{D}-06$
30	9	$0.190829606163\mathrm{D}-07$	$0.748199973868\mathrm{D}-08$
30	10	$0.151424615947\mathrm{D}-06$	$-0.149848875474\mathrm{D}-06$
30	11	$-0.506452664529\mathrm{D}-07$	$-0.511478064836\mathrm{D}-07$
30	12	$-0.472245666954\mathrm{D}-07$	$-0.126463035464\mathrm{D}-06$
30	13	$-0.686620817548\mathrm{D}-07$	$-0.301290297354\mathrm{D}-07$
30	14	$-0.644928596505\mathrm{D}-07$	$-0.103442599115\mathrm{D}-06$
30	15	$0.198259697799\mathrm{D}-07$	$0.142813624743\mathrm{D}-07$
30	16	$0.954211318720\mathrm{D}-08$	$-0.128425190460\mathrm{D}-07$
30	17	$-0.740571217819\mathrm{D}-07$	$0.160644875889\mathrm{D}-09$
30	18	$-0.632182859890\mathrm{D}-07$	$0.167255288181\mathrm{D}-07$
30	19	$-0.218807547947\mathrm{D}-06$	$0.956651882656\mathrm{D}-07$
30	20	$0.669054417752\mathrm{D}-07$	$0.176680838599\mathrm{D}-06$
30	21	$-0.660337940756\mathrm{D}-07$	$0.108816870025\mathrm{D}-06$
30	22	$0.181893657998\mathrm{D}-06$	$0.186209510667\mathrm{D}-07$
30	23	$-0.203992006684\mathrm{D}-07$	$0.152631702462\mathrm{D}-06$
30	24	$0.100696925740\mathrm{D}-06$	$-0.119717867652\mathrm{D}-06$
30	25	$-0.627326740285\mathrm{D}-08$	$0.177969559312\mathrm{D}-06$
30	26	$0.470134044765\mathrm{D}-07$	$-0.382366062798\mathrm{D}-06$
30	27	$0.136556723990\mathrm{D}-06$	$-0.881741675474\mathrm{D}-07$
30	28	$-0.229768035089\mathrm{D}-06$	$-0.216666763860\mathrm{D}-06$
30	29	$-0.693734336361\mathrm{D}-07$	$-0.104515943248\mathrm{D}-07$
30	30	$0.267308346821\mathrm{D}-06$	$-0.107681673725\mathrm{D}-06$
31	1	$-0.504193570881\mathrm{D}-07$	$-0.269842497494\mathrm{D}-07$
31	2	$-0.366902881005\mathrm{D}-07$	$0.375165824885\mathrm{D}-07$
31	3	$-0.167904852075\mathrm{D}-07$	$0.149002408440\mathrm{D}-06$
31	4	$-0.941952907338\mathrm{D}-08$	$0.523266625865\mathrm{D}-07$
31	5	$0.151682429011\mathrm{D}-06$	$0.437812018751\mathrm{D}-07$
31	6	$0.439686117468\mathrm{D}-07$	$0.472415368574\mathrm{D}-07$
31	7	$0.179914395640\mathrm{D}-06$	$-0.658078666371\mathrm{D}-07$
31	8	$0.464288761977\mathrm{D}-07$	$-0.735256362974\mathrm{D}-07$
31	9	$0.225285783369\mathrm{D}-07$	$-0.108899304318\mathrm{D}-06$
31	10	$-0.867888321499\mathrm{D}-07$	$-0.517049158445\mathrm{D}-07$

Table A-4: (cont.) Tesseral and Sectorial Harmonic Coefficients for Mars50c

n	m	$\bar{C}_{nm}$	$\bar{S}_{nm}$
31	11	$-0.657695326927D-07$	$0.982642950041D-08$
31	12	$-0.106886329987D-06$	$0.182884565319D-07$
31	13	$-0.773696990473D-07$	$0.978748763220D-07$
31	14	$-0.779060432588D-07$	$0.435124198987D-07$
31	15	$0.156681089978D-07$	$-0.286798476556D-08$
31	16	$-0.642460313855D-07$	$0.362744102459D-07$
31	17	$-0.156125180588D-07$	$0.946910813953D-07$
31	18	$0.606478695511D-07$	$0.389682962021D-07$
31	19	$0.346738378504D-07$	$0.108785818687D-06$
31	20	$0.195065667993D-06$	$0.130671606331D-06$
31	21	$0.125251897380D-06$	$-0.385373510597D-07$
31	22	$0.788792597977D-07$	$-0.438653544861D-07$
31	23	$-0.396321080875D-07$	$-0.100145158352D-06$
31	24	$0.746954224506D-07$	$0.331136839180D-07$
31	25	$-0.159171730914D-06$	$-0.259337283970D-07$
31	26	$0.118196731282D-06$	$-0.169904439562D-06$
31	27	$-0.706785105308D-07$	$-0.825218043825D-07$
31	28	$-0.858495461937D-07$	$-0.101778873432D-06$
31	29	$-0.214301534187D-07$	$0.191043101006D-06$
31	30	$-0.117746054355D-06$	$0.119803723594D-06$
31	31	$-0.107907708261D-06$	$0.632346288384D-07$
32	1	$0.358102681849D-08$	$0.545532802585D-08$
32	2	$0.853495385671D-07$	$0.145928890723D-07$
32	3	$0.171766348472D-07$	$0.387164509960D-07$
32	4	$0.127032770824D-06$	$-0.962194638611D-07$
32	5	$0.869260113776D-07$	$-0.167258285166D-11$

Table A-4: (cont.) Tesseral and Sectorial Harmonic Coefficients for Mars50c

n	m	$\bar{C}_{nm}$	$\bar{S}_{nm}$
32	6	$-0.406810525617\text{D}-07$	$-0.185529132996\text{D}-06$
32	7	$0.854034273560\text{D}-07$	$-0.620082213882\text{D}-07$
32	8	$-0.199240926794\text{D}-06$	$-0.307846524967\text{D}-07$
32	9	$-0.586392277381\text{D}-08$	$-0.923271909208\text{D}-07$
32	10	$-0.859316549338\text{D}-07$	$0.972758509090\text{D}-07$
32	11	$-0.703395572210\text{D}-07$	$0.100631419434\text{D}-07$
32	12	$0.108278010490\text{D}-07$	$0.820745310113\text{D}-07$
32	13	$0.103988249320\text{D}-06$	$0.779830335095\text{D}-07$
32	14	$0.795603193908\text{D}-07$	$0.369537699138\text{D}-07$
32	15	$0.599753226177\text{D}-07$	$-0.486497854688\text{D}-07$
32	16	$-0.854824162872\text{D}-07$	$0.931976053554\text{D}-08$
32	17	$0.772084270376\text{D}-07$	$0.718635012013\text{D}-08$
32	18	$0.116784548071\text{D}-07$	$-0.301918988455\text{D}-07$
32	19	$0.912492473453\text{D}-07$	$-0.892044717763\text{D}-07$
32	20	$0.591947463335\text{D}-07$	$-0.315396133426\text{D}-07$
32	21	$0.624114357232\text{D}-07$	$-0.137285188157\text{D}-06$
32	22	$-0.118989994522\text{D}-06$	$-0.708418755814\text{D}-07$
32	23	$-0.640542119897\text{D}-07$	$0.196309948309\text{D}-07$
32	24	$-0.115456220810\text{D}-06$	$0.810331092651\text{D}-07$
32	25	$-0.884767268722\text{D}-09$	$-0.524770166539\text{D}-07$
32	26	$-0.184523174167\text{D}-07$	$0.783851592846\text{D}-09$
32	27	$-0.283630744890\text{D}-07$	$-0.362881099935\text{D}-08$
32	28	$0.144125897760\text{D}-07$	$0.159300188010\text{D}-06$
32	29	$0.120170397272\text{D}-06$	$0.131661341905\text{D}-06$
32	30	$-0.177224409360\text{D}-07$	$-0.896833370862\text{D}-07$
32	31	$0.155996815722\text{D}-06$	$0.602689415123\text{D}-07$
32	32	$0.404759216025\text{D}-07$	$0.202046100901\text{D}-07$
33	1	$0.320501452065\text{D}-07$	$-0.802485664121\text{D}-07$
33	2	$0.267431533459\text{D}-07$	$0.345212535594\text{D}-07$
33	3	$-0.111194934912\text{D}-07$	$-0.683855716851\text{D}-07$
33	4	$0.774477232887\text{D}-07$	$-0.500172647723\text{D}-07$
33	5	$-0.917200067602\text{D}-07$	$0.395097322034\text{D}-07$

Table A-4: (cont.) Tesseral and Sectorial Harmonic Coefficients for Mars50c

n	m	$\bar{C}_{nm}$	$\bar{S}_{nm}$
33	6	$-0.644833170870\text{D}-07$	$-0.114251363184\text{D}-06$
33	7	$-0.110827101449\text{D}-06$	$0.112308078281\text{D}-06$
33	8	$-0.427736233621\text{D}-07$	$-0.118349173737\text{D}-07$
33	9	$0.291907162660\text{D}-07$	$0.557915193090\text{D}-07$
33	10	$-0.232904704376\text{D}-08$	$0.436256005118\text{D}-07$
33	11	$0.621242361992\text{D}-07$	$0.216790548520\text{D}-08$
33	12	$0.103363169850\text{D}-06$	$-0.570629766649\text{D}-08$
33	13	$0.388066549289\text{D}-07$	$-0.129551680193\text{D}-06$
33	14	$0.573416865123\text{D}-07$	$-0.983447238218\text{D}-08$
33	15	$-0.365753054166\text{D}-07$	$-0.244705725517\text{D}-07$
33	16	$0.325680999131\text{D}-07$	$-0.653146977881\text{D}-07$
33	17	$0.135751384032\text{D}-07$	$0.122700204140\text{D}-07$
33	18	$-0.967639185595\text{D}-07$	$-0.407344621493\text{D}-07$
33	19	$0.576133583062\text{D}-08$	$-0.733450938952\text{D}-07$
33	20	$-0.893105729027\text{D}-07$	$-0.325883873287\text{D}-07$
33	21	$-0.437508152933\text{D}-07$	$-0.917286725323\text{D}-07$
33	22	$-0.862688642576\text{D}-07$	$0.159544037492\text{D}-07$
33	23	$-0.666631308760\text{D}-07$	$0.102767566859\text{D}-06$
33	24	$0.322430237801\text{D}-07$	$0.103867404497\text{D}-06$
33	25	$0.496412352243\text{D}-07$	$-0.309163263912\text{D}-09$
33	26	$0.206295958953\text{D}-07$	$-0.521991685951\text{D}-07$
33	27	$0.172410908282\text{D}-06$	$0.570655940475\text{D}-07$
33	28	$0.266917167052\text{D}-07$	$0.272664356600\text{D}-07$
33	29	$0.158040152633\text{D}-06$	$-0.319261796289\text{D}-08$
33	30	$0.109053040145\text{D}-07$	$-0.243649932407\text{D}-06$
33	31	$-0.174216804485\text{D}-06$	$-0.752489701504\text{D}-07$
33	32	$0.162097677426\text{D}-06$	$-0.218089179047\text{D}-06$
33	33	$0.650121096304\text{D}-07$	$-0.212512515463\text{D}-06$
34	1	$0.215201879593\text{D}-07$	$-0.208871745456\text{D}-07$
34	2	$-0.101394321672\text{D}-06$	$0.190538276685\text{D}-07$
34	3	$0.149688694992\text{D}-07$	$-0.908834768782\text{D}-07$
34	4	$-0.460618824505\text{D}-07$	$0.855353830871\text{D}-07$
34	5	$-0.931339546479\text{D}-07$	$-0.416854615213\text{D}-07$
34	6	$0.605522795007\text{D}-07$	$0.991633093344\text{D}-07$
34	7	$-0.514627909045\text{D}-07$	$0.906040667168\text{D}-07$
34	8	$0.101361305855\text{D}-06$	$-0.444084507747\text{D}-07$
34	9	$0.822071417168\text{D}-07$	$0.979597219393\text{D}-07$
34	10	$0.158328903099\text{D}-07$	$-0.551398481619\text{D}-07$

Table A-4: (cont.) Tesseral and Sectorial Harmonic Coefficients for Mars50c

n	m	$\bar{C}_{nm}$	$\bar{S}_{nm}$
34	11	0.124026200410D−06	−0.569776782267D−07
34	12	0.334276220438D−09	−0.643899704816D−07
34	13	−0.616247666036D−07	−0.105209274794D−06
34	14	−0.349974216228D−07	0.506267303711D−07
34	15	−0.138174701564D−06	0.103069904672D−07
34	16	0.490551151389D−07	−0.383243982947D−07
34	17	−0.842530224440D−07	0.587555483518D−07
34	18	0.629222773793D−08	−0.373978583817D−07
34	19	−0.287446737164D−07	0.109907145710D−06
34	20	−0.225983591738D−07	−0.360103782951D−07
34	21	0.335010622825D−07	0.108258570389D−06
34	22	0.302249827954D−07	0.434424138997D−07
34	23	−0.957827573282D−08	0.691549884444D−08
34	24	0.124472669062D−06	−0.135187696359D−07
34	25	−0.349031947668D−07	−0.568792054466D−07
34	26	0.919683535295D−07	−0.152418998282D−06
34	27	0.300813295177D−07	0.466129989468D−07
34	28	0.741118757319D−07	−0.113838645542D−06
34	29	0.246701760672D−07	0.652324058126D−07
34	30	−0.393709943284D−07	−0.139658980970D−06
34	31	−0.171069318821D−06	−0.317489536829D−07
34	32	0.165035950038D−06	0.564203185987D−07
34	33	−0.321248509652D−06	0.386273370800D−07
34	34	0.254205433403D−07	0.879674432385D−07
35	1	0.603509720708D−08	0.115727541508D−06
35	2	−0.613481561554D−07	−0.545660727606D−07
35	3	0.782089202819D−07	0.175332860963D−07
35	4	−0.753348934847D−07	0.605428058618D−07
35	5	0.901851767545D−07	−0.430803421502D−07
35	6	0.435194508540D−07	0.116683870523D−06
35	7	0.177017658578D−07	−0.146703228677D−06
35	8	0.880347609809D−07	0.236578935423D−07
35	9	−0.862564714355D−07	−0.847928977258D−07
35	10	0.725814912163D−07	−0.100647403941D−06
35	11	−0.116525670203D−06	0.536141656717D−08
35	12	−0.892209301752D−07	−0.620244135771D−07
35	13	−0.178771755862D−07	0.580702448885D−07
35	14	−0.383485817337D−07	0.834301788301D−07
35	15	0.316448854364D−07	0.376950527826D−07

Table A-4: (cont.) Tesseral and Sectorial Harmonic Coefficients for Mars50c

n	m	$\bar{C}_{nm}$	$\bar{S}_{nm}$
35	16	0.230080554527D−07	0.397613266980D−07
35	17	−0.481723705245D−07	−0.523344518521D−07
35	18	0.104301947751D−06	0.790118707725D−08
35	19	−0.143582767498D−07	0.529456962190D−07
35	20	0.623713564902D−07	−0.572919727945D−07
35	21	0.746597184260D−07	0.107417887427D−06
35	22	0.349691139677D−07	−0.739900144266D−07
35	23	0.354014347241D−07	0.312704546360D−07
35	24	−0.419898710525D−07	−0.416087438051D−07
35	25	−0.269188912010D−09	−0.883824445039D−07
35	26	0.891911760032D−08	0.818852296959D−08
35	27	−0.116812716266D−06	−0.822541310319D−07
35	28	0.124912578978D−06	0.126925038974D−07
35	29	−0.120494483309D−06	0.659737995662D−08
35	30	0.879411478535D−07	0.183588539645D−07
35	31	−0.649905446225D−07	0.557337066315D−08
35	32	0.159858300531D−06	0.144656802197D−06
35	33	−0.133775605053D−06	−0.233676402760D−06
35	34	0.241067883151D−06	0.251615746158D−06
35	35	0.143225952106D−06	0.205275005522D−06
36	1	−0.332288776170D−07	0.249859863781D−07
36	2	0.852051567616D−07	−0.104806506209D−06
36	3	0.455746656885D−08	0.100494458216D−06
36	4	−0.580688714756D−07	−0.108125778601D−06
36	5	0.116504520501D−06	0.326472068831D−07
36	6	−0.904770462356D−07	−0.911861899639D−08
36	7	0.691222275000D−07	−0.982725350448D−07
36	8	−0.239053131160D−07	0.457402612177D−07
36	9	−0.974637706875D−07	−0.748160837880D−07
36	10	−0.114702216118D−08	0.293799316124D−07
36	11	−0.883577782430D−07	0.710270337946D−07
36	12	−0.104779382028D−07	0.219706699381D−07
36	13	0.661558795643D−08	0.920558189558D−07
36	14	−0.151050076649D−07	−0.126243362263D−07
36	15	0.142681543982D−06	0.245847678265D−07
36	16	−0.258794508499D−07	0.326316597265D−07
36	17	0.151432398226D−07	−0.881976189463D−07
36	18	0.162116050666D−07	0.526484333490D−07
36	19	−0.285666612353D−07	−0.885895695772D−07
36	20	0.358438594964D−07	0.538287988630D−07

Table A-4: (cont.) Tesseral and Sectorial Harmonic Coefficients for Mars50c

n	m	C_{nm}	S_{nm}
36	21	$-0.843586039920\text{D}-08$	$-0.451276740069\text{D}-07$
36	22	$0.474261503945\text{D}-09$	$-0.151331172033\text{D}-07$
36	23	$0.130998443696\text{D}-08$	$0.165334318968\text{D}-07$
36	24	$-0.674692126348\text{D}-07$	$-0.240099935452\text{D}-07$
36	25	$0.583025363205\text{D}-07$	$-0.264642684240\text{D}-07$
36	26	$-0.715942087191\text{D}-07$	$0.479459518485\text{D}-07$
36	27	$0.413003624860\text{D}-07$	$-0.356643291953\text{D}-07$
36	28	$0.101476926638\text{D}-07$	$0.106282036385\text{D}-06$
36	29	$-0.402219726617\text{D}-07$	$-0.818305945642\text{D}-07$
36	30	$0.748533650500\text{D}-07$	$0.197038857863\text{D}-06$
36	31	$-0.317674522524\text{D}-07$	$-0.949276447761\text{D}-07$
36	32	$0.127046522426\text{D}-06$	$0.127842798900\text{D}-06$
36	33	$-0.266316045749\text{D}-07$	$-0.251658370920\text{D}-06$
36	34	$0.337485570574\text{D}-07$	$0.139705942611\text{D}-06$
36	35	$0.171526194164\text{D}-06$	$-0.155008287807\text{D}-06$
36	36	$-0.324684069683\text{D}-08$	$-0.115396118812\text{D}-06$
37	1	$-0.826758067454\text{D}-07$	$-0.961814196324\text{D}-07$
37	2	$0.688270635589\text{D}-07$	$0.131483456178\text{D}-07$
37	3	$-0.163499558245\text{D}-06$	$-0.545375606805\text{D}-09$
37	4	$0.509970486400\text{D}-07$	$-0.713066773311\text{D}-07$
37	5	$-0.730793465371\text{D}-07$	$0.766658751158\text{D}-07$
37	6	$-0.286613796838\text{D}-07$	$-0.118231445372\text{D}-06$
37	7	$0.363090487987\text{D}-07$	$0.815255330827\text{D}-07$
37	8	$-0.147534877112\text{D}-06$	$-0.745902789063\text{D}-08$
37	9	$0.775297246543\text{D}-07$	$0.559157600951\text{D}-07$
37	10	$-0.699240578670\text{D}-07$	$0.139829077323\text{D}-06$
37	11	$0.877049204389\text{D}-07$	$-0.462371457355\text{D}-08$
37	12	$0.764595386468\text{D}-07$	$0.774914572566\text{D}-07$
37	13	$-0.133923989830\text{D}-08$	$0.291203108238\text{D}-07$
37	14	$0.303281164895\text{D}-07$	$-0.708715760096\text{D}-07$
37	15	$0.370940987892\text{D}-07$	$-0.135690599700\text{D}-07$
37	16	$-0.405444492172\text{D}-07$	$-0.235528210099\text{D}-07$
37	17	$0.193128876564\text{D}-07$	$0.201869739461\text{D}-07$
37	18	$-0.632380174724\text{D}-07$	$-0.393088874057\text{D}-08$
37	19	$0.337303262694\text{D}-07$	$-0.191848908125\text{D}-07$
37	20	$-0.196829812978\text{D}-07$	$0.104416411334\text{D}-06$

Table A-4: (cont.) Tesseral and Sectorial Harmonic Coefficients for Mars50c

n	m	$\overline{C}_{nm}$	$\overline{S}_{nm}$
37	21	$-0.217165056028D-07$	$-0.766201104360D-07$
37	22	$0.625586552117D-07$	$0.109433498206D-06$
37	23	$-0.480312784460D-07$	$-0.869256728946D-07$
37	24	$0.104676817103D-07$	$-0.108241655887D-07$
37	25	$-0.243545602539D-07$	$0.223567408674D-07$
37	26	$0.193788144886D-07$	$-0.416192330857D-07$
37	27	$0.126955997355D-06$	$0.297177189485D-07$
37	28	$-0.634996385550D-07$	$0.431575553487D-07$
37	29	$0.935151109262D-07$	$-0.551247794194D-07$
37	30	$-0.119217642336D-06$	$0.126083834820D-06$
37	31	$0.656662734014D-07$	$-0.973240196885D-07$
37	32	$-0.991240782875D-07$	$0.111875223486D-06$
37	33	$0.360629429301D-07$	$-0.176795059378D-06$
37	34	$-0.665659299092D-07$	$0.315373266753D-07$
37	35	$0.139033442787D-06$	$-0.347605873848D-08$
37	36	$-0.263647615958D-06$	$0.348679870001D-07$
37	37	$-0.188488009146D-07$	$0.119088151134D-06$
38	1	$-0.104180053389D-07$	$-0.547347825594D-07$
38	2	$-0.476234573871D-07$	$0.142033456975D-06$
38	3	$-0.340111959930D-07$	$-0.536900106208D-07$
38	4	$0.923791896488D-07$	$0.126800312134D-06$
38	5	$-0.112073052356D-06$	$-0.873692632137D-08$
38	6	$0.977545172962D-07$	$-0.137081922151D-07$
38	7	$-0.500709084979D-07$	$0.865414836347D-07$
38	8	$0.253527170187D-07$	$-0.208239703016D-07$
38	9	$0.482114431823D-07$	$0.722867685959D-07$
38	10	$0.247590276893D-07$	$-0.144166130329D-07$
38	11	$0.540135192867D-07$	$-0.337585658047D-07$
38	12	$0.192099712667D-07$	$-0.536012175186D-08$
38	13	$0.180888946595D-07$	$-0.274485223054D-07$
38	14	$0.150855556730D-07$	$-0.179738552732D-07$
38	15	$-0.469429455503D-07$	$-0.269267158879D-07$
38	16	$0.228554201119D-07$	$0.114507776004D-07$
38	17	$0.112247430523D-07$	$0.602419970788D-07$
38	18	$-0.276798120968D-08$	$-0.296716872269D-07$
38	19	$0.647157820593D-07$	$0.731644347077D-09$
38	20	$-0.135412720926D-07$	$-0.128088648683D-07$

Table A-4: (cont.) Tesseral and Sectorial Harmonic Coefficients for Mars50c

n	m	$\bar{C}_{nm}$	$\bar{S}_{nm}$
38	21	0.191735398633D−07	−0.140520415263D−07
38	22	0.617967904451D−08	−0.282961005435D−07
38	23	−0.629105127331D−07	−0.385438422347D−07
38	24	0.118345028774D−07	0.448120955855D−07
38	25	−0.659553657235D−07	0.206636607367D−07
38	26	0.673963049438D−07	−0.819708492112D−07
38	27	0.826343135622D−09	0.271801991274D−07
38	28	0.142605816387D−07	−0.913069270859D−07
38	29	0.659613263509D−07	0.128769296319D−06
38	30	−0.174886858254D−06	−0.444945672485D−07
38	31	0.162734682672D−06	0.320811481705D−07
38	32	−0.191954519195D−06	0.144424046565D−07
38	33	0.161926092193D−06	−0.865929283912D−07
38	34	−0.341207198516D−07	0.256835062820D−07
38	35	0.108984079023D−06	0.588107403607D−07
38	36	−0.139408992733D−06	−0.992096638785D−07
38	37	0.154981784944D−06	0.339944901872D−06
38	38	0.177347355638D−06	0.128444203354D−07
39	1	0.972572911130D−07	0.110468007034D−06
39	2	−0.534527238977D−07	0.169491704223D−07
39	3	0.138799695349D−06	−0.117487990240D−07
39	4	−0.236862398060D−07	0.724688168017D−07
39	5	0.388587993592D−07	−0.106684408260D−06
39	6	0.506485095798D−07	0.726704573318D−07
39	7	−0.573870128877D−07	−0.329791375702D−07
39	8	0.127163864951D−06	0.169798699664D−08
39	9	−0.315023038683D−07	0.296030653176D−08
39	10	0.332953431561D−07	−0.876037290826D−07
39	11	0.435572652088D−08	0.575127907097D−08
39	12	−0.113057568081D−07	−0.462242150388D−07
39	13	−0.556780840526D−10	−0.315683559479D−07
39	14	−0.336833807317D−07	−0.876340493518D−08
39	15	−0.667827731475D−07	−0.527494428809D−09
39	16	0.547265440404D−07	0.435360612940D−07
39	17	−0.920810203637D−08	0.905902648196D−08
39	18	0.432631777227D−07	−0.336804614179D−07
39	19	−0.636941489513D−07	−0.142204862752D−07
39	20	0.188085656600D−08	−0.746062971245D−07

Table A-4: (cont.) Tesseral and Sectorial Harmonic Coefficients for Mars50c

n	m	$\bar{C}_{nm}$	$\bar{S}_{nm}$
39	21	$-0.587311784291\mathrm{D}-08$	$0.298451371707\mathrm{D}-07$
39	22	$-0.831499697198\mathrm{D}-07$	$-0.706676290712\mathrm{D}-07$
39	23	$-0.121120975302\mathrm{D}-07$	$0.552273572246\mathrm{D}-07$
39	24	$-0.819739239209\mathrm{D}-08$	$0.373061175582\mathrm{D}-07$
39	25	$0.397195682752\mathrm{D}-07$	$0.896974368405\mathrm{D}-08$
39	26	$0.272913529740\mathrm{D}-07$	$0.763019986651\mathrm{D}-08$
39	27	$-0.412775812261\mathrm{D}-07$	$-0.303840079082\mathrm{D}-07$
39	28	$0.820086435039\mathrm{D}-07$	$-0.294452391141\mathrm{D}-07$
39	29	$-0.470826515698\mathrm{D}-07$	$0.715147591018\mathrm{D}-07$
39	30	$0.373792970079\mathrm{D}-07$	$-0.109813897128\mathrm{D}-06$
39	31	$0.225722834703\mathrm{D}-07$	$0.120745269117\mathrm{D}-06$
39	32	$-0.730957639798\mathrm{D}-07$	$-0.154670839312\mathrm{D}-06$
39	33	$0.128152655888\mathrm{D}-06$	$0.952490146596\mathrm{D}-07$
39	34	$-0.654458754648\mathrm{D}-07$	$-0.126536854463\mathrm{D}-06$
39	35	$0.636249816901\mathrm{D}-08$	$0.523668854811\mathrm{D}-07$
39	36	$-0.349210756191\mathrm{D}-07$	$-0.971623891758\mathrm{D}-07$
39	37	$0.114627736557\mathrm{D}-07$	$0.209298564911\mathrm{D}-06$
39	38	$0.972093655914\mathrm{D}-07$	$-0.251476447338\mathrm{D}-06$
39	39	$-0.514419355165\mathrm{D}-08$	$-0.240972380157\mathrm{D}-06$
40	1	$0.250274945464\mathrm{D}-07$	$0.377114938280\mathrm{D}-07$
40	2	$0.386998948406\mathrm{D}-07$	$-0.140542192027\mathrm{D}-06$
40	3	$0.699109237105\mathrm{D}-07$	$0.378756222386\mathrm{D}-07$
40	4	$-0.945718377425\mathrm{D}-07$	$-0.619848862477\mathrm{D}-07$
40	5	$0.767647797399\mathrm{D}-07$	$-0.690083613680\mathrm{D}-08$
40	6	$-0.669153444288\mathrm{D}-07$	$0.276414894633\mathrm{D}-07$
40	7	$0.211324081823\mathrm{D}-07$	$-0.613224044740\mathrm{D}-07$
40	8	$-0.100514615299\mathrm{D}-07$	$0.194294062941\mathrm{D}-07$
40	9	$-0.178753170888\mathrm{D}-07$	$-0.539164232031\mathrm{D}-07$
40	10	$-0.812527723734\mathrm{D}-08$	$0.137962958007\mathrm{D}-08$
40	11	$-0.341294453195\mathrm{D}-07$	$-0.275330007909\mathrm{D}-07$
40	12	$-0.128311735973\mathrm{D}-07$	$0.484603306444\mathrm{D}-08$
40	13	$-0.197441087166\mathrm{D}-07$	$-0.705196695595\mathrm{D}-08$
40	14	$0.269808785894\mathrm{D}-08$	$0.374082082076\mathrm{D}-08$
40	15	$-0.278580282664\mathrm{D}-07$	$-0.899777115103\mathrm{D}-08$
40	16	$0.250831286379\mathrm{D}-07$	$-0.171750456445\mathrm{D}-07$
40	17	$-0.195041944419\mathrm{D}-07$	$-0.936508566650\mathrm{D}-08$
40	18	$0.146232172124\mathrm{D}-07$	$-0.869688367154\mathrm{D}-08$
40	19	$-0.509464214500\mathrm{D}-07$	$0.298764296498\mathrm{D}-07$
40	20	$-0.268693656210\mathrm{D}-09$	$0.547369627861\mathrm{D}-08$

Table A-4: (cont.) Tesseral and Sectorial Harmonic Coefficients for Mars50c

n	m	$\overline{C}_{nm}$	$\overline{S}_{nm}$
40	21	$-0.280219212184\mathrm{D}-07$	$0.270595260402\mathrm{D}-07$
40	22	$0.501351719707\mathrm{D}-09$	$0.271360885134\mathrm{D}-07$
40	23	$0.351088941146\mathrm{D}-07$	$0.432738331193\mathrm{D}-07$
40	24	$0.100294816122\mathrm{D}-07$	$-0.145965150664\mathrm{D}-07$
40	25	$0.624659912028\mathrm{D}-07$	$-0.862672380669\mathrm{D}-08$
40	26	$0.227775191022\mathrm{D}-07$	$0.451135586900\mathrm{D}-07$
40	27	$-0.294475751854\mathrm{D}-08$	$-0.223333918063\mathrm{D}-07$
40	28	$0.291014058239\mathrm{D}-07$	$0.442476749826\mathrm{D}-07$
40	29	$-0.661175975454\mathrm{D}-07$	$-0.185076323979\mathrm{D}-07$
40	30	$0.964544975999\mathrm{D}-07$	$-0.213893882324\mathrm{D}-07$
40	31	$-0.969664303146\mathrm{D}-07$	$0.255343101914\mathrm{D}-08$
40	32	$0.755816598316\mathrm{D}-07$	$-0.944678298934\mathrm{D}-07$
40	33	$-0.643329151689\mathrm{D}-07$	$0.117095555806\mathrm{D}-06$
40	34	$0.603671920061\mathrm{D}-07$	$-0.129359556260\mathrm{D}-06$
40	35	$-0.361763904489\mathrm{D}-07$	$0.117029860485\mathrm{D}-06$
40	36	$0.245698259179\mathrm{D}-07$	$-0.689164587127\mathrm{D}-07$
40	37	$0.222888979790\mathrm{D}-07$	$0.145359358390\mathrm{D}-06$
40	38	$0.676770129424\mathrm{D}-07$	$-0.919619527478\mathrm{D}-07$
40	39	$-0.135952644743\mathrm{D}-06$	$0.217565582224\mathrm{D}-07$
40	40	$-0.216332039882\mathrm{D}-07$	$0.159932510098\mathrm{D}-07$
41	1	$-0.639997389006\mathrm{D}-07$	$-0.856436869881\mathrm{D}-07$
41	2	$0.176406377825\mathrm{D}-07$	$-0.357541184689\mathrm{D}-07$
41	3	$-0.642885368390\mathrm{D}-07$	$0.283669747782\mathrm{D}-07$
41	4	$-0.509637109381\mathrm{D}-08$	$-0.581045091539\mathrm{D}-07$
41	5	$-0.194708990476\mathrm{D}-08$	$0.828360935135\mathrm{D}-07$
41	6	$-0.626186555679\mathrm{D}-07$	$-0.274741274357\mathrm{D}-07$
41	7	$0.420364966365\mathrm{D}-07$	$0.181288359596\mathrm{D}-07$
41	8	$-0.487553625019\mathrm{D}-07$	$0.820556167360\mathrm{D}-09$
41	9	$0.154192210514\mathrm{D}-07$	$-0.106935948991\mathrm{D}-07$
41	10	$-0.453722546452\mathrm{D}-08$	$-0.506759738572\mathrm{D}-08$
41	11	$-0.166093769630\mathrm{D}-07$	$0.519348586670\mathrm{D}-08$
41	12	$-0.145013548885\mathrm{D}-07$	$0.427182849824\mathrm{D}-08$
41	13	$0.272510910741\mathrm{D}-07$	$-0.172305035691\mathrm{D}-07$
41	14	$0.265082866404\mathrm{D}-09$	$0.360069189825\mathrm{D}-07$
41	15	$0.230807775181\mathrm{D}-07$	$-0.935758069842\mathrm{D}-08$
41	16	$-0.222342025177\mathrm{D}-07$	$-0.187268999194\mathrm{D}-07$
41	17	$0.457786075028\mathrm{D}-08$	$-0.267249649123\mathrm{D}-07$
41	18	$-0.135828085388\mathrm{D}-07$	$0.355264556142\mathrm{D}-07$
41	19	$0.214141470067\mathrm{D}-07$	$0.392576934187\mathrm{D}-08$
41	20	$0.888623051090\mathrm{D}-08$	$0.370284099104\mathrm{D}-07$

Table A-4: (cont.) Tesseral and Sectorial Harmonic Coefficients for Mars50c

n	m	C_{nm}	S_{nm}
41	21	0.154277057910D−07	0.270909182178D−08
41	22	0.282650452760D−07	0.856904219285D−08
41	23	0.212304669390D−07	−0.274963096656D−07
41	24	0.173812033497D−07	−0.389130450089D−07
41	25	−0.665733799191D−08	−0.348501757223D−07
41	26	0.165811947543D−07	−0.300407467856D−07
41	27	0.313910553976D−07	0.310374854740D−07
41	28	−0.235363474825D−07	0.417389481036D−07
41	29	0.225383939270D−07	−0.177975106301D−07
41	30	0.200007875979D−08	0.557390082322D−07
41	31	−0.826563973611D−07	−0.517149916109D−07
41	32	0.752431414137D−07	0.634062044730D−07
41	33	−0.791475757890D−07	−0.450859701444D−08
41	34	0.150598414501D−06	−0.132362013852D−07
41	35	−0.900348640389D−07	0.602789224430D−07
41	36	0.118286570038D−06	−0.617036591402D−07
41	37	−0.362247232870D−07	0.114988382919D−06
41	38	0.525472969045D−08	−0.695908238484D−07
41	39	−0.787776345143D−07	0.615255690783D−07
41	40	0.125207846921D−06	0.130142466573D−06
41	41	0.168702568712D−06	0.247317410177D−07
42	1	−0.212229746495D−07	−0.407827798210D−07
42	2	−0.212936668847D−07	0.744224967159D−07
42	3	−0.585867147064D−07	−0.164491788946D−07
42	4	0.689571291733D−07	0.335698917561D−07
42	5	−0.311411949988D−07	0.129259999221D−07
42	6	0.479031444602D−07	−0.415563130926D−07
42	7	−0.171355174891D−07	0.203849319756D−07
42	8	0.789234923057D−08	−0.388115551628D−07
42	9	−0.460081944386D−08	0.282140679676D−07
42	10	−0.203476828638D−07	−0.339933172268D−07
42	11	0.748285169146D−08	0.468386855860D−07
42	12	−0.168943126683D−07	−0.199321658554D−07
42	13	0.660183874490D−08	0.202109016626D−07
42	14	−0.411506191575D−07	−0.792862252550D−08
42	15	0.344336152255D−07	0.421621559701D−07

Table A-4: (cont.) Tesseral and Sectorial Harmonic Coefficients for Mars50c

n	m	$\bar{C}_{nm}$	$\bar{S}_{nm}$
42	16	$-0.736754186192D-07$	$0.365832689086D-08$
42	17	$0.146978533688D-07$	$-0.494537620075D-08$
42	18	$0.124557602270D-07$	$0.339829840707D-07$
42	19	$0.173829558607D-07$	$-0.349344532129D-07$
42	20	$0.404595264107D-08$	$0.159126267311D-09$
42	21	$0.312968067022D-07$	$-0.271541480016D-07$
42	22	$-0.301150331045D-07$	$0.708911726273D-08$
42	23	$0.212089595663D-08$	$-0.480983790654D-07$
42	24	$-0.268459368822D-07$	$-0.120997381994D-07$
42	25	$-0.381066108601D-07$	$-0.266336841359D-07$
42	26	$-0.294781582683D-07$	$-0.432363462127D-08$
42	27	$0.144976560856D-07$	$0.975954092126D-08$
42	28	$-0.507888330819D-08$	$0.251974046622D-07$
42	29	$0.375600111029D-07$	$0.148575061068D-07$
42	30	$-0.678436617681D-07$	$0.209461953880D-07$
42	31	$0.452059098041D-07$	$0.818733425912D-08$
42	32	$-0.298020391873D-07$	$0.620357836706D-07$
42	33	$0.512433283852D-07$	$-0.909887528282D-07$
42	34	$0.488949021924D-07$	$0.461083060749D-07$
42	35	$-0.573714124331D-07$	$-0.765992001649D-07$
42	36	$0.877511775179D-07$	$0.287653392919D-07$
42	37	$-0.122501631535D-06$	$0.282383386515D-07$
42	38	$0.970295652507D-08$	$-0.674644987863D-07$
42	39	$-0.435257847171D-07$	$0.882531294135D-07$
42	40	$0.313408347172D-07$	$0.507426916499D-07$
42	41	$0.630634169325D-07$	$-0.121779688730D-06$
42	42	$0.513972277409D-07$	$-0.114062277421D-06$
43	1	$0.181384256910D-07$	$0.617154795813D-07$
43	2	$-0.217282478893D-07$	$0.597994991407D-07$
43	3	$0.424748212299D-07$	$-0.256710329575D-07$
43	4	$0.109031505155D-07$	$0.189279461460D-07$
43	5	$-0.189187166492D-07$	$-0.511007408564D-07$
43	6	$0.195689987524D-07$	$0.580742520047D-09$
43	7	$-0.262721904723D-07$	$-0.104193613288D-07$
43	8	$-0.196125204257D-07$	$0.209906178716D-07$
43	9	$-0.117526087885D-07$	$0.530042519511D-08$
43	10	$0.198798487029D-07$	$0.297996869056D-07$

Table A-4: (cont.) Tesseral and Sectorial Harmonic Coefficients for Mars50c

n	m	$\bar{C}_{nm}$	$\bar{S}_{nm}$
43	11	$-0.374147074569D-07$	$-0.762704615095D-08$
43	12	$0.169767521026D-07$	$0.166070163282D-08$
43	13	$-0.397318149140D-07$	$0.511608063447D-07$
43	14	$0.164300143535D-07$	$-0.199157446090D-07$
43	15	$0.308076885519D-07$	$0.397963672466D-07$
43	16	$-0.346406300374D-07$	$-0.225130676264D-07$
43	17	$0.165185391923D-07$	$0.139100288036D-07$
43	18	$-0.130825323516D-07$	$-0.289764121092D-07$
43	19	$0.334744422096D-07$	$-0.164737289883D-08$
43	20	$-0.223033614272D-07$	$0.228302953112D-08$
43	21	$-0.571849665100D-08$	$-0.223637307416D-07$
43	22	$-0.141528157805D-08$	$0.379964280377D-07$
43	23	$-0.610710742030D-08$	$-0.965948858929D-08$
43	24	$-0.325581034942D-07$	$0.295232589812D-07$
43	25	$-0.209631041495D-07$	$0.227467323583D-07$
43	26	$-0.516930512749D-08$	$0.384976494029D-07$
43	27	$-0.849574246841D-08$	$0.150798920831D-07$
43	28	$0.282457020448D-07$	$-0.282439540139D-07$
43	29	$-0.421224232214D-08$	$0.273753117286D-07$
43	30	$-0.438776596011D-07$	$-0.178987042221D-07$
43	31	$0.600990651801D-07$	$0.365133572981D-07$
43	32	$-0.397924884396D-07$	$-0.263876514398D-07$
43	33	$0.832260219613D-07$	$-0.184982271496D-07$
43	34	$-0.101577617008D-06$	$-0.444068311321D-08$
43	35	$0.262946010031D-07$	$-0.557906579104D-07$
43	36	$-0.357174160476D-07$	$0.111091597840D-06$
43	37	$-0.918472067565D-07$	$-0.104729421641D-07$
43	38	$0.495291240620D-07$	$0.724674680508D-07$
43	39	$-0.578801894336D-07$	$0.673505693030D-07$
43	40	$0.769913705078D-07$	$0.209985397726D-08$
43	41	$-0.235753745200D-07$	$-0.271268707320D-07$
43	42	$-0.425290749899D-07$	$0.450425637078D-07$
43	43	$-0.134343701579D-06$	$0.384733531637D-07$
44	1	$0.296239663486D-07$	$0.530439755509D-07$
44	2	$0.172860381563D-07$	$-0.140730999714D-07$
44	3	$0.290819125730D-07$	$-0.217474448266D-07$
44	4	$-0.345835825004D-07$	$-0.731004426364D-08$
44	5	$-0.162922053285D-07$	$-0.235885781493D-07$

Table A-4: (cont.) Tesseral and Sectorial Harmonic Coefficients for Mars50c

n	m	$\bar{C}_{nm}$	$\bar{S}_{nm}$
44	6	$-0.288360630889D-07$	$0.103139398479D-07$
44	7	$-0.548105792084D-09$	$0.261627866587D-08$
44	8	$-0.176407791326D-07$	$0.401631714494D-07$
44	9	$0.194771052596D-07$	$-0.131744015408D-07$
44	10	$0.634333900198D-08$	$0.514599492301D-07$
44	11	$0.962319270441D-08$	$-0.193935167500D-07$
44	12	$0.184901668239D-07$	$0.438430415931D-07$
44	13	$-0.129962925297D-07$	$-0.243092706493D-07$
44	14	$0.648160449008D-07$	$0.251378349620D-07$
44	15	$-0.200609547379D-07$	$-0.264477787244D-07$
44	16	$0.467431742041D-07$	$-0.953021725872D-08$
44	17	$-0.241611580550D-07$	$0.644313506799D-08$
44	18	$-0.104106991784D-07$	$-0.306679651729D-07$
44	19	$0.320203826101D-08$	$-0.148704574692D-08$
44	20	$-0.941838658506D-08$	$-0.847972644402D-08$
44	21	$-0.169062353117D-07$	$0.307547143580D-07$
44	22	$0.343560480080D-07$	$-0.283721575139D-07$
44	23	$-0.197856704431D-07$	$0.194745865004D-07$
44	24	$0.527300124208D-08$	$0.103226893961D-07$
44	25	$0.217843673357D-07$	$0.351907203637D-07$
44	26	$0.308526792240D-07$	$0.752964588730D-08$
44	27	$0.118305101901D-07$	$0.207486497392D-07$
44	28	$0.110509354232D-08$	$-0.216453323310D-07$
44	29	$-0.296531426738D-07$	$-0.260013333142D-08$
44	30	$0.119365226740D-07$	$-0.154266435141D-07$
44	31	$-0.168163474109D-07$	$0.104995408109D-07$
44	32	$0.155016537573D-07$	$-0.508879688271D-07$
44	33	$0.628837325052D-08$	$0.320281174218D-07$
44	34	$-0.517708931752D-07$	$-0.161143380131D-07$
44	35	$0.328961112139D-08$	$0.483391324350D-07$
44	36	$-0.468171388286D-07$	$0.562633735820D-07$
44	37	$0.197403097270D-07$	$0.213634643747D-07$
44	38	$-0.445429651097D-08$	$0.586440083612D-07$
44	39	$0.100380677593D-07$	$-0.324109717095D-07$
44	40	$0.707545597543D-07$	$0.314501059930D-07$
44	41	$-0.646249072760D-07$	$-0.694618795191D-07$
44	42	$0.473194465541D-07$	$0.738751151041D-07$
44	43	$0.138023380599D-07$	$0.282337486755D-07$
44	44	$0.503176665989D-07$	$0.153938282672D-06$

Table A-4: (cont.) Tesseral and Sectorial Harmonic Coefficients for Mars50c

126

n	m	$\bar{C}_{nm}$	$\bar{S}_{nm}$
45	1	$-0.255558728952\text{D}-07$	$-0.323062068566\text{D}-07$
45	2	$0.597131616225\text{D}-08$	$-0.390221049287\text{D}-07$
45	3	$-0.291530532504\text{D}-07$	$0.160265194970\text{D}-07$
45	4	$-0.826456373704\text{D}-08$	$0.460558913105\text{D}-08$
45	5	$0.224612302295\text{D}-08$	$0.177424982334\text{D}-07$
45	6	$0.191239782980\text{D}-07$	$0.237005231686\text{D}-07$
45	7	$0.155621554323\text{D}-07$	$0.284308598656\text{D}-07$
45	8	$0.242747305597\text{D}-07$	$-0.261099500145\text{D}-07$
45	9	$0.201247757417\text{D}-07$	$0.119355024378\text{D}-07$
45	10	$-0.353662937772\text{D}-07$	$-0.233306348701\text{D}-07$
45	11	$0.642006709993\text{D}-07$	$-0.190401371063\text{D}-07$
45	12	$-0.209682319194\text{D}-07$	$0.250503280493\text{D}-07$
45	13	$0.280283123228\text{D}-07$	$-0.538086563702\text{D}-07$
45	14	$-0.199256582456\text{D}-08$	$0.158092866067\text{D}-07$
45	15	$-0.305575923294\text{D}-07$	$-0.660890612685\text{D}-07$
45	16	$0.462619839153\text{D}-07$	$0.313346117627\text{D}-07$
45	17	$-0.490504259497\text{D}-07$	$-0.638669741655\text{D}-08$
45	18	$0.299734145260\text{D}-07$	$0.133521643447\text{D}-07$
45	19	$-0.676513967794\text{D}-07$	$0.744662855366\text{D}-08$
45	20	$0.198327020433\text{D}-07$	$-0.846356384089\text{D}-08$
45	21	$0.612970406067\text{D}-08$	$0.292662661652\text{D}-07$
45	22	$0.320207482759\text{D}-08$	$-0.359039856808\text{D}-07$
45	23	$-0.346754348583\text{D}-08$	$0.277048311391\text{D}-07$
45	24	$0.254848232723\text{D}-07$	$-0.131731406219\text{D}-07$
45	25	$0.302937360078\text{D}-07$	$-0.813140959439\text{D}-08$
45	26	$0.492198292484\text{D}-08$	$-0.218707597207\text{D}-07$
45	27	$0.107030085725\text{D}-07$	$-0.258293895255\text{D}-07$
45	28	$-0.148966764730\text{D}-07$	$0.154845150981\text{D}-07$
45	29	$-0.265731066254\text{D}-07$	$0.276050489443\text{D}-08$
45	30	$0.672067183012\text{D}-08$	$0.359613635295\text{D}-08$
45	31	$-0.342824965166\text{D}-07$	$0.933782579106\text{D}-08$
45	32	$0.217638038403\text{D}-07$	$-0.292369760763\text{D}-07$
45	33	$-0.273785892479\text{D}-07$	$0.195143743559\text{D}-07$
45	34	$0.335649549845\text{D}-07$	$0.116546947065\text{D}-07$
45	35	$-0.203024033077\text{D}-07$	$0.352588160783\text{D}-07$
45	36	$0.187171394092\text{D}-07$	$0.193935663015\text{D}-08$
45	37	$0.617820761363\text{D}-08$	$0.258079824367\text{D}-07$
45	38	$-0.184267205909\text{D}-07$	$-0.203132478388\text{D}-07$
45	39	$0.363796427303\text{D}-08$	$-0.313117433421\text{D}-07$
45	40	$-0.493072714425\text{D}-07$	$0.461947574261\text{D}-07$

Table A-4: (cont.) Tesseral and Sectorial Harmonic Coefficients for Mars50c

n	m	$\bar{C}_{nm}$	$\bar{S}_{nm}$
45	41	$-0.215643063547\mathrm{D}{-}07$	$-0.842421651678\mathrm{D}{-}07$
45	42	$-0.695670888830\mathrm{D}{-}08$	$0.127737184916\mathrm{D}{-}06$
45	43	$-0.275738365711\mathrm{D}{-}07$	$-0.919804214484\mathrm{D}{-}07$
45	44	$-0.851426636659\mathrm{D}{-}08$	$0.273159754941\mathrm{D}{-}07$
45	45	$0.807329136365\mathrm{D}{-}07$	$-0.887837253610\mathrm{D}{-}07$
46	1	$-0.840705161481\mathrm{D}{-}08$	$-0.390584539297\mathrm{D}{-}07$
46	2	$0.836130223588\mathrm{D}{-}08$	$-0.337139822795\mathrm{D}{-}08$
46	3	$-0.726844224079\mathrm{D}{-}08$	$0.456275593533\mathrm{D}{-}08$
46	4	$-0.159938483695\mathrm{D}{-}08$	$0.573144042992\mathrm{D}{-}08$
46	5	$0.154997885256\mathrm{D}{-}07$	$0.212057531769\mathrm{D}{-}07$
46	6	$0.738262029716\mathrm{D}{-}08$	$0.494775877082\mathrm{D}{-}08$
46	7	$0.118814743109\mathrm{D}{-}07$	$-0.966961181478\mathrm{D}{-}08$
46	8	$0.867298310072\mathrm{D}{-}08$	$-0.436797980844\mathrm{D}{-}08$
46	9	$-0.172414738183\mathrm{D}{-}07$	$-0.588204246984\mathrm{D}{-}08$
46	10	$0.139056200697\mathrm{D}{-}07$	$-0.283583463668\mathrm{D}{-}07$
46	11	$0.245241023077\mathrm{D}{-}08$	$0.113074639081\mathrm{D}{-}07$
46	12	$-0.862975638273\mathrm{D}{-}08$	$-0.451204924098\mathrm{D}{-}07$
46	13	$0.269199786693\mathrm{D}{-}07$	$0.101702310702\mathrm{D}{-}07$
46	14	$-0.495129733852\mathrm{D}{-}07$	$-0.808503815140\mathrm{D}{-}08$
46	15	$0.121641406506\mathrm{D}{-}07$	$-0.139195513225\mathrm{D}{-}07$
46	16	$-0.720857195508\mathrm{D}{-}08$	$0.303875255902\mathrm{D}{-}07$
46	17	$0.163311162488\mathrm{D}{-}07$	$-0.876784946719\mathrm{D}{-}08$
46	18	$-0.213525049345\mathrm{D}{-}08$	$0.195572507427\mathrm{D}{-}07$
46	19	$-0.160319260123\mathrm{D}{-}08$	$0.173261460961\mathrm{D}{-}07$
46	20	$0.152529966924\mathrm{D}{-}07$	$0.162869737030\mathrm{D}{-}07$
46	21	$-0.690802041789\mathrm{D}{-}08$	$-0.192663389756\mathrm{D}{-}07$
46	22	$-0.498510150931\mathrm{D}{-}08$	$0.198747427832\mathrm{D}{-}08$
46	23	$0.150959584082\mathrm{D}{-}07$	$0.992143099410\mathrm{D}{-}08$
46	24	$0.760130642532\mathrm{D}{-}08$	$-0.105719696759\mathrm{D}{-}07$
46	25	$0.321553989594\mathrm{D}{-}08$	$-0.172992496362\mathrm{D}{-}07$
46	26	$-0.823139772539\mathrm{D}{-}08$	$-0.384720668316\mathrm{D}{-}08$
46	27	$-0.216607535258\mathrm{D}{-}07$	$-0.176399032366\mathrm{D}{-}07$
46	28	$-0.172196835597\mathrm{D}{-}07$	$0.884504194319\mathrm{D}{-}08$
46	29	$0.338339136040\mathrm{D}{-}08$	$0.755020862366\mathrm{D}{-}08$
46	30	$-0.478279577128\mathrm{D}{-}08$	$0.241606353361\mathrm{D}{-}08$
46	31	$-0.610588053310\mathrm{D}{-}08$	$0.129984467633\mathrm{D}{-}07$
46	32	$0.226630110694\mathrm{D}{-}09$	$-0.196922305939\mathrm{D}{-}08$
46	33	$0.132431408197\mathrm{D}{-}08$	$-0.148042190965\mathrm{D}{-}08$
46	34	$0.364481228028\mathrm{D}{-}07$	$0.972289902247\mathrm{D}{-}08$
46	35	$0.553775205396\mathrm{D}{-}08$	$-0.160539611934\mathrm{D}{-}07$

Table A-4: (cont.) Tesseral and Sectorial Harmonic Coefficients for Mars50c

n	m	$\bar{C}_{nm}$	$\bar{S}_{nm}$
46	36	0.709327602633D−08	0.592529295209D−08
46	37	−0.269628604796D−07	−0.251520222525D−07
46	38	−0.358286705793D−07	−0.136413020379D−07
46	39	−0.159043770400D−07	0.659054708048D−08
46	40	−0.715959083848D−07	0.206308993298D−07
46	41	0.136403406280D−07	−0.604537265487D−08
46	42	−0.941851364016D−07	0.746936166745D−07
46	43	0.290376843697D−07	−0.670780282876D−07
46	44	−0.100746320308D−06	0.753879364383D−07
46	45	0.425923808558D−08	0.688229177532D−08
46	46	−0.119918936135D−06	−0.137497259437D−07
47	1	−0.175093096751D−07	−0.573429178360D−08
47	2	0.101454708973D−09	0.324458333753D−08
47	3	−0.620741485903D−08	0.143861187949D−07
47	4	0.243937601672D−07	0.723655287136D−08
47	5	0.276026470375D−07	−0.884346024037D−09
47	6	−0.106200004737D−07	−0.104324367595D−07
47	7	−0.684174195344D−08	−0.346693951242D−07
47	8	0.502783385677D−08	0.775831659375D−08
47	9	−0.357695154260D−07	−0.281161172790D−07
47	10	0.282746775720D−07	0.108387215990D−07
47	11	−0.465023744281D−07	0.219876499202D−07
47	12	0.195656276502D−07	−0.335680076161D−07
47	13	−0.192661293049D−07	0.356335976187D−07
47	14	−0.539687333021D−08	−0.230644495599D−07
47	15	0.308785372768D−08	0.514941486308D−07
47	16	−0.159962389976D−07	−0.247873748608D−07
47	17	0.475665372390D−07	0.197729898620D−08
47	18	−0.314934618695D−07	0.740362206568D−08
47	19	0.443943823960D−07	−0.251519469413D−07
47	20	−0.841419847088D−08	0.252880973535D−08
47	21	−0.519318599382D−08	−0.164947172045D−07
47	22	−0.162731662994D−07	0.225288621635D−08
47	23	0.112951397202D−07	−0.299786422425D−07
47	24	−0.104045236244D−07	−0.319488730762D−08
47	25	−0.973256127225D−08	−0.158541343900D−07

Table A-4: (cont.) Tesseral and Sectorial Harmonic Coefficients for Mars50c

n	m	$\bar{C}_{nm}$	$\bar{S}_{nm}$
47	26	-0.122164503799D-08	0.491486271750D-08
47	27	-0.543535150692D-08	0.202790454554D-07
47	28	-0.463435512231D-08	0.141145135770D-07
47	29	0.184020311620D-07	-0.332924186725D-08
47	30	0.126636049137D-07	-0.546436773708D-08
47	31	0.267475607094D-07	-0.124844537345D-07
47	32	-0.151736873421D-07	0.871353563089D-08
47	33	0.160931653050D-07	0.852233370157D-08
47	34	-0.735825164664D-08	-0.130313471031D-07
47	35	0.276094694491D-07	-0.300957836199D-07
47	36	-0.432959586848D-07	0.150723785719D-07
47	37	-0.141164631608D-07	-0.225439821482D-07
47	38	-0.218811730309D-07	0.221642122959D-07
47	39	-0.163891121264D-07	0.621605556579D-08
47	40	-0.230259584518D-07	0.207517815917D-07
47	41	0.219817206800D-07	0.292234503117D-07
47	42	-0.421449781396D-07	-0.221569288914D-07
47	43	0.689368017108D-07	-0.774840238348D-08
47	44	-0.821396210551D-07	-0.132598531644D-07
47	45	0.681960314902D-07	0.109885030987D-07
47	46	-0.457378653794D-08	-0.281463239245D-07
47	47	0.321487217789D-07	0.926113257620D-07
48	1	0.962878354939D-08	-0.161131407646D-07
48	2	0.420404319076D-09	-0.275155476967D-08
48	3	0.139967780711D-07	-0.348314130014D-08
48	4	0.846415696733D-08	-0.154122679845D-07
48	5	0.280114869778D-09	0.412007749684D-08
48	6	-0.158938136671D-07	-0.132139835779D-07
48	7	0.392964952877D-08	0.210074408930D-07
48	8	-0.260614059887D-07	-0.665960179089D-08
48	9	0.108043734627D-07	0.408824042569D-10
48	10	-0.108411508283D-07	0.209484809560D-07
48	11	-0.132645070593D-07	-0.264227480206D-07
48	12	0.217499700152D-07	0.253556063529D-07
48	13	-0.433811152695D-07	-0.321784075302D-08
48	14	0.222867851112D-07	-0.187457640026D-07
48	15	-0.186198178773D-07	0.395199708184D-07

Table A-4: (cont.) Tesseral and Sectorial Harmonic Coefficients for Mars50c

n	m	$\bar{C}_{nm}$	$\bar{S}_{nm}$
48	16	0.700265628247D−08	−0.453885289932D−07
48	17	0.163261947105D−09	0.104491345607D−07
48	18	0.518579487636D−08	−0.140562344813D−07
48	19	0.321818141051D−08	0.149545679899D−08
48	20	−0.259556191142D−07	−0.113973737907D−07
48	21	0.205551528959D−07	0.761600003789D−08
48	22	−0.275473325882D−07	0.227121897262D−07
48	23	0.740049105478D−08	−0.149736628011D−07
48	24	−0.172840366405D−07	0.822003366273D−08
48	25	−0.272269928783D−08	−0.859858062414D−08
48	26	−0.207349057060D−08	0.363317537920D−08
48	27	0.768428445005D−08	0.713002534165D−08
48	28	0.164088966274D−07	0.138113960425D−07
48	29	0.114228881247D−08	−0.498094481792D−08
48	30	−0.251162560060D−08	−0.178638350163D−07
48	31	0.915965765256D−08	−0.137750492759D−07
48	32	−0.144156260499D−07	0.454870095905D−08
48	33	0.133106080583D−07	0.106766276469D−07
48	34	−0.249096634381D−07	0.512025447322D−08
48	35	0.903021106740D−09	−0.118542158178D−07
48	36	−0.392571973994D−07	0.489788984245D−08
48	37	0.868260593189D−08	0.197451631164D−07
48	38	−0.146605561885D−07	0.729823703836D−08
48	39	0.244383368949D−07	0.230392691489D−07
48	40	−0.158097058404D−07	−0.144105800703D−07
48	41	0.407147721044D−08	0.126045273677D−07
48	42	−0.138002522965D−07	−0.351827843673D−07
48	43	0.185246202208D−08	0.117674239567D−07
48	44	−0.303267781100D−07	−0.684257231998D−07
48	45	0.195498413201D−09	0.509137333494D−07
48	46	−0.343825931200D−07	−0.978056947438D−07
48	47	−0.114593606207D−07	0.558723126536D−07
48	48	0.105239003076D−06	−0.515147983874D−07
49	1	0.890767072449D−09	0.785688977077D−08
49	2	−0.927347345815D−08	0.624264091062D−08
49	3	−0.600642775599D−08	−0.187929903054D−07
49	4	−0.733039233111D−08	0.770107073255D−08
49	5	−0.248941758034D−07	−0.185602824714D−08

Table A-4: (cont.) Tesseral and Sectorial Harmonic Coefficients for Mars50c

n	m	C_{nm}	S_{nm}
49	6	$-0.184939439011D-08$	$-0.644634775233D-08$
49	7	$-0.512329663944D-08$	$0.239583410990D-07$
49	8	$-0.158813043881D-07$	$-0.783981475938D-08$
49	9	$0.277009748448D-07$	$0.114366706621D-07$
49	10	$-0.153721583914D-07$	$0.441665452654D-08$
49	11	$0.115825481024D-07$	$-0.648420580579D-08$
49	12	$-0.924140888036D-08$	$0.164502062932D-07$
49	13	$0.588096232111D-08$	$-0.146714937926D-07$
49	14	$0.270482776226D-08$	$0.224430931409D-07$
49	15	$-0.909142134863D-10$	$-0.106216175236D-07$
49	16	$-0.898449108551D-08$	$0.690979364292D-08$
49	17	$-0.199185392155D-07$	$0.223719471550D-08$
49	18	$0.138983667190D-07$	$-0.127089430086D-07$
49	19	$-0.149469276176D-08$	$0.261557889487D-07$
49	20	$-0.761378315240D-09$	$0.427816490474D-08$
49	21	$-0.472437967953D-08$	$0.828424704302D-08$
49	22	$0.199287421632D-07$	$0.129551829050D-07$
49	23	$-0.488824228885D-08$	$0.777162390973D-08$
49	24	$0.849728974474D-09$	$0.246048639866D-08$
49	25	$-0.778702995964D-08$	$0.127449262319D-07$
49	26	$0.372736874804D-08$	$-0.204180143648D-08$
49	27	$-0.744370844045D-08$	$0.877819498787D-08$
49	28	$0.182158221311D-07$	$-0.198989300085D-07$
49	29	$-0.136360378084D-07$	$-0.542520164295D-08$
49	30	$-0.141658883676D-07$	$-0.212147758404D-07$
49	31	$-0.287463487799D-07$	$0.127294398078D-07$
49	32	$0.837045602151D-08$	$0.620674117466D-08$
49	33	$0.998051966027D-08$	$0.357992316744D-08$
49	34	$0.107025917638D-07$	$0.550319619203D-08$
49	35	$-0.186244707327D-07$	$0.157278390947D-07$
49	36	$-0.589076098416D-08$	$0.805269824163D-08$
49	37	$0.123358068380D-07$	$0.238106480900D-07$
49	38	$0.843824653297D-08$	$-0.203995020541D-07$
49	39	$-0.845547943243D-08$	$0.162135890883D-07$
49	40	$-0.149957070044D-07$	$-0.266093361806D-07$
49	41	$-0.146999924233D-07$	$0.986344541248D-08$
49	42	$-0.384813597143D-08$	$-0.171962588238D-07$
49	43	$-0.232540804853D-07$	$0.710961784133D-08$
49	44	$0.174492349484D-07$	$-0.358514991249D-07$
49	45	$-0.390649858513D-07$	$0.247180790970D-07$

Table A-4: (cont.) Tesseral and Sectorial Harmonic Coefficients for Mars50c

n	m	$\bar{C}_{nm}$	$\bar{S}_{nm}$
49	46	0.301359022811D$-$07	$-$0.550807270821D$-$07
49	47	$-$0.418677806307D$-$07	0.640841482442D$-$07
49	48	0.236660293171D$-$07	0.467384346853D$-$07
49	49	$-$0.378777760042D$-$07	$-$0.345483058119D$-$07
50	1	$-$0.787285329010D$-$08	0.989140285882D$-$08
50	2	$-$0.135899577076D$-$08	$-$0.594060750389D$-$08
50	3	0.120415545669D$-$07	0.585344421435D$-$09
50	4	$-$0.489728264542D$-$08	0.104678389540D$-$07
50	5	0.177906727691D$-$09	$-$0.824298508243D$-$08
50	6	0.258993966019D$-$07	0.237039635302D$-$07
50	7	$-$0.203301796205D$-$07	$-$0.404705374883D$-$08
50	8	0.434401047099D$-$07	$-$0.766126326387D$-$08
50	9	$-$0.924182639168D$-$08	0.195345884513D$-$07
50	10	0.303160864952D$-$08	$-$0.295642234914D$-$07
50	11	0.134055099418D$-$07	0.238943037428D$-$07
50	12	$-$0.311336117308D$-$07	$-$0.741172527017D$-$08
50	13	0.311055540481D$-$07	$-$0.156430019664D$-$08
50	14	$-$0.125316124307D$-$07	0.176655127009D$-$07
50	15	0.223864638486D$-$07	$-$0.237260132949D$-$07
50	16	$-$0.167149922336D$-$07	0.312760027390D$-$07
50	17	$-$0.522491668384D$-$08	$-$0.202445539944D$-$07
50	18	0.468288824408D$-$09	0.245513192267D$-$07
50	19	$-$0.860369979470D$-$08	$-$0.194357385094D$-$07
50	20	0.245035476826D$-$07	$-$0.963709230779D$-$10
50	21	$-$0.224546549250D$-$07	0.751059292039D$-$08
50	22	0.332231965530D$-$07	$-$0.238023222874D$-$07
50	23	$-$0.249627481371D$-$07	0.407567540050D$-$08
50	24	0.101779486350D$-$07	$-$0.899891292531D$-$08
50	25	$-$0.398449897069D$-$09	0.105696428942D$-$07
50	26	0.783193091491D$-$08	$-$0.925974962416D$-$08
50	27	0.847841869378D$-$08	$-$0.717144965247D$-$08
50	28	$-$0.171519999466D$-$07	$-$0.146886971999D$-$07
50	29	$-$0.124435913027D$-$07	0.512052217289D$-$08
50	30	$-$0.961231470704D$-$10	0.352228526794D$-$08
50	31	$-$0.171026418146D$-$07	0.185842185142D$-$07
50	32	0.205291866250D$-$07	$-$0.803175734166D$-$08
50	33	$-$0.784261785374D$-$09	0.192411293288D$-$08
50	34	0.143916093704D$-$07	$-$0.143951230729D$-$07
50	35	0.514051030081D$-$08	0.673505388735D$-$08

Table A-4: (cont.) Tesseral and Sectorial Harmonic Coefficients for Mars50c

n	m	$\bar{C}_{nm}$	$\bar{S}_{nm}$
50	36	$-0.661261991788\mathrm{D}-08$	$-0.413427104282\mathrm{D}-08$
50	37	$0.269950158839\mathrm{D}-08$	$-0.102371745167\mathrm{D}-08$
50	38	$0.114637501400\mathrm{D}-07$	$-0.177045608550\mathrm{D}-07$
50	39	$-0.227240322201\mathrm{D}-07$	$-0.276104380417\mathrm{D}-08$
50	40	$-0.487250964253\mathrm{D}-08$	$-0.111737702858\mathrm{D}-07$
50	41	$-0.212264862598\mathrm{D}-07$	$0.794420701636\mathrm{D}-08$
50	42	$0.185882047916\mathrm{D}-07$	$-0.543849267563\mathrm{D}-08$
50	43	$-0.241064333948\mathrm{D}-07$	$-0.598992674519\mathrm{D}-08$
50	44	$0.252988497206\mathrm{D}-07$	$-0.364125892310\mathrm{D}-08$
50	45	$-0.364323425315\mathrm{D}-07$	$-0.153391934089\mathrm{D}-07$
50	46	$0.438040640109\mathrm{D}-07$	$0.980645414486\mathrm{D}-08$
50	47	$-0.478961508495\mathrm{D}-07$	$0.256312327749\mathrm{D}-07$
50	48	$0.235574825156\mathrm{D}-07$	$0.275766753646\mathrm{D}-07$
50	49	$-0.107190301986\mathrm{D}-07$	$-0.145328042950\mathrm{D}-07$
50	50	$-0.449524473690\mathrm{D}-07$	$0.889533681887\mathrm{D}-07$

Table A-4: (cont.) Tesseral and Sectorial Harmonic Coefficients for Mars50c

Appendix B

EPOCHS FOR APPROXIMATION OF LOCAL TRUE SOLAR TIME

The equation for computing Pathfinder's hybrid solar time, HST, is

$$\text{HST}(t) = \text{LTST}(t_0) + (t - t_0)/1.02749126$$

where

$$
\begin{aligned}
t &= \text{the ET time at which HST is to be computed} \\
t_0 &= \text{the HST epoch expressed in ET} \\
t - t_0 &= \text{the time difference between the HST epoch and the time of} \\
&\quad\text{ interest expressed as SI seconds} \\
\text{LTST}(t_0) &= \text{the LTST time at the HST epoch}
\end{aligned}
$$

and 1.02749126 is the number of SI seconds in a mean solar second for Mars.

A list of HST epochs that can be used to maintain $|\text{HST} - \text{LTST}| \leq 5$ solar minutes is given in Table B-1.

| Days from | HST Epoch Times | |
July 4, 1997 UTC	UTC	seconds past J2000 ET
0	1997-07-04 01:30:35.174	−78748103.64209852
30	1997-08-03 21:13:22.489	−76085136.32799846
60	1997-09-02 16:17:45.325	−73510873.49288577
90	1997-10-02 11:24:41.020	−70936457.79770768
115	1997-10-27 03:17:06.524	−68805712.29319103
125	1997-11-06 09:55:05.286	−67917833.53124955
135	1997-11-16 16:33:49.485	−67029909.33202498
145	1997-11-26 23:13:21.344	−66141937.47317710
155	1997-12-06 05:13:37.291	−65342721.52566021
162	1997-12-13 09:54:16.136	−64721082.68012795
169	1997-12-20 14:35:16.909	−64099421.90705799
176	1997-12-27 19:16:37.820	−63477740.99626257
183	1998-01-03 23:58:16.417	−62856042.39927094
190	1998-01-10 03:59:52.675	−62323146.14062926
197	1998-01-17 08:41:55.462	−61701423.35380870
204	1998-01-24 13:24:05.623	−61079693.19196223
211	1998-01-31 18:06:18.708	−60457960.10690179
218	1998-02-07 22:48:30.079	−59836228.73615690
225	1998-02-14 02:50:17.800	−59303321.01517519
232	1998-02-21 07:32:13.826	−58681604.98902090
239	1998-02-28 12:13:55.522	−58059903.29220103
246	1998-03-07 16:55:19.220	−57438219.59442121
253	1998-03-14 21:36:21.832	−56816556.98248343
260	1998-03-21 01:36:56.846	−56283721.96822653
270	1998-03-31 08:17:13.791	−55395705.02310082
280	1998-04-10 14:56:36.405	−54507742.40970299
290	1998-04-20 21:35:03.845	−53619834.96898703
310	1998-05-10 10:09:41.200	−51932957.61421075
340	1998-06-09 05:16:04.525	−49358574.28984386
360	1998-06-29 18:23:43.499	−47583315.31692435
370	1998-07-09 00:17:34.804	−46784484.01178214
380	1998-07-19 06:50:25.204	−45896913.61251390
390	1998-07-29 13:22:58.828	−45009359.98851206
400	1998-08-08 19:55:19.792	−44121819.02523909
410	1998-08-18 01:48:19.020	−43323039.79662680

All epochs correspond to LTST noon (12:00:00) on the same calendar day.

Table B-1: Hybrid Solar Time Epochs Required to Stay within 5 Solar Minutes of Local True Solar Time